Hydrogen Production Reactions from Carbon Feedstocks: Fossil Fuels and Biomass

R. M. Navarro, M. A. Peña, and J. L. G. Fierro*

Instituto de Catalisis y Petroleoquimica, CSIC, Cantoblanco, 28049 Madrid, Spain

Received December 1, 2006

Contents

* Author to whom correspondence should be addressed (fax +34 91 585 4760; e-mail jlgfierro@icp.csic.es).

1. Introduction

Hydrogen is one of the most common elements in Earth's crust, but it does not occur to a significant extent in elemental form. It is mostly present in water, biomass, and fossil hydrocarbons. Hydrogen is considered as a nonpolluting, inexhaustible, efficient, and cost-attractive energy carrier for the future. Hydrogen gas is a versatile energy carrier that is currently produced from a variety of primary sources such as natural gas, naphtha, heavy oil, methanol, biomass, wastes, coal, solar, wind, and nuclear.[1−4] It is a clean energy carrier because the chemical energy stored in the H−H bond is released when it combines with oxygen, yielding only water as the reaction product, althought nitrogen oxides (NO_x) can also form during high-temperature combustion in air. Accordingly, a future energy infrastructure based on hydrogen has been perceived as an ideal long-term solution to energy-related environmental problems.[5,6]

It is generally understood that the renewable energy-based processes of hydrogen production (solar photochemical and photobiological water decomposition, electrolysis of water coupled with photovoltaic cells or wind turbines, etc.) would be unlikely to yield significant reductions in hydrogen costs in the next few years. Industry generates some 48 million metric tons of hydrogen globally each year from fossil fuels. Almost half of this hydrogen goes into making ammonia,[7] a major component of fertilizers and a familiar ingredient in household cleaners. Refineries use the second largest amount of hydrogen for chemical processes such as removing sulfur from gasoline and converting heavy hydrocarbons into gasoline or diesel fuel. Food producers use a small percentage of hydrogen to add to some edible oils through a catalytic hydrogenation process.[8,9]

The demand for hydrogen in the next decade, both for traditional uses, such as making ammonia, and for running fuel cells, is expected to grow.[10,11] In fact, many car manufacturers already have produced prototype vehicles powered by hydrogen fuel cells. At least in the near future, this thirst for hydrogen will be quenched primarily through

10.1021/cr0501994 CCC: $65.00
Published on Web 08/23/2007

Rufino M. Navarro received his bachelor's degree in industrial chemistry at the Complutense University of Madrid, Spain, in 1992. He started his research in applied catalysis at the Institute of Catalysis and Petrochemistry in 1994. He obtained his doctor of chemistry degree from the Autonomous University of Madrid in 1998 with a dissertation on the development of catalysts for deep hydrodesulfurization of diesel fuels under the direction of Prof. J. L. G. Fierro and Dr. B. Garcia Pawelec. After receiving his Ph.D. degree, he was recruited as a postdoctoral fellow in the Laboratoire Catalyse et Spectrochimie (CNRS, Caen, France, 1998–1999) with Dr. J. Leglise. At the end of this period he was appointed as a postdoctoral associate of the Institute of Catalysis and Petrochemistry, where he focused on hydrogen production from hydrocarbons and low molecular alcohols using traditional technologies. He assumed his current position of tenure scientist at the Institute of Catalysis and Petrochemisty in 2006. His research activities focus on heterogeneous catalysis applied to clean energy production: fuel hydrotreatments, hydrodesulfurization, hydrogenation of aromatics, hydrogen production, re-forming of hydrocarbons and alcohols, water gas shift, and preferential oxidation of CO.

Miguel A. Peña received his M.Sc. in chemistry in 1985 from the Complutense University of Madrid, Spain. He obtained his Ph.D. in chemistry in 1990 at the same university, working under the supervision of Dr. L. González Tejuca and Prof. J. L. G. Fierro at the Institute of Catalysis and Petrochemistry (CSIC). From 1990 to 1993, he was working under contract in a project of oxidative coupling of methane funded by REPSOL (the largest Spanish oil and petrochemistry company). At the end of this period, he took a staff position of researcher at the Institute of Catalysis and Petrochemistry, which is his current status. In 1996–1997 he was a Visiting Scholar in the group of Prof. A. Varma, at the University of Notre Dame (USA). Currently, he is secretary of the Hydrogen Spanish Association. His research interests are focused mainly in catalytic processes for clean energy production, specifically in catalytic applications of perovskite oxides (Ph.D. dissertation), natural gas conversion, catalytic combustion, C_1 chemistry, catalytic membrane reactors, hydrogen production, and fuel cell catalysts. He has published 50 papers, is the co-inventor of five patents, and has made 30 presentations at symposia and conferences.

the use of fossil fuels. To make hydrogen, industry uses steam methane re-forming (SMR), which is the most widely used and most economical process.[12] Although SMR is a

Jose L. G. Fierro was graduated in chemistry from the University of Oviedo (Spain) in 1973 and received his Ph.D. degree in chemistry from the Complutense University of Madrid (Spain) in 1976. He developed postdoctoral positions in the Department of Surface Chemistry at the Université Pierre et Marie Curie, Paris (France), and in the Department of Chemistry of Cork University, Cork (Ireland), and took a sabbatical leave in the Groupe of Physico-Chimie Minérale et de Catalyse of the Université Catholique de Louvain, Louvain-la-Neuve (Belgium). In 1988 he reached the position of professor in the Institute of Catalysis and Petrochemistry (CSIC). His activities cover different fields of catalysis such as natural gas conversion, selective oxidations of paraffins and olefins, synfuels, environmental catalysis, catalytic combustion, surface chemistry, heteroatom removal and dearomatization of petroleum feedstocks, catalyst preparation, hydrogen production, high-temperature chemistry, and chemical and physical characterization of solid catalysts. His scientific achievements are compiled in 730 papers spread in prestigious refereed journals, 12 reviews, 8 books (editor and/or coauthor), and 20 patents. He has been invited to more than 200 plenary lectures, seminars, and conferences in refining and petrochemical companies, specialized symposia, and public and private organizations all around the world.

complex process involving many different catalytic steps, as long as natural gas (or CH_4) remains at low or even moderate cost, including the advent of a carbon tax, SMR will continue to be the technology of choice for massive production of H_2. Over several decades of developments in catalyst technology, substantial improvements have been introduced. The SMR process also gives off carbon monoxide and carbon dioxide, the primary greenhouse gas. Although this approach generates pollution, these gases are released in a potentially more manageable way rather than in the case of billions of automobile engines. A novel re-forming technology, the membrane reactor (MR), is currently being developed[13] and promises economic small-scale hydrogen production combined with inexpensive CO_2 capture because of the high concentration and pressure of the exiting gas stream.[14] This could avoid a dedicated hydrogen infrastructure, facilitate CO_2 capture at small scale, and thus, possibly, contribute to a more rapid cut in greenhouse gas emissions. Because it is expected that significant development of a hydrogen transportation infrastructure will not occur within the next decade,[15] the time frame of this study is the medium-term future (2015−2025).

Nonetheless, shedding the habit of fossil fuel entirely is the only way a wholesale shift to hydrogen will work in the long term. One approach to this goal is to apply steam re-forming methods to alternative renewable materials. Such materials might be derived from plant crops, agricultural residues, woody biomass, etc. Not only do these biomass conversion schemes turn low-value feedstocks into a valuable product, but carbon dioxide released in the processes is slowly recycled by the planting of new crops to provide the needed biomass, even though time constants of the carbon

cycle are different. A biomass strategy of hydrogen generation could be a useful intermediate step between the current fossil fuel method and the dream of efficient water splitting. Still, any realistic contender for hydrogen generation must first suppress the re-forming of fossil fuel as the cheapest and most efficient process.

Despite the compelling attractiveness of hydrogen, the realization of a hydrogen economy faces many challenges. Perhaps the most important one is the near absence of large-scale supporting infrastructure for hydrogen distribution. Interest in hydrogen grew after World War I, but it was in 1970 that General Motors engineers coined the term "hydrogen economy".[16] Recently, many worldwide agencies have described hydrogen as the future fuel of choice.[17] The International Energy Agency described a Hydrogen Program with detailed development activities. The report describes technical options for small-scale production of hydrogen via steam re-forming of natural gas or liquid fuels. Its focus is on small stationary systems that produce pure hydrogen at refueling stations for hydrogen-fueled vehicles.[18,19]

Although hydrogen production and storage/distribution infrastructures are commercially available in chemical and refining industries around the world, existing conversion and storage technologies are too expensive for widespread use in energy schemes. Finally, as a general rule, the existing energy policies do not promote consideration of environmental and security costs of energy that would facilitate wider use of hydrogen. Developing hydrogen as a realistic, viable energy option will require an unprecedented level of sustained and coordinated activities at different levels. This area remains a fertile ground for improvements. As can be seen in the sections below, recent important approaches to hydrogen production involve methane decomposition, partial oxidation, and CO_2 re-forming of methane, together with the re-forming of low molecular weight alcohols such as methanol and ethanol. There are a few relatively complete reviews covering this field.[1−3] A review in 2002 by Rostrup-Nielsen et al.[20] provided a coherent description of the catalysis of the re-forming reactions. More recently, Ross[21] summarized the steam re-forming and CO_2 re-forming reactions, discussing some catalysts developed for these reactions.

2. Reactions with Carbon Dioxide and Carbon Monoxide Coproduction

2.1. Steam Re-forming

The steam re-forming of hydrocarbon feedstocks (eq 1) has for many decades been the preferred method used industrially for the production of hydrogen either as a pure gas or as a reactant for the production of ammonia or methanol.[20,22] Generally, the steam re-forming process involves two reactions, namely, the splitting of hydrocarbons with steam (eq 1) and the water gas shift (WGS) (eq 2):[23]

$$C_nH_m + nH_2O \rightarrow nCO + (n + m/2)H_2 \quad \text{for } n = 1:\ \Delta H^\circ_{298K} = +206.2 \text{ kJ/mol} \quad (1)$$

$$CO + H_2O \rightarrow CO_2 + H_2 \quad \Delta H^\circ_{298K} = -41.2 \text{ kJ/mol} \quad (2)$$

The steam re-forming process has been practiced since 1930. The first plant using light alkanes as feed began operation in 1930 at Standard Oil Co. in the United States and 6 years later at ICI in Billingham, England.[22] In the United States, where natural gas was available, methane steam re-forming had been performed. By contrast, in Europe during the 1950s, light naphtha became the most economic feedstock. Later, however, the discovery of natural gas reserves in The Netherlands and under the North Sea changed the feedstock situation. Due to its importance, substantial improvements have been introduced over the years, and research on catalysts, reactor materials, fluidodynamics, and heat transport continues.

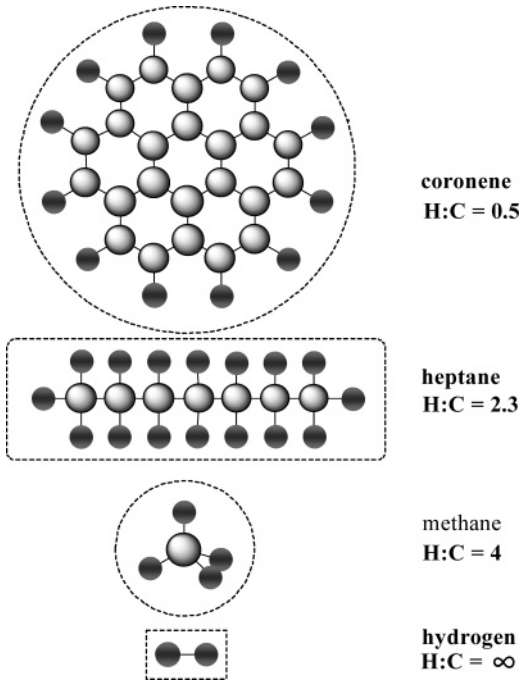

Figure 1. H/C atomic ratios in different hydrogen-containing molecules.

2.1.1. Methane

2.1.1.1. Reaction and Mechanisms. The transformation of methane to hydrogen has been a challenging task because methane is extremely difficult to activate. Among hydrocarbons, the methane molecule has the largest H/C ratio (H/C = 4), substantially higher than that of *n*-heptane (H/C = 2.3), the boiling point of which falls in the range of gasoline hydrocarbons, and much higher than that of a highly condensed polyaromatic structure such as coronene (H/C = 0.5) (Figure 1). The methane molecule is very stable, with a C−H bond energy of 439 kJ/mol; hence, methane is resistant to many reactants. In the methane molecule the sp^3 hybridization of the atomic orbitals of carbon makes the carbon−hydrogen bonds very strong. Methane is readily activated by group 8, 9, and 10 metals and is oxidized to give syngas ($CO + H_2$) first and then hydrogen after WGS and CO_2 removal. Syngas is cooled and then shifted in the WGS reactor. In older plants, CO_2 is subsequently removed by means of a chemical absorption unit. Modern hydrogen plants apply pressure swing adsorption (PSA) to separate hydrogen from the other components, which produces higher quality hydrogen (99.999% against 95−98% for scrubbing systems) at feedstock pressure (ca. 25 bar).[24] The integration of ceramic ion transport membranes with re-formers opens new possibilities for highly efficient and low-cost hydrogen production with CO_2 capture in the long term.[25]

The SMR reaction (eq 1) is highly endothermic and favored at lower pressures. The steam re-forming catalysts

usually contain nickel as the major metallic component. The noble metal catalysts were first used for steam re-forming, but the cost makes their use prohibitive. For these systems, the catalytic activity depends on the metal area, and their properties are dictated by the severe operating conditions such as temperatures in the range of 700−1250 K and steam partial pressures of up to 30 bar. The actual activity of the catalyst is not, in general, a limiting factor. Thus, a typical nickel catalyst is characterized by a turnover frequency (TOF) of ca. 0.5 s^{-1} at 723 K under conditions approaching industrial practice, which corresponds to CH_4 conversions around 10%. The main barrier of the steam re-forming reaction is thermodynamics, which determines very high conversions only at temperatures above 1170 K. In practice, a significant part of the catalyst loaded into the tubes of the re-former is poorly utilized. The catalyst activity is important but not decisive, with the heat transfer coefficient of the internal tube wall being the rate-limiting parameter.[22]

Kinetics of methane steam re-forming catalysis are reported and summarized by Rostrup-Nielsen et al.[22] and Wei and Iglesia,[26] who concluded that CH_4 reaction rates are limited solely by C−H bond activation steps and unaffected by the identity or concentration of co-reactants. According to these studies the following mechanism was proposed:

$$H_2O(g) + * \rightarrow O^*(a) + H_2(g) \quad (3a)$$

$$CH_4(g) + 2^* \rightarrow CH_3^*(a) + H^*(a) \quad (3b)$$

$$CH_3^*(a) + * \rightarrow CH_2^*(a) + H^*(a) \quad (3c)$$

$$CH_2^*(a) + * \rightarrow CH^*(a) + H^*(a) \quad (3d)$$

$$CH^*(a) + O^*(a) \rightarrow CO^*(a) + H^*(a) \quad (3e)$$

$$CO^*(a) \rightarrow CO(g) + * \quad (3f)$$

$$2H^*(a) \rightarrow H_2(g) + 2^* \quad (3g)$$

In eqs 3a−3g * denotes a Ni surface atom. According to this mechanism, H_2O reacts with surface Ni atoms, providing adsorbed oxygen and gaseous hydrogen; methane adsorbs dissociatively on the Ni surface, forming a methyl group that undergoes further stepwise dehydrogenation steps. CH− species formed in this way react with adsorbed oxygen and finally yield gaseous CO and H_2.

2.1.1.2. Carbon Formation. In the production of H_2 from methane, carbon formation usually takes place in the form of fibers or filaments with a small Ni particle at the top of each fiber.[3,27] Carbon formation may lead to breakdown of the catalyst together with carbon deposits and degradation of the catalysts. There are two major reactions for carbon formation:

$$2CO \rightarrow C + CO_2 \quad \Delta H^\circ_{298K} = -172.5 \text{ kJ/mol} \quad (4)$$

$$CH_4 \rightarrow C + 2H_2 \quad \Delta H^\circ_{298K} = +74.9 \text{ kJ/mol} \quad (5)$$

The tendency to form carbon on the catalyst surface depends on reaction kinetics, process conditions, and re-former design.[3,22] These C-forming reactions are carefully balanced by C-consuming reactions ($C + CO_2 \rightarrow 2CO$ and $C + H_2O \rightarrow CO + H_2$), which in turn also depend on the kinetic process conditions and reactor design (Figure 2). At low temperatures, the activated Ni catalyst is covered by a hydrocarbon layer, which slowly degrades into a polymeric film, blocking the nickel surface. At high temperatures, ethylene from the pyrolysis of higher hydrocarbons produces pyrolytic coke, which encapsulates the catalyst particles. Whisker carbon is the most common form of carbon produced during the steam re-forming.[22]

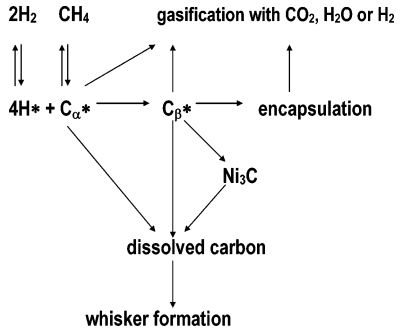

Figure 2. Carbon formation and gasification routes during the steam re-forming of methane. Adapted with permission from ref 23. Copyright 1997 Elsevier B.V.

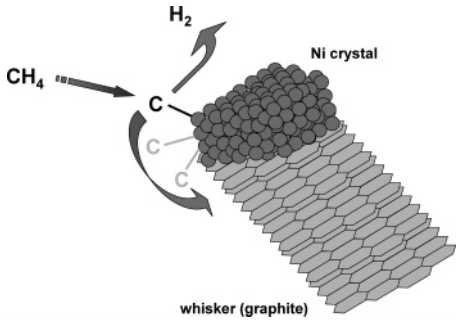

Figure 3. Schematic illustration of the process by which carbon whiskers are formed at the nickel particle during steam re-forming.

Nickel carbide is not stable under SMR conditions. As a consequence, carbon nucleates in the form of filaments after an induction period, and then the carbon filament grows at a constant rate (Figure 3). The importance of step sites on the catalyst surface for the nucleation of carbon was recently confirmed by in situ investigations by high-resolution transmission electron microscopy (TEM). These indicate the segregation of carbon when the formation of filaments takes place at specific sites on the nickel surface.[20] The size of Ni particles has a direct implication on the nucleation of carbon. The initiation of carbon formation is retarded on the smaller nickel crystallites, as demonstrated by thermogravimetric experiments with two Ni catalysts having the same activity but different metal dispersions.[28]

The rate of carbon formation was lower on noble metals than on nickel,[29] and this behavior appears to be related to the difficulty of noble metals to dissolve carbon in the bulk.[30] The carbon formed on the surface of noble metals is almost indistinguishable from the catalyst particles. High-resolution TEM images taken from a ruthenium catalyst employed in the SMR reaction reveal a structure in which a few carbon layers are deposited on the surface of the Ru particles.[29]

Several approaches can be followed to minimize coke formation on Ni or other metal surfaces. The first rests on the ensemble size control.[31] The formation of carbon—either dissolved in or deposited on the nickel—must require the polymerization of monoatomic carbon species (C_α), whereas gasification involves only one of such species. The formation of more than one species demands more surface sites. Because the SMR requires the dissociation of methane to

form a carbonaceous intermediate, coke formation would require an ensemble of surface sites that would be larger than that required for the re-forming reaction. Following this reasoning, it was inferred that by controlling the number of sites in a given ensemble it may be possible to minimize coke formation while maintaining the re-forming reaction. The basis of the ensemble size control lies in the work of Alstrup and Andersen[32] on sulfur adsorption on nickel. Those authors found that the grid sulfur did not coincide with the nickel atoms placed in the topmost layer of nickel crystallites. Adsorption of sulfur on the catalyst surface thus delineates ensembles of sites, with the critical size being reached at sulfur coverage above 0.7. Under these conditions, the rate of the steam re-forming reaction was decreased but coke formation was almost eliminated. Although sulfur adsorption is strong, it is diminished during reaction. As a result, it is necessary to add small amounts of a sulfur-producing gas to the feed.

The second approach to the control of coke formation is to prevent carbide formation.[33] The electronic structure of carbon is similar to that of sulfur and the tetra- and pentavalent p metals (Ge, Sn, and Pb or As, Sb, and Bi). The tetra- or pentavalent metals could also interact with Ni 3d electrons, thereby limiting the possibility of nickel carbide formation.[33] Alloy formation reduces carbide formation but is undesirable as active sites on the surface of nickel crystallites are lost. However, carbide formation can be developed only on the surface layer, and as a result an alloy formed at the surface layer should be preferred. On the basis of these ideas, Trimm[33] studied the effect of small amounts of dopants on the catalytic and coking behavior of nickel catalysts. The effect of tin on steam re-forming was small for Sn levels below 1.75%, whereas coke formation was significantly reduced even by the addition of 0.5% Sn. It is clear that the addition of small amounts of dopant does substantially reduce coking while having little influence on the rate of the steam re-forming reaction. Alloying nickel with copper can also reduce carbon formation,[34] but it is not feasible to reach the required high surface coverage of copper atoms, as occurs with sulfur atoms, to remove carbon deposition. The formation of a stable alloy between nickel and tin,[35] or nickel and rhenium,[36] also appears to be responsible for the reduction in carbon formation. All of these studies have shed some light on the improvement of catalyst performance in the steam re-forming reactions. However, additional work is required to understand the promoting effects of various oxides and to discern whether or not the promoters decorate the surface of nickel crystallites.

2.1.1.3. Promoter Effects. The catalysts are promoted to reduce the risk of carbon formation. Several recent investigations have reported the effect of catalyst composition on the activation of methane. Upon looking at the degree of dehydrogenation of CH_x species (measured by the number of hydrogen atoms per carbon atom) on several metals, it was observed that x was larger for nickel than for cobalt catalysts and also larger for magnesia-supported than for silica-supported catalysts.[37] Kinetics experiments revealed that MgO and alkali dissociate steam, which then transfers to the nickel particles through a spillover mechanism.[22] A similar conclusion was reached from isotope-exchange experiments,[38] which demonstrated that the enhanced adsorption of water on magnesia support leading to improved resistance to carbon formation is by nature a dynamic effect. The spillover of water probably takes place through OH groups instead of molecular water. In favor of this possibility, in a recent study on Ni/MgO and Ni/TiO_2 catalysts Bradford and Vannice[39] concluded that surface hydroxyl groups, located on the support surface, react with the CH_x fragments adsorbed on the nickel surface to yield a formate-type intermediate which decomposes into H_2 and CO. These authors also suggested that the support may serve as a sink for surface hydroxyl groups and that the active site for CH_xO formation and subsequent decomposition may be at the metal−support interface. Activation barriers were found to be higher on Ni/TiO_2 after significant time on-stream, and this was attributed to a geometric site blockage mechanism whereby migrating TiO_x moieties or inactive carbon deposits break up the large site ensembles on the nickel surface needed for CH_4 dissociation. The use of supports able to release bulk oxygen such as yttria-stabilized zirconia indicates that a spillover of lattice oxygen may be involved in the re-forming reaction.[40]

2.1.1.4. CO_2 (Dry) Re-forming. At the beginning of the past decade interest arose in so-called "dry re-forming", the re-forming of methane to syngas using CO_2 as a reactant[41] (eq 6). Carbon dioxide re-forming is typically influenced by the simultaneous occurrence of the reverse water gas shift (RWGS) reaction (eq 7), which results in H_2/CO ratios of less than unity.

$$CH_4 + CO_2 \rightarrow 2\,CO + 2H_2 \quad \Delta H^\circ_{298K} = +247.4\ \text{kJ/mol} \tag{6}$$

$$CO_2 + H_2 \rightarrow CO + H_2O \quad \Delta H^\circ_{298K} = +41.2\ \text{kJ/mol} \tag{7}$$

This reaction had been first studied by Fischer and Tropsch in 1928.[42] In a series of papers in the 1960s, Bodrov et al.[43] had also demonstrated that the steam re-forming and CO_2 re-forming reactions over Ni materials had very similar kinetics and mechanisms. The reaction is notoriously prone to giving carbon deposition, the chemical potential for carbon deposition for the stoichiometric dry re-forming reaction being significantly higher than that in the equivalent steam re-forming reaction.[44] The renewed interest in the early 1990s arose because several catalysts (e.g., noble metals supported on alumina[45]) were reported to be effective for the reaction without exhibiting the serious problems of carbon deposition found with the more conventional catalysts such as Ni supported on alumina. Most of the papers related to CO_2 re-forming were introduced with the argument that the discovery of an effective catalyst would lead to a solution to the greenhouse effect. This is untrue because at the end, after the shift reaction, 1 mol of CO_2 consumed yields 2 mol of CO_2 (eq 6). Nevertheless, the research led to a new understanding both of the conditions under which dry re-forming or a combination of dry re-forming and steam re-forming could be carried out and of the catalysts to be used.

The active catalysts, the reaction mechanisms, and the deactivation processes are similar for steam re-forming and dry re-forming reactions of methane.[41,46] The conversion of methane is restricted by the thermodynamics of re-forming reaction. The calculated thermodynamic conversion of methane for various CO_2/CH_4 ratios as a function of temperature is shown in Figure 4.[21] Assuming that the ratio chosen for operation will be close to unity, it can be seen that reasonable conversions will be achieved only at high temperatures (above ca. 1120 K). The reaction is more endothermic than steam re-forming and must be carried out at high temperature and low pressure to achieve maximum

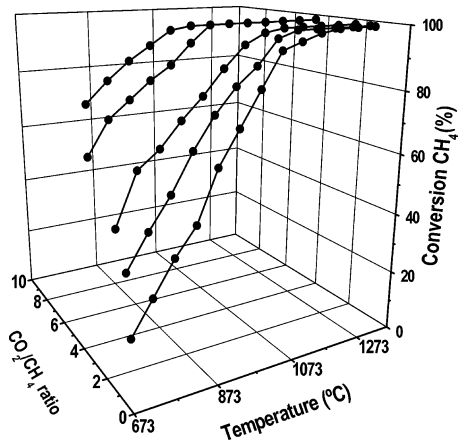

Figure 4. Thermodynamically calculated conversions of methane as a function of temperature for a series of different feed ratios. Adapted with permission from ref 21. Copyright 2005 Elsevier B.V.

conversion. Nickel[30,47] and noble metals[30,48,49] are active for the dry re-forming. In addition, perovskite oxides[50,51] and transition metal carbides (especially Mo) have been considered for CO_2 re-forming,[52−54] although under reaction conditions the later systems seem to be stable only at high pressure.

Several attempts have been made to understand the mechanism of CH_4 re-forming with CO_2 on group 8, 9, and 10 metals. Most of these employ supported platinum catalysts because Pt appears to be one of the most active and stable metals for these reactions.[55−57] Platinum supported on zirconia, for instance, has been used for the dry re-forming of CH_4 for 500 h without detectable deactivation.[57,58] Recently, Wei and Iglesia[59] reported an isotopic tracer and kinetic study aimed at probing the identity and reversibility of the elementary steps required for H_2O and CO_2 re-forming of CH_4 on supported Pt clusters and to demonstrate the mechanistic equivalence for H_2O and CO_2 re-forming and CH_4 decomposition reactions. Re-forming rates were limited by C−H bond activation of CH_4 molecule on essentially uncovered Pt crystallite surface unaffected by the concentration or reactivity of CO_2 co-reactant. Kinetic isotopic effects appeared to be consistent with the sole kinetic relevance of C−H bond activation ($k_H/k_D = 1.58-1.77$ at 873 K). These isotope effects and measured activation energies were similar for H_2O re-forming, CO_2 re-forming, and CH_4 decomposition reactions. CH_4/CD_4 cross-exchange rates are much smaller than the rate of methane conversion in the CO_2 and H_2O re-forming reactions, and thus C−H bond activation steps are irreversible.

For the supported platinum catalysts, turnover frequencies (TOF) for H_2O and CO_2 re-forming and CH_4 decomposition increase with increasing platinum dispersion, suggesting that coordinative unsaturated surface Pt atoms, present in small crystallites, are more reactive than Pt atoms in a low index surface for C−H bond activation. Platinum dispersion, but not TOF, is influenced by the type of support (Al_2O_3, ZrO_2, $Zr_{1-x}Ce_xO$).[59] This indicates that co-reactant activation on supports, if it occurs, is not kinetically relevant. The rates of structure-insensitive CO oxidation reaction are found to be similar before and after CH_4 re-forming, and hence this latter reaction does not influence the number of exposed Pt atoms via coverage or sintering by unreactive chemisorbed species. These mechanistic conclusions and metal dispersion effects appear to apply generally to CH_4 reactions on group 8, 9, and 10 metals,[59] but the reactivity of surface Pt atoms

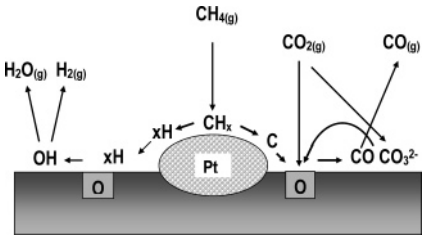

Figure 5. Model for CO_2 re-forming of CH_4 over a Pt/ZrO_2 catalyst. Adapted with permission from ref 63. Copyright 1998 Elsevier B.V.

in C−H bond activation reactions is greater than for similar crystallite size of other metals.

Others have proposed that in the mechanism for CO_2 re-forming, CH_4 and CO_2 are activated in different ways, depending on active metal.[60−62] Schuurman et al.[60] studied Ni and Ru supported on SiO_2 and Al_2O_3 by temporal analysis of products (TAP). CH_4 is activated by decomposition in both metals, producing H_2 and adsorbed carbon. However, the behavior of CO_2 is different on each metal. CO_2 is adsorbed on Ni, yielding CO and adsorbed oxygen; O_{ads} and C_{ads} react later via a Langmuir−Hinshelwood mechanism to form CO: this is the rate-determining step. Nevertheless, on Ru, CO_2 reacts directly with C_{ads} (Eley−Rideal mechanism) to produce CO. No adsorbed oxygen is present in this case, and the rate-determining step is the adsorption of methane. Other authors[61−63] also postulated that the reaction is not occurring solely on the noble metal surface but primarily on the metal−support interfacial region. Thus, a bifunctional mechanism has been proposed for CO_2 re-forming of CH_4 over a Pt/ZrO_2 catalyst.[63] In this mechanism (Figure 5), a molecule of methane reacts at the Pt surface to give carbon species and hydrogen is desorbed. Some of the carbon accumulates on the surface of the Pt crystallite, but some diffuses to the interface between the Pt and the zirconia support, where it picks up oxygen from the support and desorbs as CO. The oxygen of the support is then replaced by the reaction of a molecule of CO_2 with desorption of a further molecule of CO.

The major difficulty associated with the realization of dry re-forming is the thermodynamically favored formation of coke, which deactivates the catalysts. Thermodynamics predicts formation of coke under usual conditions of CO_2 re-forming via either CH_4 decomposition or CO disproportionation. The catalysts are promoted to reduce the risk of carbon formation by means of (i) enhancing the adsorption of CO_2, (ii) enhancing the rates of surface reactions, and (iii) decreasing the rate of methane activation. The porous structure of the support also influences the stability of the metal. On comparing α-Al_2O_3 with γ-Al_2O_3, SiO_2, and MgO of different porosities, Lu et at.[64,65] concluded that porous supports favor metal dispersion and contact between the active sites and reactants, increasing the activity for CO_2 re-forming and stability. Zhang et al.[66] found that the activity for CO_2 re-forming in supported Rh catalysts follows the order YSZ > Al_2O_3 > TiO_2 > SiO_2 > La_2O_3 > MgO, which is directly correlated with the acidity of the support. Deactivation is controlled by other parameters, becausesince in a specific support it decreases when the particle size of Rh increases. Nevertheless, the nature of the support has a stronger influence on the catalytic lifetime, which is low on TiO_2 and MgO within the mentioned support series. The enhanced adsorption of CO_2 on supports[67] seems to be important for the promoting effect when using basic materials

Table 1. Composition of Logistic Fuels[a]

	gasoline	diesel grade 2	jet-A
paraffins (% vol)	45	55	60
oleffins (% vol)	8	2	2
napthenes (% vol)	12	16	20
aromatics (% vol)	35	27	18
sulfur (wt %)	0.005	0.005	

[a] From Astarita et al. and Naidja et al.[71,72]

(La_2O_3, CeO_2) as supports for dry re-forming catalysts. Increasing the concentration of adsorbed CO_2 is suggested to reduce carbon formation via CO disproportionation. Manganese also promotes Ni/Al_2O_3 for CO_2 re-forming by decreasing carbon deposition.[68] In this case, Ni particles are partially covered by MnO_x patches, and their role is to promote the adsorption of CO_2, producing a reactive carbonate. This carbonate reacts with the CH_x fragments, preventing coke from being formed form these fragments. Additionally, the MnO_x patches break the Ni ensemble necessary for carbon formation, without reducing the activity of the catalyst. Carbon formation during CO_2 re-forming of CH_4 also depends on the choice of metal. Bradford and Vannice[61] studied different CO_2 re-forming active metals (Ni, Co, Fe, Rh, Pd, Ir, Pt) supported on TiO_2 and SiO_2. The TOF depended on the d-character of the transition metal. In general, it has been found that Ru, Rh, and Ir supported on Eu_2O_3,[48] Mg,[69] and Al_2O_3[45] exhibit much less carbon formation than supported Ni, Pd, and Pt. A beneficial effect of the addition of Sn to Pt has been described.[35] $Pt-Sn/SiO_2$ and $Pt-Sn/ZrO_2$ exhibit less carbon deposition during CO_2 re-forming than the respective monometallic Pt catalyst analogues. The reason for this behavior is possibly the formation of a Pt−Sn alloy and remains under investigation.

2.1.2. Liquid Hydrocarbons

The wide availability of gasoline, diesel fuel, and jet fuels would make them ideal as fuels for hydrogen production.[70] Logistic liquid fuels are multicomponent mixtures containing a large number of hydrocarbons: paraffins, naphthenes, olefins, aromatics, and sulfur compounds[71,72] (Table 1). The chemical nature of fuel mixtures poses several technical problems to the re-forming process; these are associated with (i) the presence of sulfur compounds, which may deactivate catalytic active sites, and (ii) the strong tendency for carbon to be deposited on catalytic surfaces under re-forming conditions

2.1.2.1. Catalytic Reaction and Mechanism. Steam re-forming of liquid fuels is performed over catalysts normally containing group 8, 9, and 10 metals (Ni, Co, Ru, Pt, Pd, Rh, etc.). The reaction of the hydrocarbons present in fuels with steam takes place by irreversible adsorption on catalyst surfaces with no intermediate formation.[73] The adsorbed hydrocarbon undergoes subsequent breakage of C−C bonds one by one until the hydrocarbon has been converted into C_1 compounds. The steam re-forming reaction (eq 1) is followed by the establishment of the equilibria of the exothermic water gas shift reaction (eq 2) and the methanation reaction (eq 8):

$$CO + 3H_2 \rightarrow CH_4 + H_2O \quad \Delta H^{\circ}_{298K} = -206.2 \text{ kJ/mol} \tag{8}$$

Hydrocarbons present in fuel feeds showed pronounced differences in reactivities in steam re-forming.[22] Long-chain hydrocarbons and olefins are more reactive than CH_4. Also, cycloalkanes are more reactive than methane. However, in the case of aromatics, due to the stable resonant structure of the rings, reactivity toward steam approaches that of CH_4.

2.1.2.2. Catalyst Sulfur Poisoning. The catalyst formulations used for liquid fuel steam re-forming are more complicated than those used for methane steam re-forming because they must be carefully formulated to achieve high resistance to both carbon deposition and sulfur poisoning. The metals included in re-forming catalysts (groups 8, 9, and 10) are highly susceptible to sulfur poisoning. Under re-forming conditions, sulfur compounds presents in fuel (10−50 ppm) react under re-forming conditions with metals, forming stable metal sulfides that deactivate the catalyst.[74,75] The desulfurization of natural gas (hydrogenation of alkyl thiol compounds and the subsequent adsorption/absorption of H_2S) is almost quantitative. However, desulfurization of the organic S compounds present in liquid hydrocarbon fuels (derivatives of dibenzothiophene) partly removes sulfur, even using novel hydrotreating catalysts or by deep adsorptive desulfurization.[76] Much work has been done to better understand the sulfur poisoning on Ni-based and noble metals-based catalysts. However, no highly active sulfur-tolerant steam re-forming catalyst has been developed, and only a few papers have been published in the area of catalysts with improved sulfur resistance.[77,78] Bimetallic Ni−Re catalysts have shown promising sulfur tolerance for the steam re-forming of mixture of hydrocarbons simulating gasoline in the presence of 20 ppm of S in the feed.[77] Also, catalysts based on Rh−Ni supported on CeO_2-modified Al_2O_3 have been presented as excellent catalysts that can successfully re-form sulfur-containing liquid hydrocarbons, such as jet fuel, as demonstrated by the re-forming of JP-8 containing 22 ppm of sulfur without deactivation for 100 h time-on-stream.[78]

2.1.2.3. Carbon Formation on Catalyst Surface. In the steam re-forming of higher hydrocarbons, the coke formation is much higher than with methane.[33] Rostrup-Nielsen and Tottrup[79] have reported data for a range of hydrocarbons (Figure 6) showing that olefins and aromatics, in particular, have the highest tendency for coke formation. Olefins are not normally present in the feedstock, but they may easily be formed by thermal pyrolysis of hydrocarbons during preheating at temperatures exceeding 873−973 K.[80]

The carbon formation from thermal pyrolysis may be solved through adiabatic pre-re-forming (see section 1.2.1.5) prior to deployment of the primary re-former or by the use of cool flames to evaporate liquid hydrocarbon mixtures without carbon residues.[81] However, steam re-forming of liquid feeds containing up to 30 wt % aromatics has been done without pre-re-forming units when using desulfurized feeds and special catalysts with very high coke resistance and under critical control of preheating temperatures and heat flux profiles on the re-forming reactor.[79]

2.1.2.4. Catalytic Promoter Effects. As in the case of methane steam re-forming, catalysts used in liquid fuel steam re-forming are mainly based on nickel. Noble metals (Ru, Rh) are more effective than Ni, because of their higher intrinsic rates for the activation of C−C and C−H bonds, and less susceptible to carbon formation, but are more expensive. Two strategies are employed in the formulations of catalysts to re-form liquid fuels in order to decrease carbon deposits on the catalyst: (i) the enhancement of water adsorption on catalysts and (ii) the modification of active

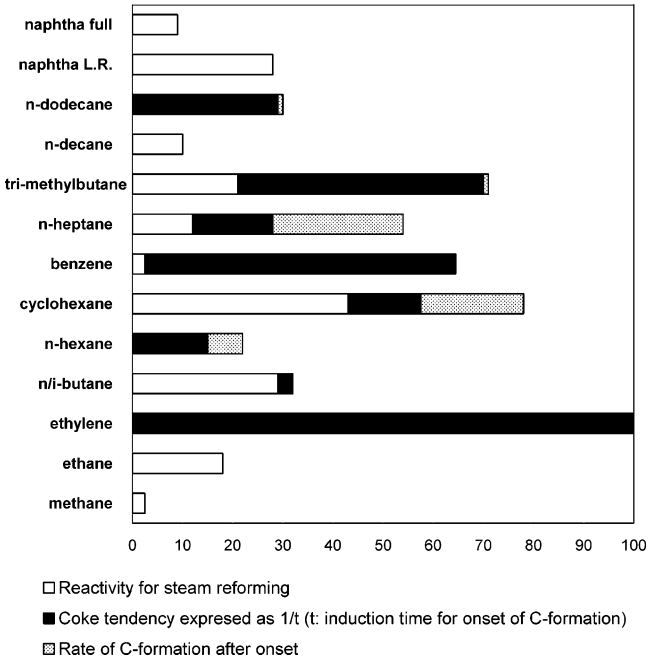

Figure 6. Steam re-forming activity and coking tendency of different hydrocarbons. Adapted with permission from ref 23. Copyright 1997 Elsevier B.V.

metal surfaces via the presence of other metals. Enhanced water adsorption can be achieved using carefully engineered supports with the addition of alkali, especially potassium, or magnesium oxides. The improved resistance to carbon formation on alkali and magnesium supports is caused by an increase in the rate of dissociation of water on the supports. As a result, the amount of OH species present on active metal surfaces is increased, thereby enhancing the removal of CH_x and delaying the full dehydrogenation of CH_x species of the atomic C precursor of carbon deposition on metal surfaces. Supports of the types mentioned above have been used in industrial naphtha steam re-forming catalysts.[82] The addition of lanthanides to supports also improves the stability of re-forming catalysts and decreases carbon formation during steam re-forming of higher hydrocarbons.[83−85] Wang and Gorte[84] investigated the effect of cerium oxide as the promoter of noble metal catalysts for the steam re-forming of various hydrocarbons. Cerium promotion revealed a beneficial effect by both decreasing the rate of carbon deposition and increasing the catalytic activity. Ozkan et al.[83] reported that the presence of lanthanide elements (La, Ce, and Yb) significantly enhances catalytic activity and stability, due in part to the fact that lanthanides help to inhibit both the growth of nickel crystallites and the carbon deposition on catalyst surfaces. Studies carried out at the Argonne National Laboratory (ANL) have shown that group 8, 9, and 10 metals dispersed on doped ceria supports are active catalysts for re-forming of a wide range of hydrocarbons, including gasoline and diesel.[86,87] The improvement in the catalytic performance of catalysts with regard to their resistance to coke deposition has been attributed to the high oxygen mobility associated with CeO_2, which facilitates coke gasification.[88,89]

Another approach to minimizing carbon formation on catalysts is by modifying the Ni phases. The addition of Co,[90] Mo, W,[91] Re,[92] Sr,[93] and Sn[94] to Ni catalysts has been shown to increase coking resistance under steam re-forming conditions. It was suggested that the major carbon-preventing effect of these promoters is to block the steps sites on Ni particles and hence remove the nucleation sites for graphite formation.[95,96]

Table 2. Operating Conditions for Adiabatic Pre-re-forming[a]

	naphtha	diesel	jet-A
inlet temperature (K)	723	753	753
H_2O/C ratio (mol/mol)	1.55	2.45	2.40
relative deactivation rate	0.28	2.2	1.2

[a] Adapted from Christiansen.[101]

Recently there has been increasing interest of investigation in noble metal-based catalysts (Ru, Rh, and Pd), despite their cost, because they exhibit the highest intrinsic rates for steam re-forming and prevent carbon deposition. The rate of carbon formation was found to be far less on noble metals than on Ni.[29] This result has been explained by the fact that the noble metals do not dissolve carbon.[30] Some patents and literature papers have reported on the application of supported Rh or Ru in the steam re-forming of high aliphatic hydrocarbons or of naphtha[97,98] A Ru-based (Ru/Al_2O_3) catalyst has been used for steam re-forming of hydrocarbons while preventing carbon deposition.[97,98] Suzuki et al.[98] have successfully conducted long-term (8000 h) tests of steam re-forming of desulfurized kerosene using $Ru/Al_2O_3-CeO_2$ catalysts.

2.1.2.5. Catalytic Pre-re-forming. The problem of carbon formation may be solved through adiabatic pre-re-forming prior to the primary re-former. In the pre-re-former all high hydrocarbons are converted directly into C_1 components (methane and carbon oxides) in the low-temperature range, typically from 673 to 823 K.[99] The products from the pre-re-former can be heated to temperatures up to 1073 K, reducing the risk of carbon formation from thermal cracking of the fuel before it reaches the re-forming catalyst bed.[100] Carbon formation is the most critical parameter for selecting operating conditions for pre-re-forming. The steam-to-carbon ratio and operating temperatures depend on the feedstock. Heavier feeds require higher steam-to-carbon ratio and higher operating temperature[101] (Table 2). The pre-re-forming catalyst is especially prone to carbon deactivation due to the low operating temperature. Specially precipitated high nickel-loaded catalysts (Ni = 20−30 wt %) with supports with alkaline properties (MgO = 60−70 wt %) and high surface area are used in the pre-re-forming process. Catalysts based on noble metals have also been used for the pre-re-forming of heavy hydrocarbon feeds such as kerosene and diesel.[101] The low operating temperature also requires catalysts with high resistance to sulfur poisoning. Sulfur poisoning on Ni catalysts varies with temperature, the effect of sulfur poisoning being more important at lower temperatures.[76] Taking into account the difficulty involved in removing the organic S compounds present in fuels (derivatives of dibenzothiophene) through the conventional hydrodesulfurization process, sulfur must be removed using deep hydrodesulfurization with novel hydrotreating catalysts or by deep adsorptive desulfurization.[78]

2.1.2.6. Steam Re-forming in Supercritical Water. A novel noncatalytic re-forming process using supercritical water has been described.[102] In this process, supercritical water works both as a highly energized re-forming agent and as an extraordinary solvent. The process has been tested for a number of hydrocarbon fuels including diesel and jet fuel. The original efforts were targeted at converting JP-8 fuel into hydrogen that could be used directly in PEM fuel cells, and preliminary results show that there is excellent potential for this process in more generally applicable on-site produc-

Table 3. Selectivity Data Obtained in Supercritical Water Re-forming of JP-8 Fuel[a]

pressure (MPa)	T (K)	water flow rate (g/min)	JP-8 flow rate (g/min)	product gas composition (mol %)					
				H_2	C_2H_4	CO	CO_2	CH_4	C_2H_6
32.9	909	20.0	2.4	5.4	2.0	2.0	64.4	20.9	0.7
23.9	978	20.7	0.3	37.3	17.1	8.0	30.0	2.3	0.0

[a] Adapted from Lee et al.[102]

tion of hydrogen from a variety of hydrocarbon and oxygenate feedstocks. In the supercritical region, water is an excellent solvent for oxygen and hydrocarbons, excluding hydrogen.[103,104] As a consequence of this high solubility the re-forming reactions are homogeneous, and hence no catalyst is required. Thus, hydrocarbon molecules are directly re-formed by water according to eq 1.

In the supercritical water re-formation process there is virtually no equilibrium limitation due to the insolubility of hydrogen, which maintains hydrogen concentration in the reaction mixture below the ultimate chemical equilibrium of the reaction. The large amounts of CO produced according to eq 1 are further converted to additional hydrogen via the water gas shift reaction. A side reaction that takes place simultaneously in the re-formation process, regardless of being supercritical or not, is the pyrolysis of hydrocarbon (eq 9):

$$C_xH_y \rightarrow C_aH_b + C_cH_d \quad (x = a + c; y = b + d) \quad (9)$$

This pyrolysis reaction is largely responsible for the formation of lighter hydrocarbons such as methane, ethane, and ethylene. It is irreversible under the reaction conditions and operates over a wide range of temperatures. As a result of repeated pyrolytic fragmentation, the resulting fragments become favorable for coking[103] via cyclization processes. All hydrocarbons present in the diesel boiling range fraction and also polycyclic aromatic hydrocarbons of low polyaromaticity (number of cycles below 4) are completely soluble in supercritical water, thus allowing chemical reactions before coking takes place.

Supercritical water re-forming of JP-8 fuel at 909 K and 32.9 MPa yields a very low proportion of carbon oxides (CO + CO_2 = 4.0 mol %) and H_2 (5.4 mol %), whereas methane (64.4 mol %) and ethane (30.8 mol %) are the major reaction products. The lack of re-forming products shows that the temperature is too low to re-form the hydrocarbons present in the JP-8 fraction into a syngas mixture. In contrast, a product gas composition containing up to 37.3 mol % is obtained by supercritical water re-forming at 978 K and 23.9 MPa overall pressure. The reaction conditions and product selectivity employed in both cases are summarized in Table 3. It is likely that higher H_2 yields can be achieved at somewhat higher temperature, although the experimental process device does not allow 978 K to be surpassed.[102]

2.1.3. Methanol

Methanol is industrially produced under high temperature and high pressure (523−573 K, 80−100 bar), using a copper−zinc-based oxide catalyst developed by Imperial Chemical Industries Co. Methanol can be converted to a H_2-rich gas mixture by chemical or chemical−physical methods. In the next section, the steam re-forming reaction is examined. Because decomposition of methanol in the absence of oxidant usually takes place, this reaction is first considered.

2.1.3.1. Methanol Decomposition. Methanol decomposition (eq 10) is an on-site source of H_2 and CO for chemical processes and fuel cells.

$$CH_3OH \rightarrow CO + 2H_2 \quad \Delta H^\circ_{298K} = +90.1 \text{ kJ/mol} \quad (10)$$

The reaction is endothermic and can be performed on metals; group 10 and 11 metals of the periodic table are active for this reaction, among which Ni and Pd have been the most widely studied. These metals have been supported on different oxide substrates such as Al_2O_3, TiO_2, SiO_2, CeO_2, ZrO_2, and Pr_2O_3.[105−116] Palladium seems to be the most effective for methanol decomposition and, in the case of Pd supported on CeO_2, it has been observed that the decomposition reaction of methanol on Pd catalysts depends on the metal crystallite size.[116] Usami et al.[106] tested a number of metal oxide-supported Pd catalysts and found that Pd/CeO_2, Pd/Pr_2O_3, and Pd/ZrO_2 catalysts prepared by a coprecipitation procedure were active for the selective decomposition of methanol at temperatures below 523 K. TOF values showed that CeO_2 and Pr_2O_3 systems are better candidates than ZrO_2 for supporting palladium. As CeO_2 and Pr_2O_3 substrates are slightly reduced during activation, a strong metal−support interaction is developed, and as a consequence the C−O bond cleavage of CH_3OH becomes inhibited while the decomposition reaction into CO and H_2 prevails. Additionally, it was observed that the interaction of Pd and the support influences the performance of catalysts, in which smaller metal particles[106] and a stronger contact with the support are favorable for the decomposition reaction. For high metal loadings, a coprecipitation method is preferred in comparison with the impregnation procedure, which produces larger particles and lower interaction with the support. In carbon-supported platinum catalysts, the mechanism of CO adsorption has been shown to depend on the structure,[117] and the effect of the particle size has been reported as well when other supported transition metals, such as iron and/or copper, are tested in the methanol decomposition reaction.[118]

In addition, La_2O_3 is a particularly attractive support because it allows high selectivity and specific activity in the methanol synthesis reaction. La_2O_3-modified palladium catalysts have been reported to be very active for the synthesis of methanol from (CO + H_2) mixtures.[119] As the reverse reaction of methanol synthesis from (CO + H_2) gas mixtures, the methanol decomposition reaction was also tested over a series of Pd/SiO_2 catalysts promoted with lanthanum oxide.[120] In keeping with these ideas, La-modified Pd/CeO_2 catalysts were prepared and tested in the reaction of methanol decomposition.[121] The addition of La_2O_3 to a 2% Pd/CeO_2 catalyst significantly improved the catalytic behavior, and a complete conversion of methanol can be achieved at around 548 K, which in turn is nearly 40 K lower than the temperature required for the 2% Pd/CeO_2 catalyst. The TPR profiles reveal that the presence of La_2O_3 shifts the reduction temperature of CeO_2 to lower values, while at the same time hindering the reduction of PdO crystallites due to an accelerated diffusion of oxygen at the La_2O_3−CeO_2 interface. A different effect has been found when noble metals are used as promoters of supported Pd catalysts. Kapoor et al.[122] found that 3% gold loading in a 4% Pd/CeO_2 catalyst increases the conversion at 453 K from 20 to 40%. This effect is associated with the formation of the new

active sites in Au−Pd bimetallic clusters, where both Au and Pd are involved in the reaction mechanism.

2.1.3.2. Methanol Steam Re-forming. Currently, increasing attention is being paid to the low-temperature steam re-forming of methanol to produce high-purity hydrogen to be used as a fuel for on-board power generation in fuel cell vehicles.[123] The importance of methanol as a chemical carrier for hydrogen lies mainly in its ready availability, high-energy density, and easy storage and transportation. Among the reactions to be used for the production of hydrogen from methanol, the most widely applied one is the steam re-forming reaction (eq 11):

$$CH_3OH + H_2O \rightarrow CO_2 + 3H_2 \quad \Delta H^\circ_{298K} = +49.4 \text{ kJ/mol} \tag{11}$$

A large variety of catalysts for steam re-forming of methanol including copper in their composition have been reported.[124−131] Commercial Cu/ZnO water gas shift and methanol synthesis catalysts[127,128] have been found to be active for the steam re-forming reaction. Shimokawabe et al.[129] have also described that highly active Cu/ZrO_2 can be prepared by impregnation of a ZrO_2 substrate with aqueous solutions of the $[Cu(NH_3)_4](NO_3)_2]$ complex, which proves to be more active than the corresponding Cu/SiO_2 catalysts. This particular interest of ZrO_2 as a substrate for the copper phases has led to the study of highly active Cu/ZrO_2 catalysts that have been prepared according to a variety of different methods, including impregnation of copper salts onto the ZrO_2 support,[132−134] precipitation of copper,[132−137] formation of amorphous aerogels,[138,139] microemulsion technique,[140] and CuZr alloys.[141] The central idea in all of these works is to maintain the zirconia support in the amorphous state under the calcination and reaction conditions in order to retain a high level of activity. The major drawback when zirconia crystallization is produced consists in the drop in both copper surface area and support specific surface. Additionally, a high copper−zirconia interfacial area must be maintained to prevent catalyst deactivation. Tetragonal zirconia can be stabilized by incorporation of aluminum, yttrium, and lanthanum oxides,[142] thus preventing, or at least minimizing, its crystallization.

Breen and Ross[143] found that $Cu/ZnO/ZrO_2$ catalysts are active at temperatures as low as 443 K but that they deactivate severely at temperatures above 590 K. However, deactivation is inhibited upon incorporation of Al_2O_3. As stated above, the deactivation may be explained by considering the transformation of amorphous zirconia into a crystalline metastable tetragonal ZrO_2 phase. It has been shown that the temperature of crystallization of zirconia is reduced to a large extent in the presence of steam,[142] which accelerates crystal growth. The improvement of catalyst stability brought about by Al_2O_3 incorporation comes from the increase in the temperature of crystallization of ZrO_2, which remains amorphous at the reaction temperature. Furthermore, the incorporation of alumina increases both the copper and BET surface areas, increasing also the catalyst's activity.

2.2. Catalytic Partial Oxidation

As stated above, steam re-forming is currently the most important industrial and economic process for the production of hydrogen from hydrocarbons. Nevertheless, steam re-forming is a very energy-intensive process, in which overheated steam in a H_2O/HC molar ratio slightly higher than stoichiometric value is used to avoid carbon deposition. In this context, new processes for the production of H_2 from hydrocarbons, at lower energy costs, are needed. The partial oxidation processes (PO) are attractive alternatives because they avoid the need for large amounts of expensive superheated steam. Partial oxidation technology, like steam re-forming, has a long history but attracted much less atention because supported metal catalysts rapidly become deactivated under typical reaction temperatures of about 950 K. After an intensive research period during the 1980s, when the oxidative coupling of methane (OCM) was considered to be the future of natural gas conversion, several research groups noted that, under similar reaction conditions, some catalytic systems yielded large amounts of hydrogen, with no catalyst deactivation.[45] Since then, intensive work has been developed to address the mechanism of the reaction and the parameters necessary for obtaining a stable catalyst.

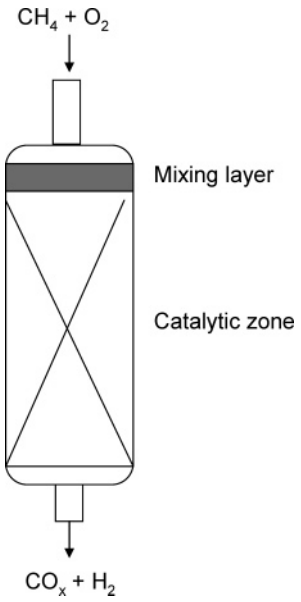

Figure 7. Illustration of the catalytic partial oxidation principle.

2.2.1. Methane

2.2.1.1. Reaction and Mechanisms. Partial oxidation of methane (POM) to synthesis gas is represented by eq 12:

$$CH_4 + {}^1/_2O_2 \rightarrow CO + 2H_2 \quad \Delta H^\circ_{298K} = -35.6 \text{ kJ/mol} \tag{12}$$

The principle of catalytic partial oxidation is illustrated in Figure 7. The POM reaction has been known from the 1990s, as described by York et al. in a recent review.[144] Although great efforts have been made, the industrial application of POM is still limited, mainly owing to the requirement of an oxygen plant,[145,146] and as yet no clearly stable supported metal catalyst is available. This is a mildly exothermic reaction, and hence no external heating energy is required. Equilibrium calculations for the POM reaction revealed an increase in both conversion and $CO + H_2$ selectivity with increasing temperature. In this sense, at atmospheric pressure and 1073 K, the equilibrium predicts a methane conversion of higher than 90% and selectivity of close to 100% (Figure 8). According to stoichiometry of the reaction, the increase of pressure has a detrimental effect on the conversion.

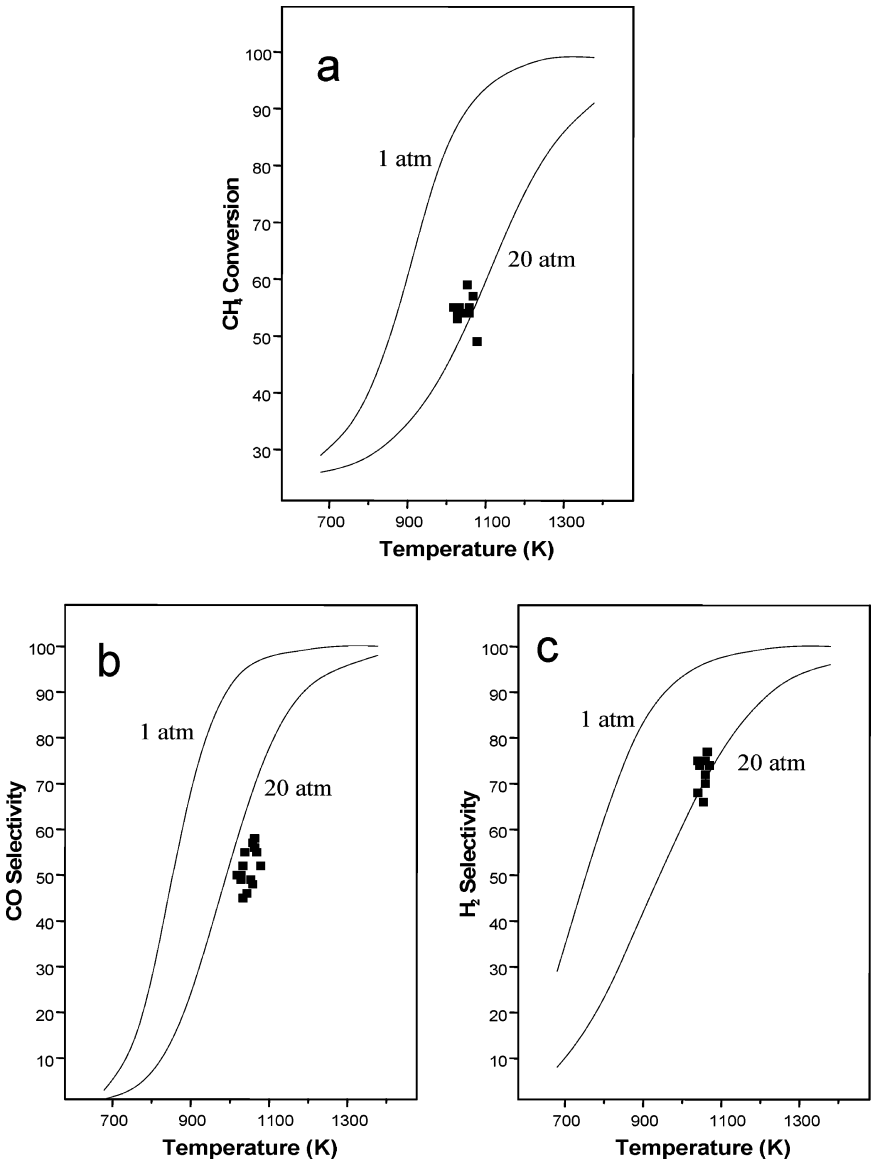

Figure 8. Methane partial oxidation equilibrium: calculated CH_4 conversion (a), CO selectivity (b), and H_2 selectivity (c) at pressures of 1 and 20 atm for a 2:1 CH_4:O_2 molar feed. Symbols indicate experimental results using a Ni/Al_2O_3 catalyst. Reprinted with permission from ref 4. Copyright 2005 Imperial College Press.

The active catalysts for POM are very similar to the supported metals used in SRM. They all are metals from groups 8, 9, and 10 (Ni, Co, Fe, Ru, Rh, Pd, Ir, Pt), among which supported nickel, cobalt, and noble metal catalysts (Ru, Rh, Pt) have been the systems most studied. Pyrochlore oxides ($Ln_2Ru_2O_7$[45]), perovskite oxides ($LaNiO_3$,[147] $LaNi_xFe_{1-x}O_3$[148]), and hydrotalcite type materials (Ni−Mg−Al hydrotalcites[149−151]) are other systems that have been used as catalyst precursors for POM reactions.

Two mechanisms have been proposed for the POM reaction: (i) the combustion and re-forming reactions mechanism (CRR)[152] and (ii) the direct partial oxidation (DPO) mechanism.[153−155] In CRR, the methane is combusted in the first part of the catalytic bed, producing CO_2 and H_2O. Along the rest of the bed, and after total oxygen conversion, the remaining methane is converted to CO + H_2 by SMR and CO_2 re-forming reactions. In DPO a CO + H_2 mixture is produced directly from methane by recombination of CH_x and O species at the surface of the catalysts.

Dissanayake et al.[152] validated the CRR mechanism in a Ni/Al_2O_3 catalyst, obtaining an almost complete conversion of methane at temperatures higher than 973 K, with a selectivity to CO + H_2 of nearly 95%. Analysis of the different phases present in the catalytic bed leads to the conclusion that it is divided into three regions: the first, in contact with the CH_4/O_2 reacting mixture, is a $NiAl_2O_4$ spinel, of moderate activity for methane combustion; the second part is NiO/Al_2O_3, of high activity for methane combustion and where the total conversion of oxygen occurs; and, finally, the rest of the catalytic bed consists of Ni/Al_2O_3, which is active for SRM and CO_2 re-forming. The distribution of these different regions is temperature-dependent and is the reason for the observed changes in the behavior of the catalyst, which is activated in the presence of the reactive mixture at 1023 K, maintains different degrees of activity when the temperature decreases to 773 K, and deactivates at lower temperatures (Figure 9).

Besides these results confirming the CRR mechanism, the DPO mechanism is operative in other systems. Hickman and Schimdt[153−155] found that the oxidation reaction of methane could be achieved in Pt and Rh monoliths under adiabatic conditions at very short residence times. In this

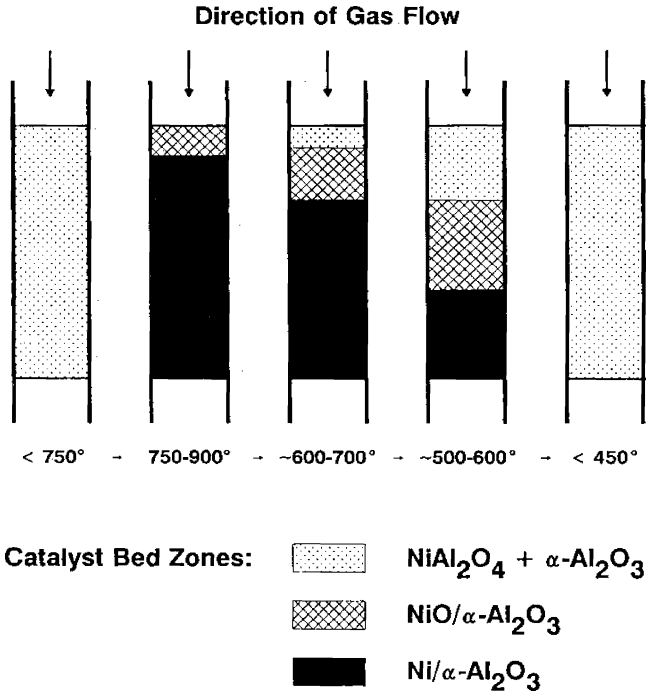

Figure 9. Schematic representation of Ni/Al_2O_3 catalyst bed composition during catalytic partial oxidation of methane at various temperatures. Reprinted with permission from ref 152. Copyright 1991 Elsevier B.V.

proposed mechanism, the CO + H_2 gas is produced as primary product:

$$CH_4 \rightarrow C(ads) + 4H(ads) \quad (13a)$$

$$C(ads) + [O]s \rightarrow CO\ (ads) \rightarrow CO \quad (13b)$$

$$2H(ads) \rightarrow H_2 \quad (13c)$$

The reaction intermediates formed on the surface of the catalysts, and the way in which they participate in the reaction mechanism, are different, depending on the active metal, the support, and their interaction. Li et al.[156] have followed the surface state of Ni/Al_2O_3 by a transient response technique; they concluded that if oxygen is the most abundant surface intermediate, the catalyst is not activr and that a catalyst in the reduced state, covered by adsorbed carbon, is essential for the activation of the reactants. This reduced state of the metal surface as a condition for the activation of the reactants has also been observed in Rh/Al_2O_3 in TAP experiments,[157] because CH_4 is adsorbed dissociatively on the metal and the pre-adsorbed oxygen reduces this activation. Moreover, the degree of oxygen coverage changes the mechanism of reaction: from DPO at low oxygen coverage to CRR at high oxygen coverage.

2.2.1.2. Catalyst Deactivation and Promoter Effects. Because several supported catalytic systems have high activity for the POM reaction, the main topic of research is the stability of the catalysts. There are three main processes for the deactivation of the catalyst: carbon deposition, sintering of metal crystallites, and oxidation of metal atoms by oxygen or steam. Carbon deposition is due to the process of decomposition of CH_4 (eq 5) and CO (eq 4). Two different kinds of carbon can be formed on the surface of the catalyst: encapsulated carbon, which covers the metal particle and is the reason for physical−chemical deactivation; and whiskers of carbon, which do not deactivate the particle directly but may produce mechanical plugging of the reactor.

The catalysts are promoted to reduce the extent of carbon formation. The improvement of the catalyst's stability can be achieved using an appropiate support. In the design of catalysts for re-forming reactions, the influence of the support has been one of the issues most investigated. Tsipouriari et al.[158] compared Ni/Al_2O_3 with Ni/La_2O_3 and found that in the former system the deposition of carbon increases with the time on stream. In the lanthana-supported catalyst, carbon is also accumulated, but this carbon deposited on the surface is constant and does not increase with time. The same effect is detected on magnesia-supported catalysts due to the formation of a $Mg_{1-x}Ni_xO$ solid solution.[159] In contrast, the use of ZrO_2 as a support is not effective, because metal particles become rapidly sintered due to the low $Ni-ZrO_2$ surface interaction. The effect of the support has been also investigated in other metals, and the tendencies are not the same in all cases. Bitter et al.[160] found that the trend in stability on supported platinum follows the order ZrO_2 > TiO_2 > Al_2O_3. This trend is different in supported nickel, Al_2O_3-supported nickel being more stable than the corresponding TiO_2-supported catalyst.[161] In the case of Pt, there is no evidence of sintering, and deactivation is produced by blockage of the active centers by carbon. The support, in this case, plays a very active role for the reducible oxides (e.g., TiO_2). In the Pt/TiO_2 system, it is well-established that small TiO_x moieties decorate the metal particles[162] and may so allow the reaction of coke fomation to occur close to the metal, affecting adversely the reaction on the metal. Also, some differences are found in supported Ir catalysts, with an activity trend for the POM in the order TiO_2 > ZrO_2 > Y_2O_3 > MgO > Al_2O_3 > SiO_2.[163] In these systems, SRM does not change with the support, and the trends for POM and CO_2 re-forming are the same. Therefore, a CRR mechanism can be concluded for these catalysts. On the Rh/Al_2O_3[157] system, water is adsorbed on the alumina surface, which plays the role of the oxygen source in the POM reaction. Also, in Ni and Ru supported in Al_2O_3, a similar effect is produced, due to the formation of hydroxyl groups at the surface of Al_2O_3 that provide oxygen to the active metal sites. In contrast, when these metals are supported on SiO_2, the support does not participate in the reaction mechanism.

Improvements in catalyst stability can be achieved not only by the use of an appropriate support but also by doping the catalyst with other metals. In Ni/Al_2O_3, a beneficial effect of the addition of noble metals (Pt, Pd, Ru) has been described.[164] Nichio et al.[165] promoted Ni/Al_2O_3 by adding a tin organometallic complex to the catalyst in the reduced state (metallic Ni). This procedure allows the collection of bimetallic Sn−Ni systems with a good interaction between metals and, at concentrations of Sn in the 0.01−0.05% range (Sn/Ni^{surf} < 0.5), the deposition of carbon upon reaction decreases with no appreciable change in the catalytic activity. The Sn causes breaking of the Ni ensembles, active for carbon deposition (this is a structure-sensitive reaction),[165] but is not enough to affect the active sites for POM. The most typical way to promote nickel catalysts is by the use of alkaline and alkaline earth metals. Chang et al.[166] explained the promotion with K and Ca of a Ni/NaZSM-5 zeolite by the formation of carbonaceous species, produced by the interaction of CO_2 with the promoters. In isotopic effect experiments, they also observed that the activation of CH_4

at the nickel surface is not the rate-determining step in the DPO mechanism. The rate is determined by the reaction of $O_{ads} + C_{ads}$, as previously shown by Schuurman et al.[60] in Al_2O_3- and SiO_2-supported Ni catalysts. The reduction of carbon deposition has been also successfully achieved in Ni/γ-Al_2O_3 catalysts promoted with Li and La.[167−169]

2.2.2. Liquid Hydrocarbons

2.2.2.1. Reaction and Mechanisms. In recent years, the catalytic partial oxidation of high hydrocarbons employing very short reaction times (milliseconds) and high temperatures (1123−1273 K) over noble metals supported on porous ceramic monoliths has been the subject of much research.[154,155,170] Catalytic partial oxidation of hydrocarbons is described by the idealized eq 14.

$$C_nH_m + {}^{n}/_{2}O_2 \rightarrow nCO + {}^{m}/_{2}H_2 \quad (14)$$

The oxygen-to-fuel ratio (n) determines the heat of reaction and the hydrogen yield. The direct catalytic partial oxidation reaction is much faster than the corresponding catalytic steam re-forming reaction by roughly 2 orders of magnitude, but the H_2 yield per carbon in the fuel is lower. Despite the simplicity of eq 14, the catalytic partial oxidation of liquid fuels is a complicated process in terms of the number of catalytic reactions involved. Partial oxidation commonly includes total oxidation, steam re-forming, CO_2 re-forming, hydrocarbon cracking, methanation, and water gas shift. No detailed mechanism of hydrogen production from higher hydrocarbons has yet been established. A basic scheme[171] assumes that the reaction is initiated near the catalyst entrance by complete dissociation of hydrocarbons due to multiple dehydrogenation and C−C cleavage reactions. This is followed by reaction of the absorbed oxygen with carbon and hydrogen to form CO, CO_2, and H_2O, which desorb along with H_2. Aromatics tend to be less reactive than *n*-alkanes in partial oxidation reactions.[171] They are strongly adsorbed to the metal sites, causing kinetic inhibition, and are also more prone to carbon formation than paraffins and cycloparafins.[172] The complexity of the process and the nature of liquid fuels, with hundreds of different components, have produced slow development at the industrial scale, the process still being in the exploratory stage.

2.2.2.2. Catalyst Deactivation and Promoter Effects. There are relatively few experimental studies on the catalytic partial oxidation of liquid fuels. Results on catalytic partial oxidation of *n*-hexane,[173] *n*-heptane,[174] *n*-octane,[175] isooctane,[171,173] and mixtures simulating liquid fuels have shown that deactivation by both sulfur and carbon deposition are key challenges to the use of catalytic partial oxidation. Catalysts for partial oxidation of liquid fuels have been primarily based on nickel,[175] platinum,[175,176] rhodium,[173,176,177] and bimetallics.[176] Direct comparison among these catalysts is reported in only a few cases, rhodium generally being the most active and the most selective to hydrogen.[173,176] The advantage of rhodium is attributed to a lower tendency of surface H atoms to become oxidized to surface hydroxyl radicals, leading to the formation of water. As a result, desorption of the H atoms as H_2 molecules is the favored process on rhodium. A recent work[178] has reported the use of oxygen-ion conducting systems as supports of noble metals applied to partial oxidation of diesel fuels. The study shows that ceria and zirconia were found to be effective in minimizing carbon deposition, a mixed ceria−zirconia support being superior to either. The authors attributed this behavior to a temperature-dependent mechanism involving the dissociative adsorption of oxygen on the metal following its spillover to the support.

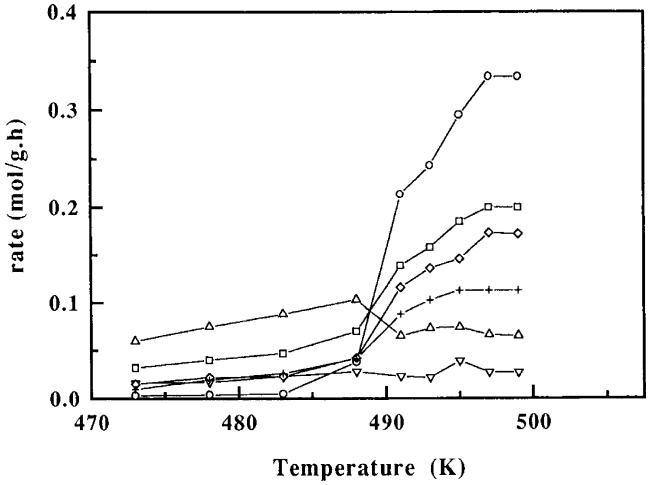

Figure 10. Partial oxidation of methanol over the catalyst $Cu_{40}Zn_{60}$: (□) CH_3OH conversion; (+) O_2 conversion; (○) H_2; (◇) CO_2; (△) H_2O; (▽) CO. Reprinted with permission from ref 179. Copyright 1997 Elsevier B.V.

2.2.3. Methanol

Among the different methods employed to produce hydrogen from methanol (decomposition, steam re-forming, and partial oxidation), selective production of H_2 by partial oxidation has some obvious advantages, because it is an exothermic reaction and a higher reaction rate is expected, which shortens the reaction time to reach the working temperature from the cold start-up conditions. In this section, catalysts and promoters employed and the reaction mechanism are examined.

2.2.3.1. Copper−Zinc Catalysts. Copper−zinc catalysts have been found to be very active for the partial oxidation of methanol[179] (eq 15):

$$CH_3OH + {}^{1}/_{2}O_2 \rightarrow CO_2 + 2H_2 \qquad \Delta H^{\circ}_{298K} = -192.2 \text{ kJ/mol} \quad (15)$$

The partial oxidation reaction starts at temperatures as low as 488 K, and the rates of methanol and oxygen conversion increase strongly with temperature to selectively produce H_2 and CO_2 (Figure 10). The rate of CO formation is very low across the temperature range explored (473−498 K), and H_2O formation decreases for temperatures above 488 K. As a general rule, methanol conversion to H_2 and CO_2 increases with copper content, reaching a maximum with $Cu_{40}Zn_{60}$ catalysts (40:60 atomic percentage) and decreasing for higher copper loadings. The $Cu_{40}Zn_{60}$ catalyst with the highest copper metal area has been found to be the most active and selective for the partial oxidation of methanol. Unreduced copper−zinc oxide catalysts display very low activity, mainly producing CO_2 and H_2O and only traces of H_2, although the catalysts become eventually reduced under reaction conditions at high temperatures. From the reaction rates and copper areas, turnover frequency (TOF) values have been calculated as a function of copper content at constant temperature (497 K). It was observed that both the apparent activation energy (E_a) and the TOF were higher for the low copper content catalysts and then decreased slightly, tending to constant

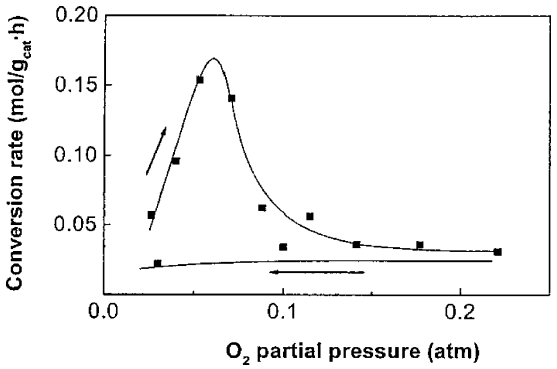

Figure 11. Effect of O_2 partial pressure on CH_3OH conversion in the reaction with the $Cu_{40}Zn_{60}$ catalyst at 488 K. Reprinted with permission from ref 182. Copyright 2003 Springer.

value at Cu loadings above 50% (atomic). The simultaneous variation of E_a and TOF suggests that the enhancement in reactivity would be a consequence of a change in the nature of the active sites rather than induced by a simple spillover type synergy. Activity data for the methanol partial oxidation reaction to hydrogen and carbon dioxide over Cu/ZnO catalysts obtained with different catalyst compositions and different Cu^0 metal surface areas have shown that the reaction depends on the presence of both phases: ZnO and Cu^0. Additionally, Wang et al.[180] found that the presence of ZnO in silica-supported Cu catalysts allows a higher dispersion of metallic copper, although a high concentration of zinc gives Cu_2O crystallites. On the other hand, for Cu−Zn catalysts, with Cu concentrations in the 40−60 wt % range, the copper metal surface area seems to be the main factor determining the reaction rate.[181]

The O_2/CH_3OH molar ratio in the feed has a strong influence on catalyst performance. As illustrated in Figure 11, CH_3OH conversion rates and H_2 and CO_2 selectivities increase almost linearly for O_2 partial pressures in the range of 0.026−0.055 bar (O_2/CH_3OH ratios = 0.03−0.063).[182] A further increase in O_2 partial pressure leads to a sharp drop in CH_3OH conversion and an almost complete inhibition of H_2 formation, with the simultaneous production of H_2O and CO_2. When lower O_2 partial pressures are returned to, the conversion and selectivity to H_2 and CO_2 remain constant and at very low values, producing a hysteresis curve. As revealed by X-ray diffraction patterns, a thick layer of copper oxide grows on the surface of copper crystallites when exposed to O_2 pressures above 0.055 bar. Thus, it is inferred that Cu^+ sites appear to be responsible for the partial oxidation reaction of methanol. Cu^0 metal has low reactivity to methanol, and activity is optimized at intermediate surface coverages by oxygen.

TPD experiments with pure Cu^0, pure ZnO, and the Cu/ZnO catalyst show that methanol can be activated by both ZnO and copper.[182] On the ZnO surface, methanol may form intermediates, which in the presence of copper might react and desorb more easily, probably via a reverse spillover process. Isotopic product distribution of H_2, HD, D_2, H_2O, HDO, and D_2O in the temperature-programmed reaction of CH_3OD shows a slight enrichment in products with H, suggesting that during methanol activation on the ZnO some of the D atoms might be retained by the support.[182] CH_3OH activation via O−H bond cleavage occurs easily on group 8, 9, and 10 metals at temperatures as low as 100−200 K.[183] Nevertheless, CH_3OH bond activation on copper catalysts requires higher temperatures or the presence of oxygen atoms on the copper surface. It has been proposed that the basic character of O_{ads} atoms on copper surfaces would facilitate H-transfer from the O−H bond to form a surface methoxy intermediate.[184] The kinetic isotope effect (k_H/k_D = 1.5) observed for CH_3OH conversion[182] can be related to this H-transfer, suggesting that during the CH_3OH oxidation O−H bond cleavage is at least partially involved in the rate-determining step, especially for the water yield with an isotopic effect of k_H/k_D = 2.0. However, for H_2 formation (k_H/k_D = 0.9), the rate-determining step is related to C−H bond activation, because the C−O bond does not break during the reaction (no CH_4 formation is observed). These kinetic results obtained for the partial oxidation reaction on Cu/ZnO catalysts are in agreement with the data found for the decomposition and steam re-forming reactions of methanol. For these reactions, it has been suggested that a methoxide species would be rapidly formed and that the rate-determining step would be the cleavage of the C−H bond to form the H_2CO species.[181,182,184−190]

It has been suggested that oxygen atoms participate in methanol activation through the abstraction of the hydroxyl H atom to form methoxide and OH_{surf}. This OH_{surf} species rapidly loses H to the surface, regenerating the O surface species.[182] Although all of these reactions occur on the copper surface, ZnO also plays some role in the reaction. The results of TPD experiments carried out after the pre-adsorption of the O_2/CH_3OH mixture on pure ZnO are conclusive in the sense that CH_3OH is partly converted into H_2, CO, CO_2, and H_2CO.[182] Of the two peaks observed in the TPD profiles, the one at low temperature (573 K) for H_2 and CO_2 suggests the participation of bulk oxygen, whereas that seen at a slightly higher temperature (590 K) is related to the formation of H_2CO. As stated above, the Cu metal area determines the reaction rate, but the combination of copper with a certain amount of ZnO seems to be of fundamental importance for the partial oxidation reaction. Thus, ZnO might also participate in methanol activation and, through a reverse spillover effect, transfer species to the metallic surface for further reaction.

The incorporation of small amounts of Al_2O_3 (up to 15% Al at.) to the Cu/ZnO system results in lower activity, indicating that aluminum has an inhibiting effect on the partial oxidation of methanol.[177] For the $Cu_{40}Zn_{55}Al_5$ catalyst, this inhibition is clear at lower temperatures, although the activity approaches that of the Al-free $Cu_{40}Zn_{60}$ counterpart at temperatures close to 500 K. Other catalysts with higher Al loadings ($Cu_{40}Zn_{50}Al_{10}$ and $Cu_{40}Zn_{45}Al_{15}$) do not show significant activity in the temperature range studied.[177] In terms of stability, the behavior of $Cu_{40}Zn_{60}$ and $Cu_{40}Zn_{55}Al_5$ catalysts is very different: whereas the $Cu_{40}Zn_{60}$ catalyst loses 43% of activity, with a less marked drop in the selectivity of H_2 and CO_2, after 110 h of on-stream operation at 503 K, no significant deactivation is observed for the $Cu_{40}Zn_{55}Al_5$ catalyst. The addition of aluminum as Al_2O_3 to the Cu−ZnO favors the dispersion of the copper phase and improves catalyst stability by preventing the sintering of metal particles. This stabilization effect due to the presence of aluminum is, in this way, very similar to the one observed for the steam re-forming of methanol.[191]

For both binary Cu−ZnO and ternary Cu−ZnO(Al) systems, reduction pretreatments control the structural and morphological characteristics of the catalyst surface.[192] These initial characteristics play a central role in the evolution of the oxidation state and structural morphology during the

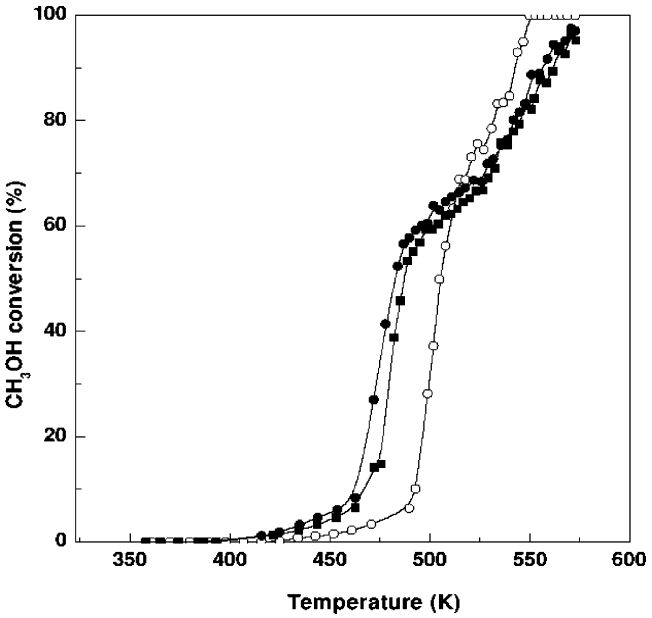

Figure 12. Temperature dependence of CH_3OH conversion during temperature-programmed start-up over the $Cu/ZnO/Al_2O_3$ catalyst in different initial states: (○) oxidized; (●) reduced; (■) reduced + air exposed. Atmospheric pressure, feed ratio $O_2/CH_3OH = 0.3$, heating rate = 0.1 K/min. Reprinted with permission from ref 192. Copyright 2002 Elsevier B.V.

reaction, because the dynamic behavior of the catalyst surface is determined by the conditions of the gas atmosphere during the reaction. The temperature dependence of CH_3OH conversion on a $Cu_{55}Zn_{40}Al_5$ catalyst in its oxidized, reduced, and air-exposed pre-reduced states during the partial oxidation reaction in an $O_2/CH_3OH = 0.3$ (molar) mixture is shown in Figure 12.[192] All conversion profiles display a sigmoidal-like shape, with a marked increase in CH_3OH conversion within a narrow temperature range. The reaction starts at 416 K on the reduced sample, whereas this point shifts to 422 and 434 K in the air-exposed and oxidized samples, respectively. Conversely, however, product selectivity is the same in all cases. For a CH_3OH conversion of around 0.6, where oxygen is completely consumed, the slope of the curves changes as a consequence of the overlapping of the decomposition reaction. From the data in Figure 11 it is clear that the oxidized sample becomes reduced during the partial oxidation reaction, and this reduction process leads to surface reconstruction with a higher CH_3OH decomposition capacity than that of the pre-reduced counterparts. These differences are related to changes in the number, but not the characteristics, of the active sites induced by the different reduction potentials of the reacting gases.

2.2.3.2. Palladium Catalysts. Group 10 metals, and more specifically palladium, are highly active in the partial oxidation reaction.[193,194] High yields to H_2 have been obtained on pre-reduced Pd/ZnO catalyst under O_2/CH_3OH feed ratios of 0.3 and 0.5. For the 1 wt % Pd/ZnO catalyst, CH_3OH conversion reaches 40−80% within the 503−543 K temperature range. Upon increase of the reaction temperature, CH_3OH conversion increases, with a simultaneous increase in H_2 selectivity at the expense of water. Because the oxygen is completely consumed, this selectivity trend suggests some contribution of the methanol steam re-forming produced by the water byproduct. Important structural changes take place at the Pd−ZnO interface during on-stream operation. With X-ray diffraction, temperature-programmed reduction, and X-ray photoelectron spectroscopy techniques, a PdZn alloyed phase was seen.[193,195] The formation of this alloy has been also detected in used Pd/ZnO catalysts prepared according to different methods (microemulsion and impregnation)[196] and in Pd/ZnO catalysts used in the steam re-forming of methanol.[197] The reactivity of the PdZn alloy is somewhat different from that of small Pd clusters, as illustrated by the behavior of a 5 wt % Pd/ZnO catalyst, which exhibited fairly high selectivity to HCHO and CO and where PdZn alloy is formed to a larger extent than in 1 wt % Pd catalyst. It is likely that processes such as CH_3OH decomposition, the inability to oxidize the intermediate HCHO, and the low oxidation rate of CO would be involved in large PdZn alloy particles, whereas the H_2 selectivity is favored in small Pd and PdZn alloy clusters. Pd/ZnO catalysts prepared by the microemulsion method also show higher CO yield when Pd particle size is larger.[196]

The nature of the support to a large extent determines the performance of supported catalysts. Thus, the 1 wt % Pd/ZrO_2 catalyst exhibits not only oxidation products (H_2 and CO_2), as happens on the parent Cu−ZnO catalysts, but also the decomposition reaction seems to occur to a greater extent.[194]

2.3. Autothermal Re-forming

Hydrogen production using autothermal reforming (ATR) has recently attracted considerable attention due to its high energy efficiency with low investment cost due to its simple system design. The ATR process has been used to produce hydrogen- and carbon monoxide-rich synthesis gas for decades. In ATR the heat for the re-forming reactions is supplied by internal combustion. Consequently, there is no need to supply heat to the reactor over and above the amount provided in the preheating of the reactants. The overall chemical reactions taking place in the ATR include partial oxidation (eq 14), steam re-forming (eq 1), and water gas shift (eq 2).

The main advantages of the use of the autothermal process with respect to the steam re-forming process are related to economics of scale; much larger single-stream units are possible with adiabatic ATR than with steam re-forming, and the size of equipment is smaller, because ATRs are very compact units compared to steam re-formers. Furthemore, re-former tube materials limit the outlet temperature from steam re-formers to a maximum of about 1223 K, whereas autothermal processes easily exceed 1273 K. This makes higher conversion of the feed possible, even at low steam-to-carbon ratios. The main disadvantage of ATR, especially with oxygen as oxidant, is that it requires an oxygen source. Oxygen plants are expensive, and the associated investments constitute the major part of the total investments.

2.3.1 Methane

The overall chemical reactions taking place in the ATR reactor are partial oxidation, steam re-forming, and water gas shift. The ATR reactor operates in three zones: (i) combustion zone, (ii) thermal zone, and (iii) catalytic zone (Figure 13). The combustion zone is a turbulent diffusion flame where CH_4 and oxygen are gradually mixed and combusted. Combustion in ATR is substoichiometric with an overall oxygen to hydrocarbon ratio of 0.55−0.60. Typically, the ATR operates at high temperatures of ca. 2200 K in the combustion zone. In the thermal zone above the catalyst bed further conversion occurs by homogeneous gas-

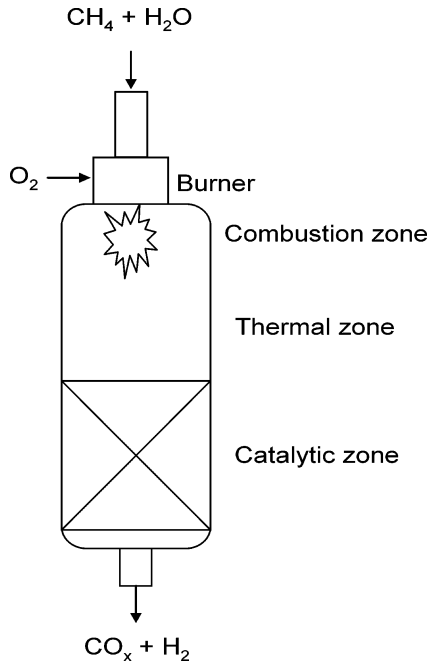

Figure 13. Illustration of an ATR reactor.

phase reactions. The main reactions in this zone are the homogeneous gas-phase steam methane re-forming and shift reaction. In the catalytic zone the final conversion of hydrocarbons takes place through heterogeneous catalytic reactions at 1200−1400 K including methane steam re-forming and shift reactions. The H_2/CO ratio at the outlet of the reactor can be precisely adjusted by varying the H_2O/CH_4 and/or O_2/CH_4 molar ratios in the feed.

As ATR is a combination of homogeneous partial oxidation with catalytic steam re-forming, the active catalysts used are the same as those for the steam process, namely, the group 8, 9, and 10 metals, especially Ni, Pt, Pd, Rh, Ru, and Ir. However, the high temperature of operation requires catalysts with a high thermal stability. The preferred catalyst for ATR is a low loaded nickel-based catalyst supported on alumina (α-Al_2O_3) and magnesium alumina spinel ($MgAl_2O_4$). Spinel has a higher melting point and in general a higher thermal strength and stability than the alumina-based catalyst. Recent studies[198] also propose the use of a temperature-stable support for nickel phases, consisting of a low surface area macroporous zirconia−haffnia carrier that shows excellent resistance to high-temperature treatments. Alternative catalyst formulations for methane ATR based on bimetallics have been studied because the activity of nickel catalysts can be increased by the addition of low contents of noble metals (Pt, Pd, Ir). These findings have stimulated the study of several bimetallic nickel catalysts. Ni−Pt bimetallic catalysts show higher activity during ATR than separate nickel and platinum catalysts blended in the same bed, although the real mechanism for this increase in activity is not clear. Explanations advanced includd (i) the increase in the reducibility of Ni due to the formation of an alloy or hydrogen spillover[199] and (ii) the increase in exposed Ni surface area under reaction conditions assisted by the noble metal.[200]

2.3.2. Liquid Hydrocarbons

As for methane, the overall reactions taking place in the ATR reactor include partial oxidation ($n = 1$ in eq 14), steam re-forming (eq 1), and water gas shift (eq 2). For liquid fuels, ATR conditions have been achieved using a re-former including a partial oxidation zone and a separate steam re-forming zone. The oxygen-to-carbon (O/C) and the steam-to-carbon (S/C) ratios determine the energy released or absorbed by the reaction and define the adiabatic temperature and consequently the concentration of H_2 in the fuel gas.[201] Higher H_2O/C ratios reduce the CO yield with lower equilibrium temperature.[202] In the ATR of diesel fuel, thermodynamic equilibrium can be achieved at a H_2O/C ratio of 1.25, an O_2/C ratio of 1, and an operating temperature of 973 K.

The operating conditions in ATR process require catalysts and supports with high resistance to thermally induced deactivation. Coking can be controlled with excess steam (and/or oxygen injection), whereas the low sulfur coverage on catalysts at the elevated temperatures of ATR makes desulfurization prior to ATR not necessary.

Noble metal catalysts (Pt, Rh, and Ru) modified with promoters with high oxygen storage capacity (CeO_2−ZrO_2, CeO_2, $CeGdO_2$) have exhibited excellent re-forming activity, with good thermal stability and sulfur tolerance in the ATR of liquid fuels.[203−209] In recent years, research into catalysts for the ATR of hydrocarbons has paid considerable attention to systems with a perovskite structure of general formula ABO_3.[210−212] Perovskite oxides (ABO_3) are strong candidates as precursors of re-forming catalysts due to the possibility of obtaining well-dispersed and stable active metal particles on a matrix composed of metal oxides that may allow the small particles of the metal to be stabilized in position B under the reaction conditions. Investigation into the application of non-precious group metal-based catalysts for ATR of high hydrocarbons has attracted some attention in the past few years. The use of group 6 metal carbides in re-forming a range of high hydrocarbons was successfully demonstrated.[212−214] In contrast with noble metal- and nickel-based catalysts, bulk molybdenum carbide shows stable performance in the ATR of higher hydrocarbons, such as gasoline and diesel, performed under much lower steam/carbon ratios.

2.3.3. Methanol

An even more appealing option than steam re-forming (eq 11) and partial oxidation (eq 15) is to combine these two reactions, providing the possibility of producing hydrogen under almost autothermal conditions (eq 16):[181,215−219]

$$CH_3OH + (1 - 2n)H_2O + nO_2 \rightarrow CO_2 + (3 - 2n)H_2 \quad (0 < n < 0.5) \quad (16)$$

Copper-based catalysts also display good performance in ATR. Agrell et al.,[219] using a Cu−ZnO catalyst, reported that, at differential O_2 conversions, water is produced by combustion of methanol. When oxygen conversion is complete, water production levels off and H_2 formation is initiated. Then, CH_3OH conversion and H_2 and CO selectivity increase, whereas water selectivity decreases. If ZrO_2 and Al_2O_3 are incorporated to the Cu−ZnO catalyst, the resulting catalyst exhibits the best performance for steam re-forming, although the light-off temperature for the partial oxidation reaction is lower for the Cu−Zn binary catalyst. CO formation over these ZrO_2-loaded Cu−ZnO catalysts is less pronounced than in the other catalysts and still lower than in the steam reaction. Purnama et al.[220] also found this beneficial effect of the oxygen addition to the feed during steam re-forming of methanol on Cu/ZrO_2 catalysts.

The oxidative methanol re-forming reactions of methanol have also been investigated over Cu−ZnO(Al) catalysts derived from hydrotalcite-like precursors.[190,218,221] The oxy-re-forming reactions under $O_2/CH_3OH/H_2O = 0.3:1:1$ molar ratios in the feed lead to high activity for CH_3OH conversion and very high selectivity for H_2 production. All of the catalysts exhibit higher CH_3OH conversions than that attained under the conditions of the partial oxidation process. Another interesting result is that CO levels at the exit stream are much lower than in the case of the reaction performed under the conditions of partial oxidation reaction. Despite the complexity of the mechanism of the oxy-re-forming of methanol, it is likely that the water gas shift reaction may contribute to the reduction in CO selectivity at the expense of water.

2.4. Gasification of Coal and Heavy Hydrocarbons

Gasification is another choice technology for the large-scale production of hydrogen. Gasification involves the reaction at high temperatures (1200−1400 K) and moderate pressures (5−10 bar) of a source of carbon, associated or not with hydrogen, with a source of hydrogen, usually steam, and/or oxygen to yield a gas product that contains CO, H_2, CO_2, CH_4, and N_2 in various proportions. Proportions of these component gases depend on the ratio of the reactants used and on the reaction conditions. It is a versatile process that can use all carbon-based feedstocks, including coal, petroleum residues, biomass, and municipal wastes, and is the only advanced power generation technology for coproducing a wide variety of commodity products to meet market needs. Gasification-based systems are the most efficient and environmentally friendly alternatives for the production of low-cost electricity and other useful products and can be coupled to CO_2 concentration and sequestration technologies.[222]

The first companies to convert coal to combustible gas through gasification were chartered in 1912. During the 1930s, the first commercial coal gasification plants were constructed, followed by town gas applications in the 1940s. In the 1950s, chemical process industries started applying gasification for hydrogen production. At present, gasification is a commercially proven mature technology with about 40 GW total syngas production capacity around the world.[223]

2.4.1. Chemistry

The chemistry of gasification is quite complex, involving cracking, partial oxidation, steam gasification, water gas shift, and methanation. In the first stages of the gasification, the feedstock becomes progressively devolatilized upon increasing temperature and yielding simultaneously oils, phenols, tars, and light hydrocarbon gases[224−229] followed by the water gas shift reaction[230,231] and methanation reactions. In a simple form, the basic reaction network in an oxygen and steam fed gasifier can essentially be summarized as follows:

fast pyrolysis:

$$C_nH_mO_y \rightarrow \text{tar} + H_2 + CO_2 + CH_4 + C_2H_4 + \ldots \quad (17a)$$

steam re-forming:

$$\text{tar} + xH_2O \rightarrow xCO + yH_2 \quad (17b)$$

CO_2 re-forming:

$$\text{tar} + CO_2 \rightarrow xCO + yH_2 \quad (17c)$$

partial oxidation:

$$C_nH_m + {}^{n}/_{2}O_2 \rightarrow nCO + {}^{m}/_{2}H_2 \quad (17d)$$

WGS:

$$CO + H_2O \rightarrow CO_2 + H_2 \quad (17e)$$

methanation:

$$CO + 3H_2 \rightarrow CH_4 + 2H_2O \quad (17f)$$

Partial combustion predominates at high temperatures, whereas total combustion predominates at lower temperatures. The water gas shift reaction alters the H_2/CO ratio but does not modify to a significant extent the heating value of the syngas mixture. Methane formation is favored under high pressures (above 8 bar) and low temperatures (about 1100 K), and therefore its formation plays a major role in lower temperature gasifiers. The rates and degrees of conversion for the various reactions involved in gasification are functions of temperature, pressure, and the nature of the hydrocarbon feed being gasified. At higher operating temperatures, the conversion of hydrocarbons to CO and H_2 increases, whereas the production of methane, water, and CO_2 decreases. Depending on the gasification technology, significant amounts of CO_2, CH_4, and H_2O can be present in the synthesis gas as well as trace amounts of other components.[232] Under reducing conditions of the gasifier, most of the organic sulfur is converted to hydrogen sulfide (H_2S), whereas a small fraction, usually not surpassing 10%, forms carbonyl sulfide (COS). The nitrogen present in organic heterostructures forms ammonia (NH_3) and smaller amounts of hydrogen cyanide (HCN). Most of the chlorine present in the fuel reacts with hydrogen to form hydrogen chloride and some particulate-phase inorganic chloride. Trace elements usually associated with inorganic matter, such as mercury and arsenic, are released during gasification and partitioned between the gas phase and ash fraction. The formation of a given species and its partition between the gas phase and solid phase depend strongly on the operating conditions and gasifier design.

Several metals and metal oxides catalyze the reactions involved in gasification and may, therefore, modify the values of their kinetic constants. For example, several authors[233−235] have found how iron-based species (Fe_2O_3, Fe_3O_4) affect the rate of the overall steam gasification of coal and/or biomass. Reactions 17c, 17e, and 17f are also catalyzed by nickel.[232,236] Calcium-based catalysts are also known to promote steam gasification under moderate reaction conditions. High-temperature X-ray diffraction studies have demonstrated that the addition of calcium decreases the reaction temperature and increases the gasification rates.[237] Balasubramanian et al.[238] found that the addition of NiO/Al_2O_3 and CaO catalysts successfully achieved near equilibrium conditions for re-forming of CH_4, water gas shift, and the separation of CO_2 simultaneously in a single reactor at 823 K.

2.4.2. Gasification with Simultaneous CO_2 Capture

The in situ capture of CO_2 during gasification is an especially attractive process because it allows very high H_2 content with very low (near zero) CO_2 and tar contents in

the gasification gas.[226,239] Attempts to use CaO in a CO_2 acceptor process were first conducted by Curran et al.[240] and McCoy et al.[241] In these studies only half of CO and CO_2 was immobilized in CaO. A new method that combines the gas production and separation reactions (hydrogen production by reactions integrated gasification, HyPr-Ring) in a single reactor was proposed by Lin et al.[242] In this process, the energy required for the endothermic re-forming reactions is supplied by the heat of CO_2 absorption. Wang and Takarada[243] reported complete fixation of CO_2 with $Ca(OH)_2$ for a Ca/molar ratio of 0.6 (stoichiometry dictates the ratio to be 1) along with enhanced decomposition of tar and char. In addition, the overall conversion rate of CO to CO_2 can be enhanced by the inclusion of an oxygen donor in the reaction zone. The steam re-forming rate of CH_4 and other light hydrocarbons released during coal pyrolysis may also be enhanced by incorporation of a suitable oxygen donor. Thermodynamic calculations also show that the enthalpy of the Fe^{2+}/Fe^{3+} oxide system is suitable for the water gas shift reaction, a necessary reaction required to convert the CO + H_2 mixture to additional hydrogen (eq 17e). However, Fe_2O_3 oxidizes H_2 at a rate 2−10 times higher as compared to CO.[243] This unwanted reaction results in a reduction in the yield of H_2.

Mondal et al.[235] reported that selection of Fe_2O_3 and CaO as the oxygen transfer compound and CO_2 removal material, respectively, provides additional benefits in H_2 production by gasification. The net result of these reactions is exothermic, so additional CO_2 and H_2 are produced by CH_4 re-forming. Then, the reduced FeO is regenerated in an air (or O_2) stream and the heat released from this exothermic reaction is used to regenerate the carbonated CaO. Thus, the products would result into three separate streams: (i) high-purity H_2 for use in fuel cells; (ii) sequestration-ready CO_2; and (iii) high-temperature oxygen-depleted air for use in gas turbines. The following are the reactions involved in the process, for which the heats of reaction are reported at 1073 K.[235]

Hydrogen Enrichment Stage

coal gasification: $C + H_2O \rightarrow CO + H_2 \quad \Delta H_{1073K} = +135.7$ kJ/mol (18a)

steam reforming: $CH_4 + H_2O \rightarrow CO + 3H_2 \quad \Delta H_{1073K} = +206.0$ kJ/mol (18b)

water gas shift: $CO + H_2O \rightarrow CO_2 + H_2 \quad \Delta H_{1073K} = -33.1$ kJ/mol (18c)

Boudouard reaction: $2CO \rightarrow CO_2 + C \quad \Delta H_{1073K} = -169.4$ kJ/mol (18d)

CO oxidation: $CO + Fe_2O_3 \rightarrow CO_2 + 2FeO \quad \Delta H_{1073K} = -4.8$ kJ/mol (18e)

CO_2 sorption: $CaO + CO_2 \rightarrow CaCO_3 \quad \Delta H_{1073K} = -167.6$ kJ/mol (18f)

Hydrogen Enrichment Stage

CaO hydration: $CaO + H_2O \rightarrow Ca(OH)_2 \quad \Delta H_{1073K} = -94.1$ kJ/mol (18g)

dry re-forming: $CH_4 + CO_2 \rightarrow 2CO_2 + 2H_2 \quad \Delta H_{1073K} = +260.8$ kJ/mol (18h)

methanation: $C + 2H_2 \rightarrow CH_4 \quad \Delta H_{1073K} = +21.7$ kJ/mol (18i)

carbon oxidation: $C + Fe_2O_3 \rightarrow CO + 2FeO \quad \Delta H_{1073K} = +9.4$ kJ/mol (18j)

H_2 oxidation: $H_2 + Fe_2O_3 \rightarrow H_2O + 2FeO \quad \Delta H_{1073K} = +29.0$ kJ/mol (18k)

Oxide Regeneration Stage

decomposition: $CaCO_3 \rightarrow CaO + CO_2 \quad \Delta H_{1073K} = +167.6$ kJ/mol (18l)

oxidation: $FeO + O_2 \rightarrow Fe_2O_3 \quad \Delta H_{1073K} = -281.4$ kJ/mol (18m)

The efficacy of the simultaneous gasification−hydrogen enrichment process can be demonstrated by using a fluid bed reactor configuration.[235] Under typical reaction conditions, that is, temperature of 1143 K and 85% steam, the incorporation of both CaO and Fe_2O_3 [CaO/FeO_2O_3 = 2:1 (wt)] yields a gas with the highest H_2 purity along with maximum coal conversion. The use of CaO alone increases the H_2 yield and purity, whereas incorporation of Fe_2O_3 alone has a negative effect on the H_2 yield.

2.5. Commercialization Status of Fuel Re-formers

The H_2 demand for chemical processing in the United States increased from about 23 M Nm^3 in 1996 to about 38 M Nm^3 in 2000. A similar growth in H_2 consumption was observed for electronics, food-processing, and metal-manufacturing markets.[244] As stated above in this section, steam methane re-forming, coal and residues gasification, and methanol decomposition processes are mature technologies for H_2 production. However, as long as natural gas (or CH_4) remains at low or even moderate cost, SMR will continue to be the technology of choice for massive H_2 production. This trend is expected to continue due to the rapidly growing interest in fuel cells (FCs) in stationary and mobile applications. Accordingly, distributed hydrogen production via small-scale re-forming at refueling stations could be an attractive near- to mid-term option for supplying hydrogen to vehicles. A brief account of the present status and/or commercialization of H_2 production technologies based in fossil precursors is summarized in the next sections.

2.5.1. Steam Methane Re-formers

2.5.1.1. Conventional Steam Methane Re-formers. Steam methane re-formers have been built over a wide range of sizes. For large ammonia, refining, and methanol plants (0.5×10^6 Nm^3/day), capital costs (including the re-former, shift reactor, and PSA unit) are about $200/kW H_2 output, and these decrease to about $80/kW H_2 for a 5×10^6 Nm^3/day plant. On the contrary, scale economics in the capital cost is increased up to about $4000/kW H_2 for small 2300 Nm^3/day plants. This technology can be, in principle, used for other applications which require much lower H_2 production rates such as that required for hydrogen refuelling station applications. However, the large size of standard re-former tubes (12 m long) and high cost, due to costly alloy materials for high-temperature and high-pressure operation, make then unsuited for small-size re-formers. For these reasons, hydrogen needs for FC technology and other niche applications require more compact, lower cost re-formers.[245]

2.5.1.2. Compact Annular Catalyst Bed Re-formers. For small sizes, a more cost-effective approach is to use a low-temperature, lower pressure re-former, with lower cost components. Steam methane re-formers for FCs in the range of 0.4−3 kW have been developed and have also been recently adapted for stand-alone H_2 production. In these designs, the re-former operates at lower temperature and pressure (3 bar, 970 K), which facilitates materials availability and cost. Estimate costs for small FC type steam methane re-formers show that the capital cost for H_2 production plants in the 20−200 Nm^3/day would be \$150−180/kW H_2 for 1000 units sold. Energy conversion efficiencies of 70−80% are achieved with these re-formers.

A number of industries have developed compact steam methane re-formers for FC applications. Major players in this technology are Haldor Topsoe, Ballard Power Systems, Sanyo Electric, International Fuel Cells (IFC), and Osaka Gas Corp. Praxair, in a joint venture with IFC, has recently commercialized a small stand-alone H_2 production system based on these annular bed re-formers. Sanyo Electric and Dais-Analytical Co. built residential PEMFCs powered by H_2 also generated by steam methane re-forming. This technology is being commercialized and offers the attractiveness of reduced capital costs as compared to conventional small-scale re-formers, as well as compactness.

2.5.1.3. Plate-type Steam Methane Re-formers. Another design alternative for steam methane re-formers for FC systems is the plate-type reformer. This type of re-former is more compact than the conventional long tube or annular re-formers. The re-former plates are arranged in a stack. One side of the plate is coated with a steam re-forming catalyst, and in the other side, the anode exhaust gas from the FC undergoes catalytic combustion, providing the heat to drive the endothermic steam re-forming. The advantages of this design are its compactness, low cost, good heat transfer, and fast start-up.

Osaka Gas Co. has developed a plate steam methane re-former for use in PEM FCs.[246] In this design, the different elements, that is, desulfurizer, steam re-former, water gas shift, and CO cleanup, are made up of plates of standard dimensions, greatly reducing the cost. Before commercialization of this technology, the energy conversion efficiency is expected to increase from 70 to 77% by reducing heat losses and increasing the lifetime from 5 to 10 years. Another plate-type methane steam re-former design has been provided by GASTEC. During the development of a 20 kW re-former the performances of various re-formers and combustion catalysts, coatings, and substrate materials were reported. A joint venture between GASTEC and Plug Power was undertaken to develop this plate re-former for residential size fuel cells.

2.5.1.4. Membrane Reactors. In the membrane reactors the steam re-forming, water gas shift, and CO cleanup processes take place in the same reactor. The reactor, which operates under pressure, incorporates on one side a palladium membrane through which hydrogen permeates with a high selectivity. Depending on the temperature, pressure, and reactor length, methane can be quantitatively converted, and pure H_2 is obtained. As H_2 is removed once produced, the equilibrium is shifted, thus allowing lower reaction temperature and lower cost materials. There are many patents issued on membrane reactor re-forming to a number of companies involved in fuel processor design for FC application and on related ion-transport membranes to oil companies (BP Amoco, Exxon, Standard Oil) and industrial gas companies such as Air Products and Praxair. Argon National Laboratory and Praxair launched a program to develop compact, low-cost hydrogen generators based on a ceramic membrane. Natural gas, steam, and oxygen are re-formed in an autothermal reactor, for which oxygen is obtained from air by means of an oxygen transport ceramic membrane that works at temperatures of about 1200 K.[247] The oxygen transport membrane has been developed by Praxair, beginning in 1997, and is now undergoing pilot demonstration.

2.5.2. Partial Oxidation, Autothermal, and Methanol Re-formers

A number of companies are involved in developing small-scale partial oxidation re-formers. Small POX re-formers have been built by Arthur D. Little, Epyx, and Nuvera for use in FCs. Epyx is supplying the on-board gasoline processors for the U.S. DOE's gasoline FC prototype. Similarly, Nuvera shipped gasoline re-formers to automotive companies for testing in FC-powered vehicles. In addition, the consortium McDermott Technology/Catalytica and Hydrogen Burner Technologies are developing a multifuel processor for a 50 kW FC.

Autothermal re-formers (ATR) are being developed by a number of companies, mostly for fuel processors of gasoline, diesel, and logistic fuels and for natural gas fuelled PEM FC cogeneration systems. Principal players in this technology are Honeywell, Daimler-Chrysler, Analytical Power, IdaTech, Hydrogen Burner Technologies, Argonne National Laboratory, Idaho National Energy and Environmental Laboratory (INEEL), and McDermott Technologies. INEEL with McDermott and Pacific Gas have recently begun the development of a 10 kW ATR system for hydrogen refuelling stations.[248] In addition, a consortium of McDermott Technologies, Catalytica Advance Technology, Ballard BWX Technologies, and Gibbs and Cox is developing a small autothermal re-former for use with diesel and logistic fuels on ships. Particularly important for this application is the design of a regenerable desulfurization system to operate with naval diesel fuel, which contains up to 1 wt % sulfur.

Experimental FC vehicles with on-board methanol re-formers have been demonstrated by Daimler-Chrysler, Toyota, and Nissan. In addition, small hydrogen production systems based on methanol re-forming are in commercial use. Although this technology is being developed for fuel processors in on-board FC vehicles, it has also been suggested H_2 might be produced by methanol steam re-forming at refuelling stations. For this latter application, a hydrogen purification step would be needed, either a pressure swing adsorption unit or a membrane separation stage. The cost of the H_2 production via steam methanol re-forming might be higher than that of H_2 from small-scale steam methane re-forming, because methanol is generally, although not always, a more expensive feedstock than natural gas. Costs for methanol are about \$11/GJ versus about \$4−5/GJ for methane at the refuelling station. Assuming an energy conversion efficiency (feedstock to hydrogen) of 75% for each system, feedstock costs alone would be higher for the methanol steam re-former (\$11/GJ − \$5/GJ)/0.75 = \$8/GJ). The European Commission also funded two projects to develop on-board processors for FC vehicles. The Mercatox project aimed to develop a prototype integrated methanol re-former and selective oxidation system. The re-former

consists of a series of catalytic plates, with combustion of anode off-gas on one side and re-former on the other side.

2.5.3. Novel Re-former Technologies

2.5.3.1. Ion Transport Membrane (ITM) Re-forming. A large consortium headed by Air Products in collaboration with the U.S. DOE and several companies (Cerametec, Norsk Hydro, McDermott Technology, Chevron, Eltron Research, and Pacific Northwest Laboratory) and academic partners (University of Pennsylvania, University of Alaska, and Pennsylvania State University) is developing a ceramic membrane technology for the generation of H_2 and syngas ($CO + H_2$) mixtures.

These membranes are nonporous multicomponent oxides suited to work at temperatures above 1000 K and have high oxygen flux and selectivity. These membranes are known as ITMs. The initial design was carried out for a hydrogen refuelling station dispensing about 12000 Nm^3 of H_2/day. Initial cost estimations show significant reduction in the cost of on-site high-pressure H_2 produced according to ITM technology in a plant of capacity in the range of 3000−30000 Nm^3 of H_2/day. For instance, the cost of the H_2 produced via ITM methodology appears to be ca. 27% cheaper than the liquid H_2 transported by road.

In this approach, oxygen is separated from air fed to one side of the membrane at temperatures around 300 K and moderate pressure (0.03−0.20 bar) and reacts on the other side with methane and steam at higher pressure (3−20 bar) to form a mixture of CO and H_2. Then this mixture can be processed downstream to produce H_2 or liquid fuels. Among the different geometries employed for the ITM reactor, the flat-plate system offers some advantages because it reduces the number of seals and thus makes for safer operation.

2.5.3.2. Sorbent-Enhanced Re-forming. Sorbent-enhanced steam methane re-forming is another technology explored recently to produce H_2.[249,250] In this concept, calcium oxide is mixed with the steam re-forming catalyst, removing the CO_2 (and CO) via carbonation of calcium oxide. The resulting H_2/CO mixture produced according to this methodology is H_2-enriched. Thus, a syngas composition of 90% H_2, 9.5% CH_4, 0.5% CO_2, and CO levels below 50 ppm has been reported. This reduces the need for downstream processing (water gas shift and preferential oxidation), which is expensive in a small-scale steam re-former. In addition, removal of CO_2 by calcium oxide makes the reaction occur at lower temperature (670−770 vs 1070−1270 K), reducing heat loss and material costs. Sorbent-enhanced re-forming technology is still at the demonstration scale and shows promise for low-cost H_2 production. Critical issues in this methodology are sorbent lifetime and system design.

2.5.3.3. Plasma Re-formers. Thermal plasma technology is also employed in the production of hydrogen and hydrogen-rich gases from natural gases and other liquid hydrocarbons. The role of plasma is to provide the energy and to create free radicals needed for fuel re-forming. Typical temperatures of thermal plasmas are 3000−10000 K, which accelerate the kinetics of re-forming reactions even in the absence of a catalyst. Basically, the hydrocarbon and steam are introduced into the reactor and H_2, plus other hydrocarbons, that is, C_2H_2, C_2H_4, CO, CO_2, are formed.[251,252] The new designs of plasma re-former are very flexible: it is possible to change the geometry of the electrodes, the reaction volume, and the interelectrode gap. It can operate in a large range of operating conditions, autothermal or steam re-forming conditions, allows the use of different feed stocks, and is very tolerant to sulfur content and carbon deposit.[253] The important advantages of this technology for the automotive applications are its very short start-up time (few seconds), the large operating range of fuel power (from 10 to 40 kW), and its compactness and robustness. The best steam re-forming showed 95% conversion of CH_4 and specific energy use of 14 MJ/kg H_2, equivalent to about 10% of the higher heating value of hydrogen.

2.5.3.4. Microchannel Reactors. Over the past few years there has been great interest in finding an improved process that decreases both the investment and operating costs of hydrogen production via steam re-forming reaction. Microchannel reactors are one of the most attractive options to reduce capital cost by intensifying reactor equipment and reducing operating costs by improving heat and mass transfer.[254,255] A conventional methane steam re-former is quite large (ca. 450000 Nm^3 of H_2/day) and operates with a contact time of the order of 1 s. However, a microchannel plant with the same capacity operates with a contact time below 10 ms, which corresponds to a plant volume of around 88 Nm^3, much lower than the 2700 Nm^3 required in conventional methane steam re-former plants.[256] Very recently, methane steam re-forming experiments have been conducted at contact times below 1 ms to demonstrate that the microchannel reactors enable high rates of heat transfer to maintain fast reactions.[257] Experiments conducted at contact times of 0.09−0.9 ms in a 0.28 mm thick porous catalyst structure held adjacent to flow gap revealed that a greater than 98% approach to equilibrium in methane conversion can be achieved at 0.9 ms, and 19.7% at 0.09 ms. In addition, a model was employed to explore microchannel reactor structures that minimize heat and mass transfer, and sensitivity results suggested that a high approach to equilibrium could also have been achieved with a 10% Rh−4.5% $MgO-Al_2O_3$ catalyst at 0.5 ms when it was washcoated on a thick porous catalyst structure up to 0.4 mm.

The use of microchannel reactors demonstrates that a highly active catalyst allows methane steam re-forming to be carried out with a contact time of less than 1 ms. Further reduction in contact time may be reasonably achieved by increasing the catalyst thickness in a manner that minimizes heat and mass transport limitations through careful design.

3. Carbon Dioxide-free Reactions

3.1. Methane Decomposition

The decomposition of methane is an attractive alternative for the production of CO_x-free hydrogen.[258−261] However, this process produces a lower yield of hydrogen per carbon atom than other processes (SMR, ATR). The process requires a metal catalyst (Ni, Co, Fe, Pt, ...) able to not only break the C−H bonds of the methane molecule but also maintain a high and sustained activity for a long time. Methane decomposition is a moderately endothermic process that requires 45.1 kJ/mol of H_2 produced at 1073 K:

$$CH_4 \rightarrow C + 2H_2 \qquad \Delta H_{1073K} = +90.1 \text{ kJ/mol} \quad (19)$$

Because only hydrogen and carbon structures are produced during methane decomposition, separation of products is not an issue. Another important advantage of the methane decomposition as compared to conventional processes of steam or autothermal processes is the absence of the high- and low-temperature water gas shift reactions and CO_2

removal steps. To achieve stable operation during methane decomposition, it is essential that the metal catalyst should remain isolated from the carbon deposit by forming nanometer-sized carbon structures such as tubes and whiskers. In contrast, if methane decomposition is accompanied by the formation of soot, amorphous or encapsulated carbon on the metal surface, then activity is very low.[262] Catalytic decomposition of other hydrocarbons has been investigated.[263]

3.1.1. Catalysts

Both monometallic and bimetallic transition metal catalysts accumulate filamentous carbon deposits when used in methane decomposition reaction. Universal Oil Products developed a process for the production of hydrogen-based on methane decomposition.[264] This process uses a 7% Ni/Al_2O_3 catalyst in a fluidized bed reactor-regenerator operated at 1150 K. The reactor exit consists of ca. 94% H_2 with the rest being mainly unreacted methane. Another alternative proposed by United Technologies Co.[265] involves methane decomposition on a nickel catalyst deposited in glass fibers. At the typical reaction temperature of 1123 K, hydrogen production is accompanied by the formation of a high-density carbon residue.

This technology is still far from commercial application for hydrogen production. The primary issues are low efficiency of conversion and carbon fouling of the catalyst. The catalyst must be often regenerated to remove accumulated carbon, but relatively low capital costs are projected due to the simplicity of the system.

The influence of reaction conditions on the rate of formation and nature of carbon deposits has been studied in some detail during the past two decades.[34,266−269] Most of these studies employ nickel catalysts because they form carbon deposits at temperatures as low as 723−823 K using CH_4, C_2H_6, or CO + H_2 feeds. The pyrolysis of methane at temperatures below 873 K produces fish-bone-type nanofibers.[269] Metallic Ni particles are sited at the tip of the carbon fibers, which catalyze CH_4 decomposition and hence determine the growth of the fibers. The edges of the stacking carbon layers are exposed at the walls of the fibers, and these layers adopt a turbostratic graphite structure as a consequence of the randomly displaced C-atoms with respect to each other.[270] The sizes of nickel particles, and hence the diameter of the carbon fibers, fall in the 10−100 nm range. Notwithstanding, the carbon structures are different on Pd−Ni bimetallic catalysts.[271] For a Pd−Ni bimetallic catalyst with a Pd/Ni = 1 atom ratio, branched carbon nanofibers of a wider size distribution (10−300 nm) are developed, which contrasts with the carbon nanofibers formed on supported-nickel catalyst (Figure 14). The growth of the carbon fibers on PdNi particles is not uniform; fibers tangle with each other and form a coarse texture. These carbon structures lead to progressive catalyst deactivation.

Nickel and iron catalysts were employed by Muradov[260] for methane decomposition over a wide range of temperatures. The results showed that catalyst activity drops with the time on-stream due to formation of carbon deposits. To circumvent the problem of carbon removal, the active components are supported on a carbon substrate. Among the different carbon materials employed as catalyst supports, activated carbon produced from coconut shells displays the highest activity, whereas graphite exhibits a poor performance. These differences can be attributed to the structure and size of the carbon crystallites. The use of methane binary

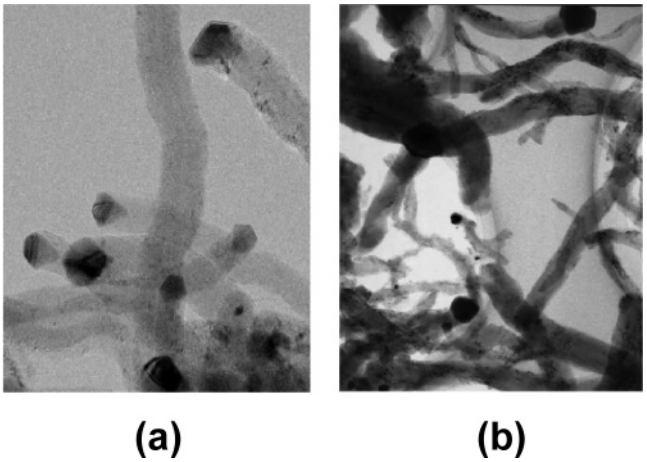

Figure 14. TEM images of carbon deposited by methane decomposition at 873 K over Ni/C (a) and Ni−Pd/C (b). Reprinted with permission from ref 271. Copyright 2003 Elsevier B.V.

gaseous mixtures of methane with a second hydrocarbon has shown that acetylene addition enhances the steady-state methane decomposition rate. The carbon deposit resulting from acetylene decomposition is seen to be more active toward methane decomposition than that resulting from methane alone.

Zhang and Amiridis[272] studied methane cracking over silica-supported metal catalysts to produce CO-free hydrogen. They showed that a 20% CH_4/He mixture reaches a 35% CH_4 conversion at 823 K, although this conversion progressively decreases with the time on-stream until the catalyst becomes completely deactivated after approximately 3 h on-stream. Very recently, methane decomposition was studied on thermally stable Ni-based catalysts prepared from hydrotalcite-like precursors.[273] Results of catalytic methane pyrolysis on two Ni/MgAlO ex-hydrotalcite precursors, containing 58 and 19 wt % Ni, show that the amount of H_2 produced before complete deactivation and the temperature of maximum H_2 production depend only slightly on the Ni loading, although there is no direct relationship between the Ni content and the amount of carbon deposit.

In contrast with nickel catalysts, there are only a few studies concentrated on the decomposition of methane over cobalt catalysts. Wang and Rukenstein[274] investigated carbon formation during methane decomposition at 1173 K over a 48 wt % Co−MgO calcined at three different temperatures (773, 1073, and 1173 K). Precursors calcined at high temperature lead to more extended cobalt crystallites and probably exhibit an ordered structure that templates an ordered nucleus for carbon formation. The carbon nucleus formed generates a graphitic filament because the free energy of the graphitic structure is the smallest. In contrast, when the Co^0 crystallites are formed from the more reducible Co_3O_4 and Co_2MgO_4 phases, present only at calcination temperatures below 1073 K, large metal particles are generated, and because their interactions with the substrate are weaker, their structure is less ordered and many more carbon nuclei are formed. Accordingly, the carbon deposits tend to coalesce during their growth, hence preventing the formation of fibers but generating shapeless tangle shell-like structures.

3.1.2. Catalyst Deactivation and Regeneration

Catalyst deactivation is a complex kinetic process controlled by the decomposition rate of methane on one side of

the Ni particle, the rate of diffusion of carbon, and the graphitization of C-atoms at the other side of the Ni particle. If the rate of these two processes is not well balanced, the catalyst becomes deactivated, presumably by accumulating carbon in the metallic phase (carbide species). No deactivation occurs when the CH_4 decomposition or C−H bond cleavage of CH_4 is the rate-determining step. Collision of a carbon nanofiber with the active Ni particle on the tip of the carbon fiber or coating of the active Ni surface on the tip of the carbon layer is suggested, among others, to be responsible for catalyst deactivation. The Ni K-edge XANES spectra of a fresh 5 wt % Ni/SiO_2 catalyst and under steady-state conditions in CH_4 decomposition are essentially the same. However, the Ni K-edge XANES spectrum for the deactivated catalyst (C/Ni ≥ 900) shows shoulders at 8332 and 8341 eV and increases in intensity with increases in the C/Ni ratio.[275] These changes in the Ni K-edge due to deactivation can be ascribed to the structural change of nickel particles from Ni metal to a nickel carbide species. For the bimetallic Pd−Ni system, the Ni K-edge XANES spectrum of the deactivated catalyst virtually coincides with that of the fresh counterpart, indicating that the local structure of the nickel atoms in the PdNi alloy do not change during the CH_4 decomposition. The longer life of the Pd−Ni catalyst for CH_4 decomposition may be ascribed to the PdNi alloy, which does not react with carbon to form a stable carbide compound.

Removal of the carbon fibers grown during CH_4 decomposition on the metal surfaces can be satisfactorily achieved by a consecutive gasification process with CO_2, O_2, and H_2O.[276] Deactivated silica-supported nickel catalysts[273] were regenerated with steam, recovering completely their original activity. Some clues as to the nature of carbon deposits and their relative reactivity were derived from TEM images. The TEM images showed that the external graphitic skin of the filamentous carbon, which roughly represented nearly 30% of the total carbon deposited, was highly resistant toward steam regeneration, whereas the inner less graphitic carbon was easily removed by steam gasification. Results of catalytic methane pyrolysis on two Ni/MgAlO ex-hydrotalcite precursors,[273] containing 58 and 19 wt % Ni, revealed that the deactivating carbonaceous deposits produced along the pyrolysis process can be removed, at least in part, by a consecutive oxidation cycle involving O_2 or CO_2. Both regeneration methods are very effective because redispersion of nickel phase along the oxidation step is followed by an increase of catalytic activity (Figure 15). Ni particle size of the regenerated sample decreased with respect to its counterpart after the first reduction, indicating redispersion of the Ni crystallites after CO_2 regeneration. Another reason for the higher activity of the regenerated catalyst is that carbon may also be active for methane decomposition.[261] On the other hand, dilution of the deposited carbon in the Ni crystallites produces nickel carbide,[277] which can be more active for methane decomposition than metallic Ni. Gasification of carbon deposits with O_2 and H_2O also reaches levels somewhat above 95%, and the process can be repeated over several cycles. The gasification of carbon fibers with CO_2, O_2, and H_2O allows the recovery of the original activity of the Ni/TiO_2 catalysts, although the TOF values of hydrogen formation on Ni/SiO_2 and Ni/Al_2O_3 catalysts do not follow the same trend as in the Ni/TiO_2 system. Indeed, TOF values for the Ni/SiO_2 catalysts decrease progressively upon increasing number of reaction−regeneration cycles as a consequence of the increase of the particle size of the Ni crystallites along the operation cycle. In contrast with this, the extent of sintering of Ni crystallites is less marked in the Ni/TiO_2 catalyst because of the strongest $Ni-TiO_2$ interaction, which prevents the formation of large Ni particles during the repeated reaction−regeneration cycles. The strongest interaction between Ni and the Al_2O_3 surface diminishes the extent of formation of Ni crystallites suitable for CH_4 decomposition, resulting in lower catalytic activity in the first few cycles. Additionally, further decomposition−regeneration cycles cause the growth of Ni metal particles, and therefore TOF values progressively decrease.[276]

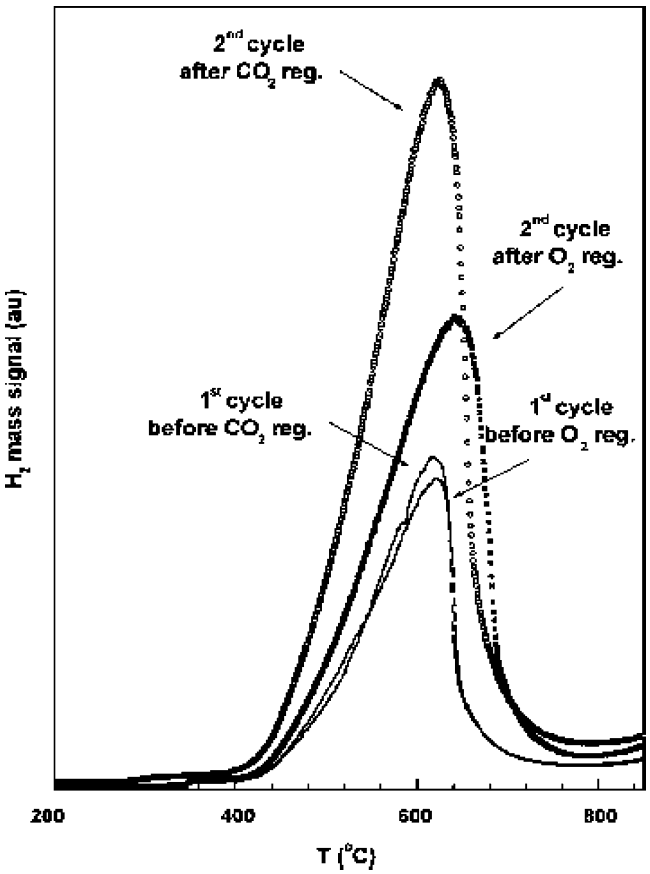

Figure 15. H_2 produced from catalytic methane decomposition on Ni/MgAlO ex-hydrotalcite precursor before and after O_2 or CO_2 regeneration. H_2 production is represented by the corresponding (m/z) mass as a function of temperature. Reprinted with permission from ref 273. Copyright 2006 Elsevier B.V.

3.2. Theoretical Analysis of Methane Decomposition on Metal Surfaces

Theoretical studies have been carried out to describe the processes taking place during CH_4 decomposition on transition metal surfaces. The dissociation of CH_4 molecules on several transition metals (M) (M = Ru, Os, Rh, Ir, Pd, Pt, Cu, Ag, Au) was analyzed theoretically by Au et al.[278] by simulating the surface by a M_{10} cluster. On the Pt_{10} cluster, the barrier for the first dehydrogenation is estimated to be 0.84 eV. The dehydrogenation of CH_x to CH_{x-1} fragments is highly endothermic in the gas phase with dissociation energy (D_e) values of 4.85, 5.13, 4.93, and 3.72 eV for x = 4, 3, 2, and 1, respectively.[278] However, there is significant reduction in the D_e values on metal surfaces due to the formation of strong $M-CH_{x-1}$ and M−H bonds. The first and second dehydrogenation steps on a Ru surface are nearly

Table 4. Effects of Acidification and Basification of Impregnating Solution on the Catalytic Performance of 2 wt % Mo/HZSM-5 Catalyst[a]

		selectivity (mol %)					yield (mol %)	
catalyst	CH_4 conversion (mol %)	C_2H_4	C_2H_6	C_6H_6	C_7H_8	$C_{10}H_8$	C_2	aromatics
Mo/HZSM-5	5.2	3.5	3.2	74.6	3.6	15.1	0.3	4.9
Mo/HZSM-5(N)	5.7	3.1	2.9	74.2	4.2	15.6	0.3	5.4
Mo/HZSM-5(S)	7.6	2.8	2.1	74.3	3.9	16.7	0.4	7.2
Mo/HZSM-5(A)	7.4	2.4	2.3	76.4	4.3	14.6	0.3	7.1

[a] Reaction temperature = 973 K, GHSV = 1600 mL h^{-1} g^{-1}, and data were recorded 1 h after the start of reaction. C_2: $C_2H_4 + C_2H_6$. Adapted from ref 284. Copyright 2007 Elsevier B.V.

thermoneutral, whereas the third and fourth steps are slightly exothermic and endothermic, respectively. On the Rh surface there is one mildly exothermic, one slightly exothermic, and two endothermic steps, but in Cu, Ag, and Au metals all of the steps tend to be endothermic. For the whole process the reaction with the highest activation barrier should be the rate-determining step. However, among the transition metals the highest barriers are found to be very similar, and hence from these results it is not easy to predict the catalytic behavior.

The summation of the energies for the four discrete steps, which gives the total dissociation energies, is seen to be a more realistic measure for the activity of the metal in methane dissociation. The calculations of these sums are conclusive in the sense that the total dissociation of methane on Rh is thermodynamically more favored than that on other transition metals,[278] and the values follow the trend Rh < Ru < Ir < Os ≈ Pt < Pd. This trend is similar to that obtained by Schmidt et al.[279] in the partial oxidation of CH_4 to syngas. By contrast, these sums prove to be highly endothermic for Ag, Au, and Cu metals. Two causes can be responsible for this behavior. First, the adsorption energy of H-atom on Ag, Au, and Cu metals is relatively small as compared with the other transition metals, and, second, the adsorption of the CH_x fragments on these metals increases only weakly from $x = 3$ to $x = 1$ and even decreases from $x = 1$ to $x = 0$. Therefore, a complete dissociation of CH_4 to surface C_s and H_s is difficult on Ag, Au, and Cu metals, in agreement with the experimental observation that these latter metals are inactive in the partial oxidation reaction.

In addition to the direct dissociation of methane on clean metal surfaces, oxygen-assisted dissociation has also been studied. The dissociation of CH_4 on Rh in the presence of surface oxygen was studied by applying the BOC-MP method,[280] in which different surface oxygens at on-top, bridge, and hollow sites were considered. The BOC-MO calculations show that oxygen atoms at on-top sites promote methane dehydrogenation. Because the H-atoms bind more strongly with oxygen at on-top sties than with the clean metal, the CH_4 dissociation reaction in the presence of surface O_s located at on-top sites has a lower reaction energy due to hydroxyl formation. This means that oxygen at on-top sites promotes the dehydrogenation of CH_x, in agreement with the BOC-MP predictions.[280] On the contrary, O-atoms at hollow locations show a different behavior toward CH_4 dissociation because they increase the adsorption energies of H on Pt, and also on Ag, Au, and Cu, but decrease those on other transition metals. Thus, only Pt, Cu, and Au metals promoted CH_4 dissociation.

3.3. Methane Aromatization

Methane dehydroaromatization (MDA) in the absence of gas-phase oxygen has received considerable attention as a promising route for the direct conversion of methane into hydrogen and highly value-added chemical coproducts such as benzene and naphthalene[281−283] (eq 20).

$$6CH_4 \rightarrow 9H_2 + C_6H_6 \qquad \Delta H^\circ_{298K} = +88.7 \text{ kJ/mol } CH_4 \tag{20}$$

Table 4 summarizes methane conversion, selectivity to different hydrocarbons, and aromatics yield on a typical Mo/HZSM-5 catalyst at temperatures in the range of 973−1073 K under nonoxidative reaction conditions.[284]

Most research work has focused on Mo/HZSM-5 catalysts, prepared according to different methodologies. It is generally accepted that both the activation of the C−H bond of methane and the formation of the initial C−C bond take place on reduced Mo carbide species, which is formed from the reduction of MoO_x species by CH_4 in the early stage of the reaction, whereas the subsequent oligomerization, cyclization, and aromatization of the C_2 hydrocarbon fragments are catalyzed by the Brønsted acid sites of the HZSM-5 zeolite.[285−295] Therefore, a catalyst structure consisting of Mo species in the close vicinity of the Brønsted acid sites located in the HZSM-5 channels appears to be essential for the formation of aromatics.

3.3.1. Catalysts

The kind of molybdenum oxide species that are precursors of the active molybdenum carbide species in MDA is a matter of debate. In the early stages of this reaction, Solymosi et al.[286,287] and Lunsford et al.[288,296] suggested that the Mo_2C species, highly dispersed on the external surface of the HZSM-5 zeolite, are the active sites and are responsible for the initial methane activation. The Mo species in the Mo/HZSM-5 catalysts are present in different states and various coordination environments.[285,290] For Mo loading below ca. 7 wt % and calcination temperature below 823 K, these molybdenum oxide species are highly dispersed on the HZSM-5 surface and interact with the Brønsted acid sites of the HZSM-5 substrate. However, with increasing Mo loading and higher calcination temperature the tendency of framework Al extraction by molybdenum oxide species becomes more significant. The Mo species on the MoO_3/HZSM-5 catalyst prepared by impregnation include the Mo^{6+}_{6c} species in distorted octahedral coordination, the Mo^{6+}_{5c} species in square pyramidal coordination, and the Mo^{6+} species associated with the Brønsted acid sites.[297] Electron spin resonance spectra provide evidence about the location of these Mo species. The former two Mo species exist mainly on the external surface of the HZSM-5 zeolite and can be readily reduced to Mo^{5+}, whereas the latter resides primarily inside the zeolite channels. Furthermore, during the MDA reaction at 973 K, two kinds of Mo^{5+} species are present in the Mo/HZSM-5 catalyst, one derived from the

Mo_{6c} species interacting with the HZSM-5 zeolite and the other associated with the Brønsted acid sites. In addition, ^1H MAS NMR spectra have revealed that the amounts of all hydroxyl groups on MoO_3/HZSM-5 remain unchanged after H_2 pre-reduction at 623 K, and hence further migration and dispersion of the Mo species onto the external surface or into the channels of the HZSM-5 zeolite does not occur during H_2 pre-reduction.[298] Stable β-Mo_2C species in hexagonally close-packed (hcp) structures can be attained by temperature-programmed treatment of MoO_3 species from room temperature to 973 K in a methane flow, whereas metastable α-MoC_{1-x} species in face-centered cubic (fcc) structure can be formed from MoO_3 species through reduction in H_2 flow at 623 K and subsequent carburization in methane.[299] The Mo species associated with the Brønsted acid sites can be only partially reduced by CH_4 to form the MoC_xO_y species and is still associated with the Brønsted acid sites.[300] The MoC_xO_y species probably forms an hcp structure when the Mo/HZSM precursor is activated in CH_4 flow, whereas it yields an fcc structure upon pretreatment in H_2. The reactivity and stability of the latter MoO_xC_y species are by far higher than those with an hcp structure for the reaction of MDA.

On fresh MoO_3/HZSM-5 catalyst prepared by mechanical mixing, the Mo species exist mainly in octahedral coordination, just as they do in bulk MoO_3. Under a reducing atmosphere due to the presence of methane and high temperature, the MoO_3 could become well dispersed on the surface of zeolite and migrate into the channels to interact with the Brønsted acid sites, resulting in the formation of Mo species associated with the Brønsted acid sites, as well as a change in the coordination environment of the Mo species.[298] Temperature-programmed reduction (TPR) and temperature-programmed oxidation (TPO) results reveal that pretreatment in H_2 could suppress the migration of the Mo species into the HZSM-5 channels. The crystalline MoO_3 existing on the external surface of the zeolite transformed to an fcc α-MoC_{1-x} carbide via reduction in hydrogen at 623 K and then carburization in methane.[299] On the other hand, the Mo/HZSM samples prepared by physical mixture exhibit very poor performance in MDA. The fcc α-MoC_{1-x} species activate methane regardless of significant coke deposition, although the amount of benzene formed on this catalyst is rather small because of the long distance between the molybdenum carbide species and the Brønsted acid sites. Consequently, both the active Mo species and the vicinal Brønsted acid sites are indispensable for the reaction of methane dehydroaromatization.

3.3.2. Reaction Mechanism

When the MDA catalytic reaction occurs at a short time scale, in the range of 10^{-3} s, which is far from that of the usual equilibrium condition, the reaction products may be strikingly different.[299] Under the imposed short contact time, desorption of intermediates takes place in the gas phase, thereby restricting interaction of reactive intermediates and/or products with the surface of the catalyst. The study reveals that the main product of the conversion of methane at 973 K in such conditions does not follow the usual thermodynamic equilibrium conversion to produce benzene. In a 3% Mo/ZSM-5 catalyst, the transformation of MoO_3 to Mo_2C is accompanied by the formation of H_2O and CO (or CO_2), but there is no detectable amount of products such as ethane and ethylene. Apart from the signals of dissociated species

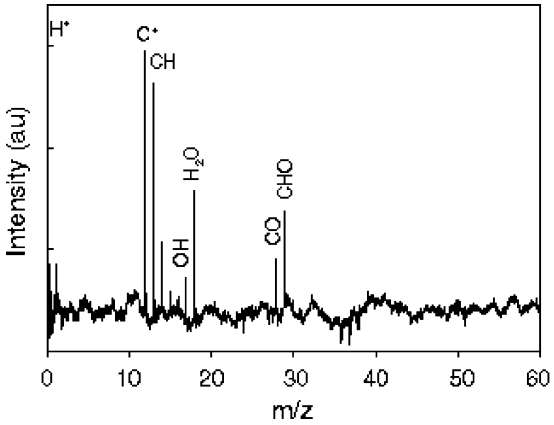

Figure 16. MS signal observed in the induction period of CH_4 dehydroaromatization at 973 K over 3% Mo/HZSM-5. Reprinted with permission from ref 299. Copyright 2006 Elsevier B.V.

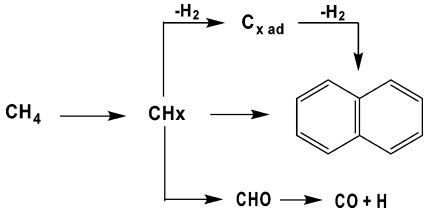

Figure 17. Mechanism of CH_4 dehydrogenation under low spatial velocity (10^{-3} s) over 3% Mo/HZSM-5. Adapted with permission from ref 299. Copyright 2006 Elsevier B.V.

of methane, signals of H^+, CH_x^+ ($x = 0-3$), H_2O^+, and CHO^+ ions are also detected (Figure 16). This suggests that the CH_x fragments produced from CH_4 decomposition react with surface oxygen of the catalyst to form a CHO radical, which then further dissociates into CO and H atoms (Figure 17). CH_4 dissociates first into CH_x ($x = 0-3$) radicals and H-atoms over Mo_2C, and then the direct oligomerization and aromatization of CH_x species in forming naphthalene occurs at the Brønsted acidic sites of HZSM-5. Ma et al.[300] precluded ethylene as an intermediate of methane aromatization reaction because ethylene in gaseous phase is not responsible for the formation of aromatic compounds. In addition, small molecules such as C_2H_4 and C_2H_6 do not appear in the gas phase at contact times of ca. 10^{-3} s due to hydrogen deficiency. Graphitic carbon on the surface of the used 3% Mo/HZSM-5 catalyst was observed with the HRTEM technique (Figure 18), and additionally encapsulated carbon originated mainly from the successive dehydrogenation and polymerization of CH_x radicals or naphthalene graphitization, which is the main reason for catalyst deactivation. On these grounds, a novel reaction mechanistic scheme for the formation of naphthalene[299] under supersonic jet expansion condition is proposed (Figure 17).

3.3.3. Coke Formation

In the course of the reaction carbon is accumulated on the catalyst surface and activity progressively drops. TPO experiments of coked Mo/HZSM catalysts show three peaks around 733, 783, and 833 K. The carbon species burning at high temperatures (833 K) comes from those formed on the Brønsted acid sites of the zeolite, whereas the carbonaceous deposits burning at lower temperatures are located on the molybdenum carbide or molybdenum oxycarbide.[300,301] In the initial period of MDA reaction, the Mo oxide species are reduced and carburized by methane and develop active

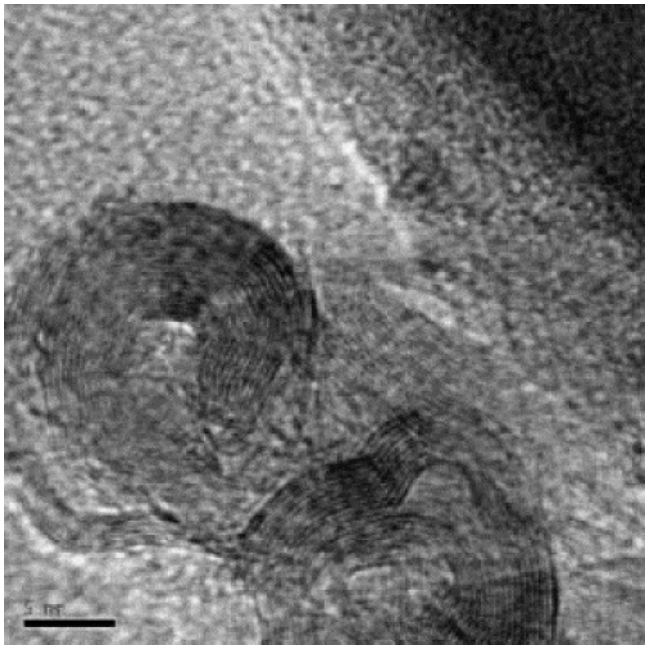

Figure 18. HRTEM images of 3% Mo/ZSM-5 catalyst used in CH_4 dehydroaromatization at 973 K under low spatial velocity (10^{-3} s). Reprinted with permission from ref 299. Copyright 2006 Elsevier B.V.

Mo species; molybdeum carbide and/or molybdenum oxycarbide are generally accepted.[294,295,302] The activated methane molecules could readsorb and become anchored to the active Mo species to form coke. Further dehydrogenation and oligomerization of monocyclic aromatic products also could lead to the deposition of aromatic-type carbon species on the Brønsted acid sites. The nature of these carbon deposits is different. Thus, the carbon deposits associated with the Mo species are reactive and reversible; however, the coke formed on the Brønsted acid sites is inert and irreversible. The latter species is responsible for the deactivation of the Mo/HZSM-5 catalysts.[303]

4. Carbon Dioxide Neutral Alternatives

Currently, hydrogen is produced almost entirely from natural gas, liquid hydrocarbons, and coal. All of these C-containing sources release massive amounts of CO_2 into the atmosphere during the production of hydrogen. Thus, renewable biomass, a product of photosynthesis, is an attractive alternative to fossil feedstocks as it can be considered as a CO_2 neutral precursor. Notwithstanding, the hydrogen content of lignocellulosic biomass is very low (ca. 6.3 wt % H_2), which contrasts with the almost 4-fold greater hydrogen content in natural gas.

4.1. Biomass Conversion

Biomass can be converted into hydrogen and other useful products through several thermochemical processes such different gasification routes, which have received much attention in recent years. In addition, there are other biochemical processes for the conversion of biomass into hydrogen, but these options are beyond the scope of this review.

4.1.1. Steam/Oxygen Gasification

Biomass is also gasified at temperatures above 1000 K in the presence of oxygen and/or water. Under these conditions biomass undergoes partial oxidation and/or steam re-forming reactions yielding gas and char product. The char is subsequently reduced to form H_2, CO, CO_2, and CH_4. This conversion process can be expressed as

$$C_xH_yO_z + H_2O + O_2 \rightarrow H_2 + CO_x + CH_4 + HCs + \text{char} \quad (21)$$

Table 5. Feedstocks and Hydrogen Production during Biomass Gasification[a]

feedstock	reactor type	catalyst	H_2 (% vol)
sawdust	fluidized bed	unknown	57.4 at 1073 K
not known	fluidized bed	Ni	62.1 at 1103 K
sawdust	fluidized bed	K_2CO_3	11.27 at 1237 K
		CaO	13.32 at 1281 K
pine sawdust	fluidized bed	unknown	26−42 at 973−1073 K
bagasse			29−38 at 973−1073 K
Eucalyptus gobulus			35−37 at 973−1073 K
Pinus radiata			27−35 at 973−1073 K
sewage sludge	downdraft	unknown	10−11
almond shell	fluidized bed	La−Ni−Fe	62.8 at 1073 K
		perovskite	63.7 at 1173 K
switchgrass	moving bed	Cu−Zn−Al	27.1

[a] Adapted from Ni et al.[324]

Unlike pyrolysis, which generates principally liquid oils and solid charcoal, gasification of biomass produces mainly gaseous products. As the products of gasification are mainly gases, this process is more favorable for hydrogen production than pyrolysis. As a general rule, the gasification process is applicable to biomass having a moisture content of less than 35%.[304,305] To optimize the process for hydrogen production, a number of efforts have been made by researchers to test hydrogen production from biomass gasification with various biomass types and at various operating conditions, as listed in Table 5.[305] Using a fluidized bed gasifier along with suitable catalysts, it is possible to achieve hydrogen production of about 60 vol %. Such high conversion efficiency makes biomass gasification an attractive hydrogen production alternative.

One of the major issues in biomass gasification is the tar formation that occurs during the process. The unwanted tar polymerizes to a more complex structure, which is not favorable for hydrogen production through steam re-forming. Currently, three methods are available to minimize tar formation: (i) proper design of the gasifier; (ii) incorporation of additives or catalysts; and (iii) control of operation variables.

Regarding method iii, the operation parameters, such as gasifying agent, temperature, and residence time, are key factors in the formation and decomposition of tar. Tar can be thermally cracked at temperatures above 1273 K.[306] In the type ii method, the use of additives (type such as dolomite, olivine, and even char), also facilitate tar reduction.[307] Dolomite is particularly suited because 100% elimination of tar can be achieved with this additive.[308] Catalysts also reduce the tar content, but are particularly effective for improving gas product quality and conversion. Dolomite-loaded nickel catalysts and alkaline metal oxides are widely used as gasification catalysts. In the type i method, a strategy consisting of a two-stage gasification and secondary air injection in the gasifier is also useful for tar minimization.[309]

The formation of ash is another problem inherent to biomass gasification. Ash may cause deposition, slagging, fouling, and agglomeration.[310] These problems have been usually alleviated by leaching and fractionation.[310−312] Leach-

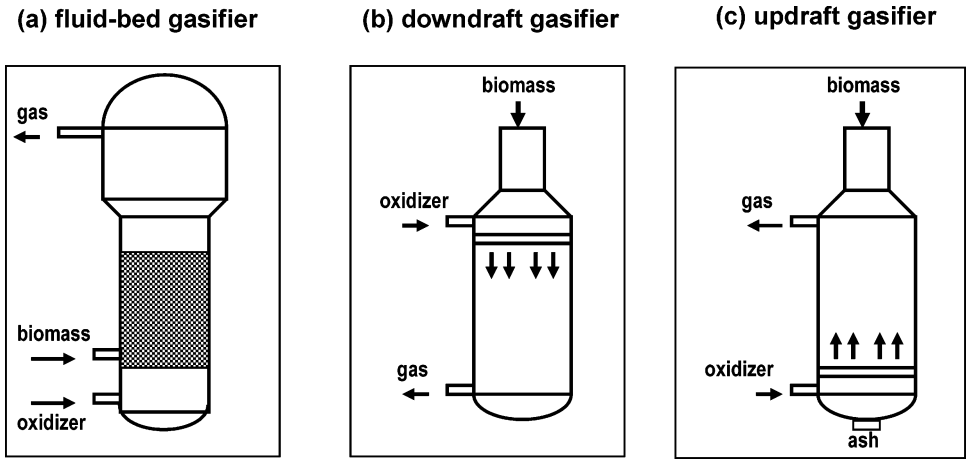

Figure 19. Sketch pictures of biomass reactors: (i) fluidized-bed gasifier; (ii) downdraft gasifier; (iii) updraft gasifier (ref 331).

ing is effective for removing the inorganic fraction, as well as for improving the quality of the remaining ash.[311] The gasification of leached olive oil waste in a circulating fluidized bed reactor was performed for gas production, showing the feasibility of leaching as a pretreatment technique for gas production.[305] Through fractionation, ash removal is achieved, but it may alter the quality of the remaining ash.

4.1.1.1. Gasifiers. A plethora of different biomass gasifiers can be found in patent bibliography. However, they can be grouped into three main types, as sketched in Figure 19: (i) fluidized bed gasifier; (ii) downdraft gasifier; and (iii) updraft gasifier.[313]

In the fluidized bed reactor (Figure 19a) the biomass, which is previously reduced to a fine powder, air, steam, or oxygen enters at the bottom of the gasifier. A high linear velocity of the gas stream forces the fine particles of biomass upward through a bed of silica beads. Pyrolysis and char gasification take place in this process. This type of gasifier is suited for large-scale applications and has a medium tar yield of around 10 g/Nm.[3] In the downdraft gasifier (Figure 19b) the air or oxygen and biomass particles of a fine powder enter at top of the reactor flow downward and the gas leaves at the bottom of the reactor. The product gas contains the lowest concentration of particulates and tars of nearly 1 g/Nm,[3] which is a much lower level than in the fluidized bed reactor, because most of the tars are combusted. The flame temperature in this reactor is 1200−1600 K. This reactor configuration is ideal when clean gas is needed. The main disadvantage of this gasifier reactor is its low overall thermal efficiency and also the difficulty in handling ash content. In the updraft gasifier (Figure 19c) biomass enters from the top and air/oxygen/steam flow upward, entering from the bottom, and the gas leaves from the top. This reactor forms primarily tars at a very high level (on the order of 100 g/Nm^3). The principal advantages of updraft gasifier include its being a mature technology for heat production, its suitability for small-scale applications, and its ability to handle feeds with high moisture content. On the contrary, the tar yield of this gasifier is very high and has slagging potential.

4.1.2. Gasification in Supercritical Water

If the moisture content of biomass exceeds 35%, it is possible to gasify biomass in supercritical water (SCW) conditions. SCW is obtained at pressures above 221 bar and temperatures above 647 K. In the absence of an added oxidant, biomass is converted under SCW conditions into fuel gases (eq 22), which are easily separated from the water phase by cooling to ambient temperature.[314−316] SCW gasification is also a promising alternative to gasify biomass with high moisture contents due to the high gasification (100% conversion) and hydrogen ratios (50% vol).

$$C_xH_yO_z + (2x - z)H_2O \rightarrow xCO_2 + (2x - z + y/2)H_2 \quad (22)$$

Detailed thermodynamic calculations in this reaction indicate that at temperatures above 873 K only a gas rich in H_2, CH_4, CO, and CO_2, with no solid carbon product, is formed.[317] Unfortunately, biomass does not react directly with steam at atmospheric pressure to yield the desired products. Instead, significant amounts of tar and char are formed, and the gas phase contains higher hydrocarbons in addition to hydrogen and other lighter gases.[317,318] These hurdles were overcome in 1985 when Modell[319] reported experiments involving the quick immersion of maple wood sawdust in supercritical water. The sawdust quickly decomposed to tars and some gas without the formation of char. Cellulose is most stable component of biomass but suffers rapid decomposition at temperatures somewhat below the critical temperature of water.[320] At temperatures above 463 K, a fraction of lignin and hemicellulose reacts via solvolysis after only a few minutes of exposure to hot water.[320,321] The initial products originated in the solvolysis undergo several reactions such as dehydrations, isomerizations, fragmentation, and condensation[322−329] and finally form gas and tars.[330] At temperatures above 873 K and pressures exceeding the critical pressure, biomass is converted into a gas mixture composed of hydrogen, methane, carbon dioxide, and carbon monoxide, together with some tar.[331,332]

4.1.2.1. Low-Temperature SCW Gasification. Typically, low-temperature gasification is conducted at temperatures within the range of 623−873 K, and in most cases solid catalysts are employed to accelerate the reaction, although complete gasification of feedstock is rarely achieved.[333] Metal catalysts are active for the gasification of biomass under nearly supercritical conditions at low temperatures, but only few of them are suited for this purpose because the metallic crystallites become oxidized in the hot water environment.[334] Furthermore, the silica and alumina substrates, usually employed as support of metal crystallites, become severely degraded in this reaction environment as a consequence of

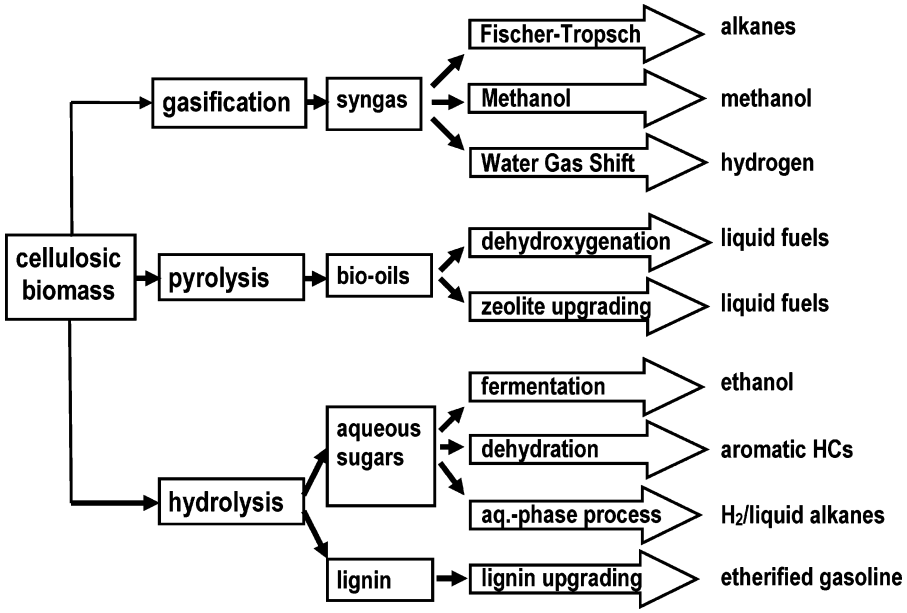

Figure 20. Strategies for production of fuels from lignocellulosic biomass. Adapted with permission from ref 388. Copyright 2006 Elsevier B.V.

their partial solubilization in high-temperature water.[335] In this respect, new catalyst formulations have been developed. These include combinations of stable metals such as ruthenium or nickel bimetallics and stable supports such as certain zirconia, titania or carbon. Indeed, the TiO_2 (rutile)- and carbon-supported nanocrystalline ruthenium particles demonstrate stable performance for times on-stream of about 2 h and reaction temperatures in the range of 523−773 K under a pressure of 40 bar. Alkali catalysts have also been used for this purpose, although their recovery from reaction media makes them less attractive. Sodium carbonate increased the gasification rate of cellulose.[336]

Some clues on the mechanism of hydrothermal degradation of biomass have been derived from experiments carried out on the conversion of cellulose and glucose in hot compressed water.[328] In the absence of catalyst, cellulose decomposes over 473 K to yield sugars, which are water-soluble products. The absence of gas, oil, or char formation indicates that hydrolysis is the primary step of the gasification reaction.[328,336] At 523 K, cellulose decomposes to form gases, oil, char, and water-soluble products, not only sugars but also other non-sugar compounds. Over 573 K, no cellulose is left in the reactor; sugars and oil decomposed, whereas char production increased. Finally, char is mainly obtained with a yield ca. 60% on a carbon basis, with 15% of non-sugar water-soluble products and 10% of gas, mainly CO_2, with very small amounts of CO. Strategies for production of fuels from lignocellulosic biomass are schematically depicted in Figure 20. Additional experiments using glucose as a feedstock conclude that hydrolysis is the first step of cellulose conversion.[329,337] For this feedstock, the product distribution and yield of gas, oil, and char at different reaction temperatures are essentially the same as that for cellulose, indicating that hydrolysis is rapid under these conditions.

Most of the mechanistic work has been conducted in the presence of catalysts. As is well-known, metal catalysts, and most specifically nickel ones, catalyze gasification reactions.[328,336] The onset temperature of cellulose degradation is similar to that found for catalyst-free operation, but the nickel phase catalyzes the gasification of water-soluble products into a CO-free mixture containing CO_2, H_2, and CH_4. Oil and char are also produced, but their yields were very low. The change of the gas composition revealed that CO_2 and H_2 are primary products, although a minor proportion of CH_4 is later formed via methanation. The gas yield increases with increasing catalyst loading, and oil and char are produced simultaneously. Separate experiments with the oil fraction have shown that it does not gasify any further.

Sodium carbonate has also been used as an alkali catalyst.[328,336] In the presence of sodium carbonate cellulose degrades at substantially lower temperatures (453 K), indicating that the alkali catalyst lowers the onset temperature of cellulose degradation. This catalyst also promotes sugar degradation, with the subsequent increase of oil and gas yields, while inhibiting char formation from the oil fraction, thus resulting in high oil yield and a low char yield even at high temperature (623 K).

4.1.2.2. High-Temperature SCW Gasification. High-temperature SCW gasification is conducted in the range of 773−1073 K. Due to the high reactivity of biomass at these temperatures, high gasification efficiency is achieved when the concentration of the precursor is low, but it falls at higher concentrations.

Organic feedstock such as glycerol and glucose can be gasified in the absence of catalysts. The gasification of glycerol under SCW and temperatures below 873 K is very slow, but the rate approaches a value asymptotically around 973 K, and complete gasification can be achieved only at concentrations below ca. 3 wt %. Under these operation conditions, the yields of H_2 and CO_2 increase sharply, whereas that of CO follows an opposite trend. These results indicate greater water gas shift activity at temperatures above 873 K, a unique property of SCW. The pressure of the process has hardly any effect on either product gas composition or gasification efficiency within a wide range of pressures, including supercritical as well as subcritical pressures (60−400 bar). Additionally, the concentration of the feedstock has a major influence on the gas yield. This is illustrated by the significant drop in the H_2 yield and carbon gasification efficiency when the concentration of the organic feedstock exceeds 5−10%.

The application of metal oxide catalysts has been reported recently. Gasification of model compounds such as glucose and pyrocatechol is enhanced in the presence of KOH, $KHCO_3$, and Na_2CO_3.[337] These alkali compounds lead to an increase in H_2 and a decrease in CO yield as a consequence of the acceleration of the water gas shift reaction.[338] SCW gasification in the presence of $KHCO_3$ leads additionally to an increased concentration of products in the aqueous mixture, less coke/char formation, a lower concentration of furfural, and a higher amount of phenol. It should be emphasized that salts catalyze many reaction steps and that whenever gasification experiments with model compounds are performed, it should be taken into account that real biomass precursors include salts and hence yield similar gas composition, such as glucose with alkali salt, which means high H_2 yield and low CO yield.

Because the major drawback of alkali salts is their recovery from the reactor effluent, solid catalysts such as zirconia (ZrO_2) were also employed. The ability of ZrO_2 to enhance the gasification of glucose and cellulose under SCW condition has been demonstrated,[339] although its effect is not as strong as that of Na_2CO_3. Similar results were obtained for partial oxidative gasification of lignin.[340]

4.1.3. Gasification with Simultaneous CO_2 Capture

Recently, several methods for one-step production of pure hydrogen from carbon or biomass were proposed. Saxena proposed the formation of hydrogen through the reactions of carbon materials with NaOH in the presence of water vapor.[341]

$$C_xH_yO_z + a\mathrm{NaOH} + bH_2O \rightarrow cH_2 + d\mathrm{Na_2CO_3} \quad (23)$$

A similar approach was undertaken by Lin et al.,[239] who examined the production of hydrogen through the reactions of organic materials (coal, wood) with water and CaO at 873−1023 K under high-pressure steam (4.2 MPa). In this method, organic materials are gasified to form H_2 and CO_2, whereas $Ca(OH)_2$ reacts stoichiometrically with CO_2 to form $CaCO_3$:

$$\mathrm{Ca(OH)_2} + \mathrm{CO_2} \rightarrow \mathrm{CaCO_3} + \mathrm{H_2O} \quad (24)$$

However, the percentages of CH_4, CO_2, and CO in the produced hydrogen are still far from satisfactory for the direct supply of the hydrogen to PEMFCs. To avoid this, a new method for the synthesis of hydrogen without CO or CO_2 for PEMFCs through the reactions of biomasses (cellulose, sucrose, glucose, starch, cotton, paper) with alkali metal hydroxides (NaOH, KOH, or RbOH) and water vapor at relatively low temperatures (473−623 K) under atmospheric pressure has been proposed.[342] In this method, cellulose $[(C_6H_{10}O_5)_n]$ reacts with NaOH in the presence of water vapor to produce CO_x-free hydrogen and Na_2CO_3 according to the overall reaction (eq 25)

$$\mathrm{C_6H_{10}O_5} + 12\mathrm{NaOH} + \mathrm{H_2O} \rightarrow 6\mathrm{Na_2CO_3} + 12\mathrm{H_2} \quad (25)$$

The results confirmed that the one-step production of pure hydrogen without CO or CO_2 is possible through the reactions of cellulose with NaOH and water vapor at 473−623 K. In addition, the rate of hydrogen production is enhanced by the addition of Ni, Co, Rh, or Ru catalyst supported on Al_2O_3 to the mixture of cellulose and NaOH, and the total yields of hydrogen dramatically improve to almost 100%. Among the catalysts tested, Ni/TiO_2 and Ni/Cr_2O_3 are promising candidates in that they maintain their catalytic activity over repeated cycles, keeping the hydrogen yield almost 100%.

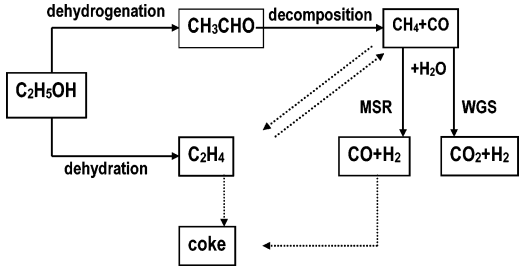

Figure 21. Reaction mechanism for steam re-forming of ethanol. Reprinted with permission from ref 361. Copyright 2004 Elsevier B.V.

4.2. Re-forming of Biomass-Derived Products

4.2.1. Ethanol

The production of ethanol by the fermentation of carbohydrates is the primary technology for the generation of liquid fuels from renewable biomass resources. Among the bio-fuel candidates for producing hydrogen, ethanol is of particular interest because of (i) its low toxicity; (ii) its moderate production cost; (iii) the fact that is a relatively clean fuel in terms of composition; (iv) its relatively high hydrogen content; and (v) its availability and ease of handling.

Hydrogen can be obtained directly from ethanol by two main processes: steam re-forming (SRE, eq 26) and partial oxidation (POE, eq 27). The overall processes summarized in eqs 26 and 27 are a complex convolution of elementary steps that involve several organic intermediates.

$$\mathrm{CH_3CH_2OH} + 3\mathrm{H_2O} \rightarrow 6\mathrm{H_2} + 2\mathrm{CO_2} \qquad \Delta H^\circ_{298\mathrm{K}} = +173.7\ \mathrm{kJ/mol} \quad (26)$$

$$\mathrm{CH_3CH_2OH} + 1.5\mathrm{O_2} \rightarrow 3\mathrm{H_2} + 2\mathrm{CO_2} \qquad \Delta H^\circ_{298\mathrm{K}} = -551.8\ \mathrm{kJ/mol} \quad (27)$$

Whereas POE offers exothermicity and a rapid response, SRE is endothermic and produces greater amounts of hydrogen, resulting in higher system efficiencies. A third option combines the advantages of both approaches by co-feeding oxygen, steam, and ethanol simultaneously through oxidative reforming process (ORE, eq 28.

$$\mathrm{CH_3CH_2OH} + x\mathrm{O_2} + (3-2x)\mathrm{H_2O} \rightarrow (6-2x)\mathrm{H_2} + 2\mathrm{CO_2} \quad (0 < x < 0.5) \quad (28)$$

$$\Delta H^\circ_{298\mathrm{K}} = (173.6-483.6x)\ \mathrm{kJ/mol}$$

4.2.1.1. Steam Re-forming. Stoichiometrically, the overall steam re-forming reaction of ethanol can be represented by eq 26. The process occurs with a catalyst at a temperature of 823−1073 K. Ethanol-re-forming reactions involve several reaction pathways (dehydration, decomposition, dehydrogenation, coking), depending on the catalysts and reaction conditions[343] (Figure 21). Therefore, the choice of catalyst plays a vital role in the re-forming process. Reactions to avoid are those that lead to C_4 and C_2H_4 inductive of carbon deposition on catalysts surfaces. Accordingly, catalysts for the steam re-forming of ethanol to produce H_2 selectively

must have catalytic surfaces able to (i) dehydrogenate ethanol; (ii) break the carbon−carbon bonds of surface intermediates to produce CO and CH_4; and (iii) re-form these C_1 products to generate hydrogen. According to the literature, different oxide catalysts,[344] metal-based catalysts (Ni, Co, Ni/Cu),[345−347] and noble metal-based catalysts (Pt, Pd, Rh)[348−351] have proven to be active in the ethanol-re-forming reaction. The metallic function and the acid−base properties of the catalysts play a central role in the re-forming reaction of ethanol. This is illustrated by the Cu/Ni/K/γ-Al_2O_3 catalyst, which exhibits acceptable activity, stability, and hydrogen selectivity at moderate temperature (573 K) and atmospheric pressure.[345] In this catalyst, copper is the active agent; the nickel promotes C−C bond rupture, increasing hydrogen selectivity, and the potassium neutralizes the acidic sites of the γ-alumina substrate and improves the general performance of the catalyst. The nature of the support hardly influences the catalytic performance of the supported catalyst for the steam re-forming of ethanol because it affects the dispersion and stability of the metal and may participate in the reaction. Lanthanum oxide is one of the best support candidates. It has been reported that Ni/La_2O_3 or Ni−La_2O_3/Al_2O_3 catalysts exhibit high activity and long-term stability for hydrogen production.[352,353] A 20% Ni/La_2O_3/Al_2O_3 catalyst exhibits good stability at 1023 K for time on-stream over 150 h, with only a small reduction in ethanol conversion from 95 to 90%, whereas hydrogen selectivity remains essentially constant. These results indicate the uniqueness of the Ni−La_2O_3 system in terms of its long stability. The unusual stability of the Ni−La_2O_3 catalyst has been attributed to the scavenging of coke deposition on the Ni surface by lanthanum oxycarbonate species existing on top of the Ni particles.[349] The effect of basic additives or promoters (K, Mg, Ca, Ce) that favor water adsorption and OH surface mobility in Al_2O_3 supports to lower the rate of coke deposition on catalyst surfaces has also been investigated on nickel-based catalysts.[354,355] Coke formation on bare and doped catalysts (Ce, K, and Mg) does occur, but with orders of magnitude lower than those claimed for Ni supported on acidic Al_2O_3.

Cobalt-based catalysts have also been proposed as appropriate for the re-forming reaction. Llorca et al.[347] studied the reaction between ethanol and water in the 573−723 K temperature range at atmospheric pressure over supported cobalt catalysts. The ZnO-supported cobalt catalyst, in which the ZnO substrate (specific area = 100 m^2/g) was prepared by thermal decomposition of zinc carbonate, exhibited the highest catalytic performance among the series. Using an $EtOH/H_2O$ = 1/13 (molar ratio) mixture, total conversion (100%) of ethanol and the highest values of H_2 (73.8%) and CO_2 (24.2%) were obtained, and in the absence of deactivation. Complete EtOH conversion was also reached on the ZnO substrate, but the yields of H_2 and CO_2 alone were found to be substantially lower. The decomposition of EtOH into acetone occurs to a large extent on Co/ZnO catalysts. Because this reaction results from consecutive reactions, such as dehydrogenation and aldol condensation, additional experiments have indicated that the re-forming reaction preferentially takes place at low contact times, whereas EtOH decomposition to acetone via aldol condensation of acetaldehyde is depressed. However, Co/ZnO shows a considerable amount of carbon deposition after the reaction, which causes the deactivation of cobalt catalysts.

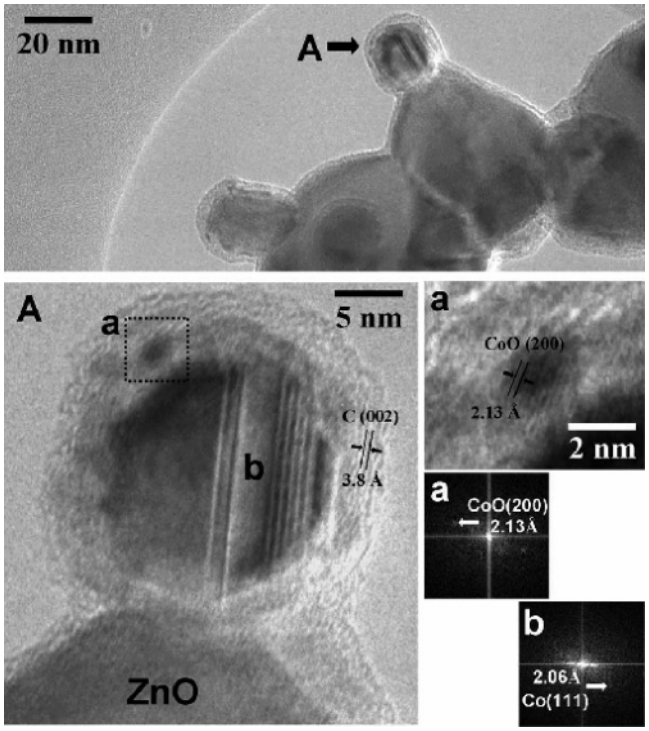

Figure 22. HRTEM images of Co/ZnO catalyst used in ethanol steam re-forming at 873 K. The size distribution of metal cobalt particles ranges from 3−4 nm to 15−30 nm. Small metal cobalt particles are located on ZnO, whereas larger cobalt particles are encapsulated in carbon filaments. Reprinted with permission from ref 374. Copyright 2004 Elsevier B.V.

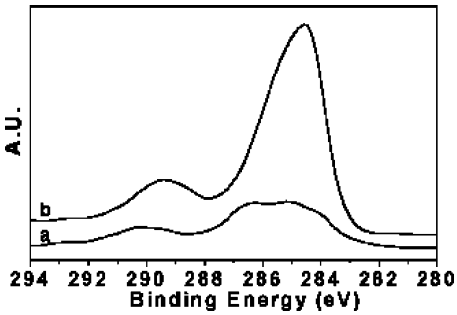

Figure 23. C1s core-level spectra of catalysts: (a) 0.98NaCoZn; (b) 0.06NaCoZn. Reprinted with permission from ref 374. Copyright 2004 Elsevier B.V.

TEM micrographs of used Co/ZnO catalyst at 873 K reveal the deposition of graphite-like carbon, as derived from the C(002) spacing of 0.346 nm calculated directly from lattice-fringe imaging (Figure 22).[356] The deactivation rate is dependent on the support used and the temperature. Sodium incorporation (0.06−0.98 wt %) to Co/ZnO catalysts results in a better performance in the ethanol-re-forming reaction. The production of hydrogen increases (5−8%) with the Na content under total conversion in the 623−723 K temperature range, and furthermore carbon deposition decreases, as evidenced by HRTEM, XPS, and Raman spectroscopy. The inhibition of carbon formation with increasing Na contents has been demonstrated by examination of the C 1s XPS core levels of the used catalysts. The C 1s spectra of two representative Na-promoted Co/ZnO catalysts (0.06 and 0.98 Na wt %) show four components at 284.3, 284.9, 286.3, and 290.0 eV (Figure 23) associated with graphitic carbon, adsorbed hydrocarbons, species containing C−O bonds, and surface carbonate species,[356] respectively. From Figure 23 it is clear that the generation of graphitic carbon is much

higher for the 0.06 Na− than for the 0.98 Na−Co/ZnO catalyst.

Noble metals supported on metal oxides of the type Al_2O_3, SiO_2, CeO_2, TiO_2, and MgO[348,351,357−363] display high activity in the steam re-forming of ethanol to CO_x and H_2. The support plays a significant role in the steam re-forming of ethanol over noble metals. When ceria/zirconia is used as the support of noble metals, ethylene formation is not observed and the order of activity at higher temperature is Pt ≈ Rh > Pd.[348] Alumina-supported catalysts are very active at low temperatures in the dehydration of ethanol to ethylene. At higher temperatures, ethanol is converted into H_2, CO, CO_2, and CH_4, with an activity order of metals as follows: Rh > Pd > Ni = Pt.[347] Auprêtre et al.[362] studied the effect of both the metal and the support in the steam re-forming of ethanol. They found that at 973 K the hydrogen yield on alumina-supported metal catalysts decreased in the following order: Rh > Pd > Pt > Ru. They concluded that the high activity of the metals in ethanol steam re-forming and their poor efficiency in the water gas shift reaction would give active and selective catalysts for ethanol re-forming. Auprêtre also reported that the H_2 yield on Rh/CeO_2 was higher than that on Rh/Al_2O_3 at 873 K.[362] It was concluded that a metal−ceria interaction affects the absorption−decomposition of ethanol to CH_4 and CO products and their subsequent re-forming reactions with steam. Cavallaro[359] reported a reaction pattern over Rh/Al_2O_3. First, ethanol is converted to ethylene by dehydration on the Al_2O_3 surface or to acetaldehyde by dehydrogenation on Rh particles. The acetaldehyde undergoes decarbonylation on the rhodium surfaces to form methane and CO, whereas ethylene is also steam re-formed on metal particles to C_1 (very fast reactions). Liguras et al.[349] also found that among the low-loaded catalysts, Rh was significantly more active and selective toward hydrogen formation than Ru, Pt, and Pd. The catalytic performance of Rh was greatly improved by the increase of metal loading. Cavallaro et al.[363] reported that 5 wt % Rh/Al_2O_3 at 923 K had good stability; only 10% of activity was lost after 95 h of reaction. Long-term experiments have demonstrated high hydrogen selectivity (up to 95%), which remains constant with time, without carbon formation.

4.2.1.2. Catalytic Partial Oxidation. The partial oxidation of ethanol (POE, eq 27) has also been investigated, but with less intensity than in the case of the steam re-forming. Partial oxidation is a very interesting process for hydrogen production because these partial oxidation systems can be run autothermally, thereby eliminating the need for external heat. Moreover, POE is much faster than the catalytic steam re-forming, which allows fast start-up and short response times to variations in H_2 production. However, use of the pure partial oxidation process is not indicated for bio-ethanol re-forming because bio-ethanol is an ethanol−water mixture in which the removal of all of the water has a significant cost. Therefore, for bio-ethanol partial oxidation the processes are usually combined with steam re-forming in autothermal schemes with the stoichiometry shown in eq 29. Additionally, adding water to the reaction stream is very useful because catalyst stability is improved while coke formation is minimized due to the fact that under pure partial oxidation conditions an extensive formation of encapsulated carbon is observed.

$$C_2H_5OH + 2H_2O + {}^1/_2O_2 \rightarrow 2CO_2 + 5H_2 \qquad \Delta H^\circ_{298K} = -68.2 \text{ kJ/mol} \quad (29)$$

The generation of hydrogen from ethanol via catalytic autothermal partial oxidation (eq 29) has been performed at temperatures of 700−1000 K using catalytic systems based on noble metals.[364,365] Ethanol oxidation follows a very complex pathway, including several reaction intermediates formed and decomposed on both the supports and active metals that integrate the catalytic systems.[366,367] In light of the above studies, it has been claimed that the ethoxy species generated on the metal and on the support can be decomposed on the metal sites, forming CH_4, H_2, and CO, whereas part of the ethoxy species generated on the supports is further oxidized to acetate species, which decompose to CH_4 and/or oxidize to CO_2 via carbonate species.[364] Thus, supports with redox properties that help the oxidation of ethoxy species and metals with a high capacity to break C−C bonds and to activate C−H bonds are suitable for use in catalysts applied to the partial oxidation of ethanol. Salge et al.[365] studied the effect of the nature of the metal (Rh, Pd, Pt) on the performance of catalysts supported on Al_2O_3 and CeO_2. The order of effectiveness in hydrogen production for catalysts supported on Al_2O_3 was Rh−Ru > Rh > Pd > Pt. Rh supported on CeO_2 was the most stable and gave greater hydrogen selectivity than noble metals supported on Al_2O_3. The better activity and stability associated with the presence of CeO_2 can be related to the capacity of CeO_2 to store oxygen and make it available for reaction via a redox reaction.[368]

4.2.2. Sugars

An innovative aqueous-phase re-forming (APR) process for the conversion of sugars and polyols into H_2 and C_1−C_{15} alkanes has been developed by Dumesic et al.[369−372] Hydrogen, CO_2, CO, and light alkanes are produced by APR of the aqueous sugar feeds under pressures ranging from 10 to 50 bar (eq 30). This technology is being commercialized by Virent Energy Systems. One of the advantages of APR is that it produces a hydrogen-rich stream with low levels of CO (100−1000 ppm), which makes it particularly suited for feeding PEM FCs.

$$C_6H_{14}O_6 + 6H_2O \rightarrow 6CO_2 + 13H_2 \qquad \Delta H^\circ_{298K} = +443.5 \text{ kJ/mol} \quad (30)$$

The reaction pathway of APR involves cleavage of C−H, C−C, and O−H bonds of sugar molecules to form adsorbed species on the catalyst surface. Adsorbed CO must be removed by the WGS reaction to form CO_2 and additional H_2. Undesired parallel reactions also occur and proceed via C−O bond splitting followed by hydrogenation to yield alcohols or even acids. Thus, good catalysts for the production of H_2 by APR reactions must be highly active for C−C bond cleavage and also capable of removing adsorbed CO by the WGS reaction, but it must not facilitate C−O bond cleavage and hydrogenation of CO_x. The H_2 selectivity depends on the feed sugar, the catalyst, and the reaction conditions. As a general trend, H_2 selectivity decreases upon increasing the size of feed molecule.

Kinetic studies were carried out for the APR of ethylene glycol (a probe molecule for sorbitol) over silica-supported Pd, Ni, Pt, Ir, Ru, and Rh catalysts at moderate temperatures (483−498 K) and moderate pressure (22 bar). The catalytic activity for APR of ethylene glycol, as measured by the rate of CO_2 formation per surface atom at 483 K follows the order Pt ∼ Ni > Ru > Rh ∼ Pd > Ir.[372] Silica-supported Ni, Ru,

and Rh catalysts displayed low selectivity for H_2 production and high selectivity for alkane production. In addition, the Ni/SiO_2 catalyst became rapidly deactivated at 498 K. On the contrary, Pt/SiO_2 and Pd/SiO_2 catalysts exhibited higher selectivity for production of H_2, with lower rates of alkane production. It was also found that both activity and selectivity of Pt-based monometallic catalysts can be enhanced by depositing Pt on TiO_2, carbon, and Al_2O_3 substrates[373] or by adding Ni, Co, or Fe to a monometallic Pt/Al_2O_3 catalyst.[374] PtNi and PtCo catalysts supported on alumina with Pt/Co or Pt/Ni atomic ratios ranging from 1:1 to 1:9 had the highest turnover frequencies for H_2 production (moles of H_2 per mole of surface site measured by CO adsorption) with values of 2.8−5.2 min^{-1} for APR of ethylene glycol solutions at 483 K, compared to a value of 1.9 min^{-1} for the monometallic Pt/Al_2O_3 under similar reaction conditions.

Nickel catalysts are also active for APR reactions; however, they have low selectivity and stability. The H_2 selectivity of Ni-based catalysts can be enhanced by adding Sn to the Ni catalyst, wheres its stability can be improved by using bulk Ni catalysts, for example, Raney Ni.[375] The rates of H_2 production by APR of ethylene glycol over a SnNi catalyst with Ni/Sn atomic ratios up to 14:1 are comparable to a 3 wt % Pt/Al_2O_3 catalyst, based on reactor volume. Incorporation of Sn to Raney Ni catalysts markedly decreases the rate of methane formation from reactions of CO_x with H_2, while maintaining the high rates of C−C cleavage necessary for the production of H_2. Notwithstanding, the reactor must operate near the bubble-point pressure of the feed and moderate space times to achieve high H_2 selectivities over Raney SnNi catalysts. These Raney SnNi catalysts are stable for more than 250 h time on stream.[375]

The alkane selectivity can be enhanced by changing the catalyst and reaction conditions. Alkanes are produced by aqueous-phase dehydration/hydrogenation (APD/H) reactions of sorbitol (eq 31) with a catalyst consisting of a metal (Pt, Pd) function and an acid substrate, for example, $SiO_2-Al_2O_3$, able to catalyze hydrogenation and dehydration reactions, respectively.[371] Hydrogen is produced for this reaction by APR (eq 30). These APR and APD/H reactions can be performed in a single reactor or two separate ones; the net reaction is exothermic, in which approximately 1.5 mol of sorbitol produce 1 mol of hexane. The APD/H reaction occurs in the liquid phase; therefore, vaporization of the aqueous feed is not needed, and accordingly the overall thermal efficiency of the process is improved. The alkane selectivity depends on the relative rates of C−C bond cleavage, dehydration, and hydrogenation reactions. The alkane selectivity can be modified not only by changing the catalyst composition, the reactor, and reaction conditions, but also by co-feeding H_2 with aqueous sorbitol, leading to a process in which sorbitol is converted to alkanes and water without the formation of CO_2.

$$C_6H_{14}O_6 + 6H_2 \rightarrow C_6H_{14} + 6H_2O \qquad \Delta H^\circ_{298K} = -264.2 \text{ kJ/mol} \quad (31)$$

Alkane production from sugars by APD/H process has the advantage that most of the alkane fraction is spontaneously separated from the aqueous phase, whereas ethanol produced by fermentation must be removed from solution by an energy-intensive distillation step. A rough estimate for the production of alkanes by APR process from corn is double the energy efficiency for the production of ethanol from corn.[369] In summary, alkanes produced by the APD/H of sugars would provide a renewable source of hydrocarbons that could fit into the current distribution infrastructure. Unfortunately, the major compound produced by the APD/H process is hexane, which in turn has a low value as a gasoline additive because of its high volatility. This limitation has been overcome at least in part by combining the APD/H reaction with a base-catalyzed aldol condensation step. This step links carbohydrate-derived units via formation C−C bonds to form heavier alkanes ranging from C_7 to C_{15}.[369] It is emphasized that the C−O−C bonds of the sugar molecules are broken under APD/H process conditions, whereas the aldol condensation produces large organic water-soluble compounds derived from sugars. Then, these molecules are transformed into alkanes in a specially designed four-phase dehydration/hydrogenation reactor.

5. Secondary Reactions in Hydrogen Production Schemes

5.1. Hydrogen Production from CO

5.1.1. Water Gas Shift Reaction

The WGS reaction (eq 2) is one of the oldest catalytic processes employed in the chemical industry (hydrogen production, ammonia, methanol, ...) for converting the CO present in re-formate streams in additional hydrogen. Currently there is great interest in the WGS reaction for the removal of carbon monoxide at small scale for future power generation using FCs for both mobile and stationary applications. The use of small WGS catalytic units coupled with small-scale re-formers imposes different requirements as compared to large-scale hydrogen production units. Among these requirements, good activity at moderately low temperature (below 553 K), stability under typical reformate conditions, non-pyrophoric formulations, durability under steady-state and transient conditions, mechanical resistance to thermal shock, stability to poisons (chlorine, H_2S), and no side reactions, that is, methanation, which consumes additional hydrogen, are all key requirements to be fulfilled by the new generation of WGS catalysts.

5.1.1.1. Conventional Catalysts. The WGS reaction is an exothermic, reversible reaction. The equilibrium constant of the reaction decreases as the temperature increases. To increase the CO conversion, it is thus desirable to perform WGS at low temperatures. However, to achieve sufficiently high reaction rates, it is often necessary to operate in two catalytic stages: a high-temperature shift (HTS) and a low-temperature shift (LTS). In industrial applications, the conventional catalyst formulations employed are $Fe_2O_3-Cr_2O_3$ and $Cu-ZnO-Al_2O_3$ for the HTS and LTS units, respectively.[376−379] For typical re-formate streams (8−10% vol CO), the HTS reactor operating at near equilibrium (623−693 K) reduces the CO level to about 4% vol, whereas the LTS working at 453−613 K achieves 0.4−0.8% vol of CO. Many studies have been conducted on the preparation,[380−382] kinetics, or reaction mechanisms of conventional WGS catalysts.[380,383,384] Notwithstanding, the debate concerning the mechanism of the reaction continues and, more specifically in the case of the LTS catalyst, about whether the mechanism takes place through associative or regenerative pathways (see section 5.1.1.3). $Fe_2O_3-Cr_2O_3$ and Cu−

$ZnO-Al_2O_3$ catalysts have some drawbacks: the low activity of the former catalyst at high temperature, the pyrophoric nature of the latter, the lengthy preconditioning of both types, and the large reactor volume dictated by the slow kinetics of the $Cu-ZnO-Al_2O_3$ catalyst. These limitations therefore make classical WGS catalysts unsuitable for use in small-scale re-formers, where fast response and low catalyst volume are mandatory. Thus, the design of new WGS catalysts for application in fuel re-formers must overcome such limitations. Improved performance of Cu−ZnO systems can be achieved upon promotion with alkali.[385,386] Moreover, better activity and durability under steady-state operation are gained upon modification of Raney Cu−ZnO catalysts with TiO_2 or ZrO_2.[217]

5.1.1.2. Alternative Catalysts. When activity and cost are balanced, two trends can envisaged in the development of new WGS catalysts for fuel re-formers: non-precious metal catalysts that are active at high temperature and precious metal formulations [Pt group metals (PG) or Au], displaying high activity over a larger temperature range.

Non-precious transition metals are particularly suited for the WGS reaction owing to their low cost in comparison with PG metal catalysts. As an alternative to commercial CuZnO, the Argonne National Laboratory has developed low specific area cobalt−vanadium binary oxides,[387] which display specific activities (normalized to surface area) that are higher than those of CuZnO. Similarly, high-surface area molybdenum carbide (Mo_2C) has been found to be an active LTS formulation, with activity comparable to or higher than that of $Cu-ZnO-Al_2O_3$.[388] These nanocrystalline Mo_2C catalysts, known as active hydrotreating catalysts, are sensitive to oxygen, and their performance under real fuel-processing conditions has yet to be studied.

For the HTS reaction, Haldor-Topsoe has recently developed a series of alkaline-promoted, sulfur-resistant oxides based on Mg, Al (magnesium aluminate spinel), La, Nd, Ce, Pr, Mn, $Co-MgAl_2O_4$, K-ZSM5, $Mg-ZrO_2$.[389] These formulations are moderately active (25−30% CO conversion) at temperatures above 673 K, but with the benefit over other high temperature formulations, such as Co- or Ni-promoted MoO_3, V_2O_5, and WO_3 oxides,[390] of the absence of methanation. Cobalt−molybdenum or nickel−molybdenum sulfide[391] catalysts or their alkaline-promoted forms are active, sulfur-tolerant HTS formulations, with a CO conversion above 40% at low space velocities ($<8000\ h^{-1}$).[392] The activity of these formulations at high temperature and their acceptable CO conversions at relatively low space velocities ($<20000\ h^{-1}$) means that, for their application in fuel re-formers, additional downstream, more active WGS catalysts are needed.

CeO_2-containing WGS catalysts have attracted interest on the basis of the oxygen storage capability (OSC) of ceria[393−395] and the cooperative effects developed at the interface between metal particles and the ceria surface. Although ceria or ceria-promoted formulations have mainly been reported in conjunction with precious metals, non-PG-loaded ceria WGS catalysts have also been developed as potentially better alternatives to $Cu-ZnO-Al_2O_3$. Li et al. reported that Cu or Ni nanoparticles deposited on high surface area Ce(La)-O_x supports, prepared by urea precipitation−gelation,[396] displayed good LTS activity at high space velocities when tested under CO concentrations in the feed stream of 2% vol. The high activity was interpreted as being due to the enhanced reducibility of ceria in the presence of the metal. Durability performance has not been reported for these formulations.

Along the development of three-way catalysts (TWC) in the early 1980s, it was discovered that ceria is the best non-noble metal oxide promoter for Pt, Pd, and Rh nanoparticles when deposited on alumina because these strongly enhance the water gas shift reaction.[393] In parallel, it was demonstrated that Pt/CeO_2 catalysts are active in both the methanation and WGS reactions.[397] Pt/CeO_2 catalysts have been reported to be active and non-pyrophoric, with activity higher than that of conventional WGS catalysts in the medium-temperature range (573−673 K), thus demonstrating their potential for use in WGS reactors. Mechanistic studies on the WGS reaction over ceria-supported Pt, Pd, Rh, Ni, Fe, and Co metals have emphasized the importance and implications of the OSC of CeO_2.[398,399] The high OSC, CO_2 coverage,[400] and surface hydration[392] are proposed as being responsible for the high activity when metal−ceria interactions are established.

The preparation method plays an important role in establishing the metal−support interaction and influences the low-temperature activity.[401] This is clearly seen on comparison of the performance of Pt/CeO_2 catalysts. The traditional methodology, consisting of the impregnation of a ceria substrate, develops a standard architecture of supported catalysts, which consists of highly dispersed nanoparticles on the CeO_2 substrate with a high concentration of interfacial sites between metal particles and the ceria surface. Notwithstanding, the microemulsion methodology gives rise to a reverse morphology dominated by the coverage of platinum particles by the cerium oxide. In addition, the microemulsion Pt/CeO_2 catalyst exhibits unusual performance. Indeed, it is highly active for the WGS reaction but does not catalyze the methanation reaction between carbon oxides and hydrogen streams at all. In contrast, the Pt/CeO_2 catalyst prepared by conventional method produces methane via hydrogenation of CO_x.

Despite the high initial activity obtained in the medium−high-temperature range (598−673 K), the $Pt-CeO_2$ catalyst loses activity. Such deactivation can be explained in terms of several mechanisms, including surface coverage with in situ formed carbonate-like species and partial loss of reoxidizing ability in the highly reducing CO/H_2 environment. An initial decrease in metal dispersion and the total BET surface area has been observed after the first hours of operation. At extended reaction times, ceria crystallite size slowly increases, leading to a further gradual decrease in total specific area and to the occlusion of Pt particles in the support. These behaviors suggest multiple operating mechanisms in addition to the redox process generally claimed, depending on the temperature and inlet concentrations. Consequently, multiple deactivation pathways are also available. The overall deactivation using typical re-formate tests leads to the partial loss of WGS activity to levels that would require overdesign of WGS reactors for long-term operation.[402] Start−stop cycles do not lead to significant additional losses in activity, indicating that the (hydroxy)carbonate buildup observed on Pt on CeO_2 surfaces during this operational mode is suppressed by the addition of ZrO_2 to the support in a mixed oxide.[403] No significant deactivation is observed during the simulated shutdown with water condensation in the catalyst particles, contrary to Pt/CeO_2. In any case, it is imperative to develop Pt catalysts that will be stable against sintering, given their nontoxicity, their lack

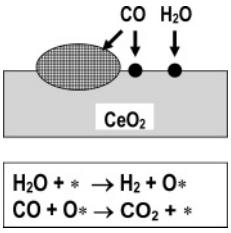

Figure 24. Scheme and sketch diagram of the regenerative (or redox) mechanism for the WGS reaction.

$$CO + * \rightarrow CO*$$
$$H_2O + 2* \rightarrow H* + OH*$$
$$OH* + CO* \rightarrow HCOO* + *$$
$$HCOO* + * \rightarrow CO_2* + H*$$
$$CO_2* \rightarrow CO_2 + *$$
$$2H* \rightarrow H_2 + 2*$$

Figure 25. Scheme of the adsorptive (or associative) mechanism for the WGS reaction.

of self-heating, and their stability against exposure to air and start−stop operations, unlike Cu−ZnO−Al_2O_3 catalysts.[404]

Besides ceria-supported precious metal catalysts, TiO_2-supported systems are also good catalysts, showing activity close to Cu catalysts in low temperature. Especially, a Pt−Re/TiO_2 catalyst has superior catalytic activity compared to a commercial Cu−Zn catalyst.[405] Characterization data of the Pt−Re/TiO_2 catalysts by TEM and XPS measurements have shown that Re acts as an anchor for the Pt particles under the reaction conditions. Thus, a high dispersion of Pt has been achieved.

Gold catalysts are attracting rapidly growing interest for WGS owing to their high activity for CO oxidation at low temperature.[406−408] Gold nanoparticles deposited on CeO_2,[409,410] TiO_2,[411] and Fe_2O_3[412] display good performance in WGS reaction; the improved WGS activity at low temperature is explained as due to the synergism of gold−metal oxide. Gold catalysts, however, are sensitive to the preparation conditions, the desired properties of the final material depending on dispersion, gold particle size, and the metal−support interaction.[409] The gold particle size has a strong impact on the activity and can easily change during the reaction. Improved stability has been reported[402] recently, but further development is needed for these catalysts to become candidates for the demanding conditions in fuel reformer applications.

5.1.1.3. Mechanisms. The kinetics and mechanism of the WGS reaction with various catalyst systems have been carried out in recent years. On the basis of kinetics results, two types of mechanisms have been proposed: the "regenerative mechanism" (Figure 24) and the "adsorptive mechanism" (involving in particular formate surface species; Figure 25). In the regenerative mechanism[376,395,398,413−417] (Figure 24), water adsorbs and dissociates on a partly reduced support, releasing H_2 and reoxidizing the support. In parallel, CO adsorbs on metallic sites to form a metal-bound carbonyl species, which then reduces the support and releases CO_2. The applicability of this redox mechanism is by nature restricted to catalysts supported on "reducible" carriers and has been proposed to explain the high WGS activity of CeO_2-supported copper[413] (Figure 24) and noble metals.[414−417]

In the adsorptive (or associative) mechanism[418−423] (Figure 25), CO and H_2O are proposed to adsorb on the catalysts and form a surface intermediate, which subsequently decomposes as H_2 and CO_2. Many research groups have tried to identify the nature of the main intermediate species mainly by isotopic labeling experiments and FT-IR spectroscopy. Formate[424,425] and carbonate species[426] have been proposed as main intermediate surface species evolved in the forward-WGS reaction.

5.1.1.4. Membrane Reactors. Inorganic and organic membrane reactors can be used to improve WGS reaction performance with the in situ separation of products. It is possible to overcome thermodynamic constraints and increase the CO conversion significantly. In comparison with organic membranes, inorganic membranes have better mechanical strength and thermal stability. The modeling results of CO_2-selective WGS membrane reactors show that a CO concentration of less than 10 ppm, an H_2 recovery of higher than 97%, and an H_2 concentration of more than 54% are achievable from autothermal re-forming syngas.[427] If steam re-forming syngas is used as the feed gas, the H_2 concentration may reach 99.6%. By using palladium or other inorganic H_2-selective WGS membrane reactors, high CO conversion values beyond the equilibrium ones or close to 100% are attained.[428−432] However, Pd membranes have a high module cost and show performance instability in the presence of hydrocarbons or steam. Therefore, silica membranes are very attractive for H_2 production by WGS reactions.

Molecular sieve silica (MSS) membrane-packed bed reactors using a classical Cu/ZnO−Al_2O_3 catalyst display good performance in low-temperature WGS.[431] By using a $CO/H_2O = 1$ (molar ratio) at the inlet, this approach allows a 99% CO conversion to be achieved at 553 K. This CO conversion level is well above the thermodynamic equilibrium and achievable bed reactor conversion. In another approach, silica−porous stainless steel composite membranes have been successfully modified using nickel and silica.[433] The silica top layer was coated on the support by repeating the whole process of dipping−drying−calcination using colloidal silica sol prepared by the hydrolysis of tetraethyl orthosilicate (TEOS). Because highly branched silica particles in colloidal sols cannot interpenetrate due to steric hindrance, a microporous thin film is formed during consolidation while a dense thin film is induced by polymeric silica sols. For a 1% CO/H_2 feed mixture, the silica stainless steel membrane reduces the CO concentration to 81 ppm.[433] Hydrophilic membranes undergo pore widening during the reaction, whereas hydrophobic membranes display no such behavior and also show increased H_2 permeation with temperature.

5.2. CO Removal Reactions

Small amounts of CO present in the H_2 streams poison the Pt electrocatalysts of PEM fuel cells. Although more effective CO-tolerant fuel cell catalysts are being developed,[378] work is needed to develop catalysts that selectively remove the 0.5−1% of CO from the H_2-rich streams prior to reaching the fuel cell. The approaches undertaken include CO preferential oxidation, catalytic methanation, and Pd-membrane separation. Among these, preferential oxidation (PROX) remains prominent because it is the lowest cost method available for reducing CO to the desired level without excessive hydrogen consumption.

5.2.1. Preferential CO Oxidation

PROX removes CO from H_2-rich gas streams by means of catalytic oxidation with molecular oxygen. In this process the main reactions involved are

$$CO + {}^1/_2O_2 \rightarrow CO_2 \quad \Delta H^\circ_{298K} = -283.0 \text{ kJ/mol} \qquad (32)$$

$$H_2 + {}^1/_2O_2 \rightarrow H_2O \quad \Delta H^\circ_{298K} = -241.8 \text{ kJ/mol} \qquad (33)$$

As both of the reactions are highly exothermic, it is important to remove heat from the reactor. Temperature control is critical to catalyst selectivity. On the basis of the relative heats of adsorption of CO and H_2 on metals that catalyze the reaction, it is very likely that the selectivity of the catalysts to preferentially oxidize CO before H_2 will be greatly reduced at higher temperatures. For that reason, multistage PROX systems with interstage cooling[434] can be used. An excellent design of PROX reactor is seen in catalyzed microchannel heat exchangers,[435] which ensure closer to isothermal operation and hence better catalyst utilization and a longer life.

High activity and selectivity are essential parameters in PROX catalysts; the catalyst should oxidize 0.5−1% CO to less than 50 ppm without oxidizing a large amount of hydrogen at the selected process temperature, usually between the outlet temperature of the WGS reactor and the inlet temperature of the PEM fuel cell (below 363 K). The lower the selectivity of the process, the higher the required O_2/CO ratio must be to completely oxidize CO to CO_2. As secondary reactions, reversed WGS and methanation of CO may occur, depending on the reaction conditions. For a typical level of CO of 1% in the feed stream, the overall CO conversion must be higher than 99.5% for a reduction of the CO level to be less than 50 ppm.

Considering the high activity required to remove CO while maintaining a high CO oxidation selectivity, catalyst formulations used for PROX involve a PG metal (Pt, Pd, Ru) loaded on high surface area supports.[436−443] Oxidation of CO on these catalysts is a multistep process obeying a single-site competitive Langmuir−Hinshelwood mechanism between CO and O_2, which compete for noble metal surface. These catalysts are characterized by operating at high temperature (about 470 K) and needing high oxygen excess for complete depletion of CO, with the corresponding lack of selectivity. However, they are resistant to deactivation by water, although slightly inhibited by CO_2. The key for improving CO oxidation is to add sites for oxygen adsorption to have a noncompetitive dual-site mechanism for CO oxidation. Following this line, new catalyst formulations are being developed by addition of promoters that enhance oxygen adsorption. In this sense, Pt-based catalysts are promoted with Fe,[436−438] Ce,[444] Co, Ni,[445,446] and alkalines.[447,448] Copper catalysts on alternative supports such as ceria, ceria−samaria, or other ceria-promoted supports are also being developed in an attempt to provide selective surface oxygen for CO oxidation at low temperatures.[449,450]

Extremely fine dispersed gold particles have been reported to be very active at very low temperatures.[439−443] However, they are very sensitive to the presence of CO_2 and steam. Using several oxide substrates, it has been shown that the reaction rates on gold particles of both CO and H_2 oxidations depend markedly on the choice of the support oxide. The variations in activity and stability are related to the different tendencies of the substrates to form surface carbonates, which impairs both CO and H_2 oxidation: Co_3O_4- and MgO-supported catalysts are the most strongly affected catalysts. Au/α-Fe_2O_3 catalysts are the most active ones assayed to date, and complete reversibility of the deactivation can be achieved simply by flushing the catalyst bed with an inert gas, suggesting the use of flushing cycles for practical applications.

There is also evidence that the ratio between the Au and support oxide particle size affects performance. Au particles of ca. 5 nm on mixed oxides have been shown to have greater activity for CO oxidation at low temperatures.[451] In the Au−MgO−MnO_x−Al_2O_3 catalyst, MgO is thought to be a stabilizer for Au nanoparticles and MnO_x for the cocatalyst. H_2 oxidation is relatively suppressed in this complex catalyst. The behavior of Au/Al_2O_3 catalysts is seen to be anomalous on comparison of their performance in CO oxidation and in selective CO oxidation (in the presence of H_2): whereas this catalyst is stable in selective CO oxidation, its activity drops rapidly in CO oxidation, although it is fully restored upon exposure to H_2 at ambient temperature. This result suggests that the active sites contain hydroxyl groups, which can be removed by CO oxidation. These weakly bonded hydroxyls, likely on the Au surface, participate in the reaction, possibly by reaction with CO to form an active intermediate in the CO formation pathway. These surface species, possibly a carbonate, can react with H_2 to regenerate the hydroxyl groups. Consistent with this interpretation is the high susceptibility of these catalysts to poisoning by chloride ions, because chloride may displace the OH groups.

The kinetics of CO oxidation on a 0.5% Pt/Al_2O_3 catalyst has also revealed that the presence of hydrogen increases the rate of CO oxidation in the low-temperature region,[452] although it falls markedly at temperatures above 523 K. This is because the reaction kinetics and selectivity depend on the steady-state coverage of the metal with CO in the presence of H_2. This simple interpretation explains the differences between Pt/γ-Al_2O_3 and Au/α-Fe_2O_3 catalysts.[453] The decrease in the selectivity of Au/α-Fe_2O_3 with temperature as compared to that of Pt/γ-Al_2O_3 is related to the difference in the CO surface coverage as a function of temperature on the two surfaces.[453] This kind of behavior explains the larger range of operation for Pt catalysts in the PROX reaction, whereas the Au formulation remains attractive for low-temperature operation.

6. Future Opportunities

There are many challenges to be overcome before hydrogen can be widely used in energy schemes. Hydrogen production, storage, and use are mature technologies that efficiently deliver large quantities of H_2 to industry. However, many existing hydrogen technologies require further development aimed at improving performance and reducing costs before they can be commercialized. As mentioned in this review, the large-scale production of hydrogen from natural gas and other available hydrocarbons through catalytic steam re-forming and other kinds of re-forming remains the cheapest source of hydrogen. Even when the cheapest production method is used (SMR), some authors deem that hydrogen production is still 4 times the cost of gasoline production for the equivalent amount of energy.[454,455] Additionally, production from methane does not reduce fossil fuel use or CO_2 emission. Furthermore, this methodology not only suffers from technical problems but also has chemical shortcomings in its advanced application for the

hydrogen energy economy, typically related to the need for extremely pure hydrogen, for example, for fuel cell applications. Such shortcomings of conventional hydrocarbon re-forming result in the production of H_2 mixed with carbon oxides, which often demands stringent and energy-consuming extraction and cleaning of hydrogen from the syngas obtained.

Some improvements in the present technologies for the bulk production of H_2 could be achieved with new catalytic systems able to inhibit the formation of carbon deposits and enhance surface re-forming reactions. Operative re-formers are heat transfer-limited rather than reaction rate-limited and are loaded with large excesses of catalysts to reach the space velocities required in the process. Improved or new alloys for the tubes of the re-former as well as improved methodologies for the transport of heat from the outside to the reaction zone are expected to increase overall yield and performance. Microchannel reactors are one of the most attractive options for reducing capital costs by intensifying reactor equipment and for reducing operating costs by improving heat and mass transfer. Experiments conducted at contact times below 1 ms in a 0.28 mm thick porous catalyst structure held adjacent to the flow gap have shown that a greater than 98% approach to equilibrium methane conversion can be achieved.

Other no less important research areas include gaining a precise knowledge of the chemical and physical processes involved in re-former operation. These include (i) sulfur passivation of highly active surface sites; (ii) growth of metal particles of the active phase due to thermal sintering; (iii) metal dust formation; and (iv) efficient use of energy. Because sulfur is present in most feedstocks, efforts should be made to address S removal as well as to develop improved S tolerant catalysts. Because re-forming reactions operate at temperatures above 1000 K, the sintering of nickel crystallites limits catalyst performance. Therefore, a better understanding of the factors responsible for particle agglomeration and ways to prevent this should be explored in detail. An understanding of the chemical processes involved in the corrosion of the reactor walls and dust formation is needed, as well as investigation of the factor(s) responsible for dust formation. Approximately 50% of the fuel spent to heat SMR tubes is indeed used to make H_2; the other 50% is recovered in steam but is not useful for making additional H_2. Research aimed at unraveling more efficient ways to utilize energy in SMR operations must be conducted with a view to increasing efficiency and reducing CO_2 emissions.

To take full advantage of the environmental benefits of hydrogen, low carbon emitting, low-polluting, low-cost hydrogen production systems are needed. Today, hydrogen production at large scale is performed by re-forming or gasification of fossil fuels. These are well-established technologies but produce massive amounts of carbon dioxide. Carbon sequestration is a process for permanently storing CO_2 gas in geologic or ocean reservoirs. If proven to be safe, permanent, and environmentally benign, sequestration could be used to reduce atmospheric CO_2 emissions from burning coal and other fossil fuels, potentially making them more acceptable sources of hydrogen or electricity in the short term. However, producing hydrogen from coal can never be an option unless such carbon can be stored safely for the long-term without other adverse environmental impacts. The safety and long-term viability of storage are uncertain, and the adverse environmental and health impacts of coal mining, mountain-top removal, and power plant waste disposal remain a problem for even the most advanced coal-fired power plants and carbon sequestration technologies.

Clean biomass, which includes sustainably grown energy crops and sustainable retrievable agricultural wastes, could also be an important short-term source of hydrogen for fuel cell vehicles and electricity generation. Clean biomass is a proven source of renewable energy that is now used for generating heat, electricity, and liquid transportation fuels. Clean biomass is an appropriate precursor to produce hydrogen through a process in which the biomass is converted to a gas and hydrogen is extracted. Virtually no net greenhouse gas emissions result because a natural cycle is maintained, in which carbon is extracted from the atmosphere during plant growth and is released during hydrogen production. Replanting and reforesting are prerequisites for maintaining a renewable hydrogen supply from biomass.

There is growing concern about the potential worldwide environmental impact that will come from the vast amounts of carbon dioxide that are released from the combustion of fossil fuels. Possible impacts range from global warming to the acidification of the ocean. Unless action is taken, future carbon dioxide emissions will dwarf those produced to date. Los Alamos National Laboratory (LANL) leads a number of scientific efforts to isolate and dispose of carbon dioxide before it ever reaches the air and to remove carbon dioxide from the atmosphere directly.

The stability of the world's economy depends on abundant energy. For economic reasons, the energy supply has been, and in all likelihood will continue to be, dominated by fossil fuels, which are still plentiful. Limiting energy use to curtail carbon dioxide emissions would stifle economies and leave the majority of the world impoverished, because energy use is an enabling agent for wealth. Left unchecked, however, the atmospheric concentration of carbon dioxide will double in the next 50 years. This doubling will take atmospheric carbon dioxide levels well beyond the highest levels recorded in geologic strata, dating back 10 million years, with the potential for severe global impacts.

For permanent sequestration of carbon dioxide, enhanced mineral carbonation is being explored. This is an accelerated version of the natural process that has maintained atmospheric carbon dioxide levels at geological time scales. LANL has pioneered the research to react carbon dioxide with naturally occurring magnesium and calcium silicates to form stable carbonates, either by an industrial, above-ground process or by the injection of supercritical carbon dioxide into appropriate geological strata. Enormous deposits of such silicates in the form of serpentinite rocks are found in a number of locations. Future power plants could be located near these deposits, allowing immediate, permanent disposal of their carbon dioxide emissions.

In the 21st century, all of these methods used in some combination could enable human-dominated systems to continue to grow while maintaining the natural environmental balance of the planet.

There is a need to develop nonconventional processes for H_2 production. One emerging technology is the decomposition of methane, either in the presence of catalysts or via plasma activation, to carbon and H_2, although its industrial application seems to be questionable, taking into account the high energy required to split C−H bonds of the CH_4 molecule into C and H_2. The advantage of this process is

the possibility of coupling this H_2 source with fuel cells, the electrocatalysts of which tolerate CO levels up to 10 ppm. Whichever process is used for the production of H_2, the fundamental objective must be to transform carbon into an inactive form that may lead to excessive carbon accumulation in Earth's atmosphere.

7. Acknowledgment

We are grateful to many of our colleagues for their stimulating contributions to our endeavors and to our research sponsor CICyT and CAM (Spain) under Grants ENE2004-07345-C03-01/ALT and S-0505/EN/0404, respectively.

8. References

(1) Peña, M. A.; Gómez, J. P.; Fierro, J. L. G. *Appl. Catal. A: Gen.* **1996**, *144*, 7.
(2) Armor, J. A. *Appl. Catal. A: Gen.* **1998**, *176*, 159.
(3) Trimm, D. L.; Onsan, Z. I. *Catal. Rev. Sci. Eng.* **2001**, *43*, 31.
(4) Fierro, J. L. G.; Peña, M. A. In *Supported Metals in Catalysis*; Fernández-García, M., Anderson, J. A., Eds.; ICP: London, U.K., 2005; Chapter 7.
(5) Bockris, J. O'M. *Int. J. Hydrogen Energy* **2002**, *27*, 731.
(6) Ogden, J. M. In *Testimony to the Committee on Science*; U.S. House of Representatives: Washington, DC, 2003.
(7) Halmann, M.; Steinfeld, A. *Energy* **2006**, *31*, 3171.
(8) Mondal, K.; Lalvani, S. *J. Am. Oil Chem. Soc.* **2000**, *77*, 1.
(9) Fernández, M. B.; Tonetto, G. M.; Crapiste, G. H.; Damiani, D. E. *J. Food Eng.* **2007**, *82*, 199.
(10) Mathiak, J.; Hienzel, A.; Roes, J.; Kalk, Th.; Kraus, H.; Brandt, H. *J. Power Sources* **2004**, *131*, 112.
(11) Seo, Y. T.; Seo, D. J.; Jeong, J. H.; Yoon, W. L. *J. Power Sources* **2006**, *163*, 119.
(12) Ogden, J. In *Proceedings of the 8th National Hydrogen Association Meeting*, Arlington, VA, March 3−5, 1998; National Hydrogen Association: Washington, DC, 1998.
(13) Sjardin, M.; Damen, K. J.; Faaij, A. P. C. *Energy* **2006**, *31*, 2523.
(14) Jordal, K.; Bredesen, R.; Kvamsdal, H. M.; Bolland, O. In *Proceedings of the 6th International Conference on Greenhouse Gas Control Technologies*; Gale, J., Kaya, Y., Eds.; Pergamon Press: Kyoto, Japan, 2003; p 135.
(15) Wurster, R. In *Fuel Cell Teach-in European Commission DGTren*; L-B-Systemtechnik GmbH: Brussels, Belgium, 2002.
(16) Dunn, S. *Int. J. Hydrogen Energy* **2002**, *27*, 235.
(17) Barretto, L.; Makihira, A.; Riahi, K. *Int. J. Hydrogen Energy* **2003**, *28*, 267.
(18) Elam, C. C.; Padro, E. G.; Sandrock, G.; Luzzi, A.; Lindblad, P.; Hagen, E. F. *Int. J. Hydrogen Energy* **2003**, *28*, 601.
(19) Collot, A.G. In *Prospects for Hydrogen from Coal*; IEA Coal Research: London, U.K., 2003.
(20) Rostrup-Nielsen, P.; Sehested, J. S.; Nørskov, J. K. *Adv. Catal.* **2002**, *47*, 65.
(21) Ross, J. R. H. *Catal. Today* **2005**, *100*, 151.
(22) Rostrup-Nielsen, J. R. In *Catalysis Science and Technology*; Anderson, J. R., Boudart, M., Eds.; Springer Verlag: Berlin, Germany, 1984; Chapter 1.
(23) Trimm, D. L. *Catal. Today* **1997**, *37*, 233.
(24) Damen, K.; van Troost, M.; Faaij, A.; Turkenburg, W. *Prog. Energy Combust. Sci.* **2006**, *32*, 215.
(25) Balachandran, U.; Lee, T. H.; Chen, L.; Song, S. J.; Picciolo, J. J.; Dorris, S. E. *Fuel* **2006**, *85*, 150.
(26) Wei, J.; Iglesia, E. *J. Catal.* **2004**, *224*, 370.
(27) Rostrup-Nielsen, J. R. *Catal. Today* **1993**, *118*, 305.
(28) Bengaard, H. S.; Nørskov, J. K.; Sehested, J. S.; Clausen, B. S.; Nielsen, L. P.; Molenbrock, A. M.; Rostrup-Nielsen, J. R. *J. Catal.* **2002**, *209*, 365.
(29) Rostrup-Nielsen, J. R.; Bak Hansen, J. H. *J. Catal.* **1993**, *144*, 38.
(30) Lobo, L. S.; Trimm, L. D. *J. Catal.* **1973**, *29*, 15.
(31) Rostrup-Nielsen, J. R. *Stud. Surf. Sci. Catal.* **1991**, *68*, 85.
(32) Alstrup, I.; Andersen, N. T. *J. Catal.* **1987**, *104*, 466.
(33) Trimm, D. L. *Catal. Today* **1999**, *49*, 3.
(34) Bernardo, C.; Alstrup, I.; Rostrup-Nielsen, J. R. *J. Catal.* **1985**, *96*, 517.
(35) Stagg, S. M.; Resasco, D. E. *Stud. Surf. Sci. Catal.* **1997**, *111*, 543.
(36) Richardson, J. T.; Jung, J. K.; Zhao, J. *Stud. Surf. Sci. Catal.* **2001**, *136*, 203.
(37) Osaki, T.; Masuda, H.; Horiuchi, T.; Mori, T. *Catal. Lett.* **1995**, *34*, 59.
(38) Alstrup, I.; Clausen, B. S.; Olsen, C.; Smits, R. H. H.; Rostrup-Nielsen, J. R. *Stud. Surf. Sci. Catal.* **1998**, *119*, 5.
(39) Bradford, M. C. J.; Vannice, M. A. *Appl. Catal. A: Gen.* **1996**, *142*, 97.
(40) Efstathiou, A. M.; Kladi, A.; Verykios, X. E.; Tsipouriari, V. A. *J. Catal.* **1996**, *158*, 65.
(41) Bradford, M. C. J.; Vannice, M. A. *Catal. Rev.* **1999**, *41*, 1.
(42) Fischer, F.; Tropsch, H. *Brennstoff Chem.* **1928**, *3*, 29.
(43) Bodrov, I. M.; Apel'baum, L. O.; Tempkin, M. I. *Kinet. Katal.* **1964**, *5*, 596.
(44) Rostrup-Nielsen, J. R. *Stud. Surf. Sci. Catal.* **2004**, *147*, 121.
(45) Ashcroft, A. T.; Cheetham, A. K.; Green, M. L. H.; Vernon, P. D. F. *Nature* **1991**, *352*, 225.
(46) Wang, S. B.; Lu, G. Q. M.; Millar, G. J. *Energy Fuels* **1996**, *10*, 896.
(47) Yamazaki, O.; Nozaki, T.; Omata, K.; Fujimoto, K. *Chem. Lett.* **1992**, 1953.
(48) Perera, J. S. H. Q.; Couves, J. W.; Sankar, G.; Thomas, J. M. *Catal. Lett.* **1991**, *11*, 219.
(49) Solymosi, F.; Kutsan, G.; Erdohelyi, A. *Catal. Lett.* **1991**, *11*, 14.
(50) Batiot-Dupeyrat, C.; Valderrama, G.; Meneses, A.; Martínez, F.; Barrault, J.; Tatibouet, J. M. *Appl. Catal. A: Gen.* **2003**, *248*, 143.
(51) Goldwasser, M. R.; Rivas, M. E.; Pietri, E.; Pérez-Zurita, M. J.; Cubeiro, M. L.; Gengembre, L.; Leclercq, L.; Leclercq, G. *Appl. Catal. A: Gen.* **2003**, *255*, 45.
(52) Brungs, A. J.; York, A. P. E.; Claridge, J. B.; Márquez-Álvarez, C.; Green, M. L. H. *Catal. Lett.* **2000**, *70*, 117.
(53) Claridge, J. B.; York, A. P. E.; Brungs, A. J.; Márquez-Álvarez, C.; Sloan, J.; Tsang, S. C.; Green, M. L. H. *J. Catal.* **1998**, *180*, 85.
(54) Xiao, T. C.; Hanif, A.; York, A. P. E.; Nishizaka, Y.; Green, M. L. H. *Phys. Chem. Chem. Phys.* **2002**, *4*, 4549.
(55) Stagg, S. M.; Noronha, F. B.; Fendley, E. C.; Resasco, D. E. *J. Catal.* **2000**, *194*, 240.
(56) Bitter, J. H.; Seshan, K.; Lercher, J. A. *J. Catal.* **1999**, *183*, 336.
(57) Bitter, J. H.; Seshan, K.; Lercher, J. A. *Top. Catal.* **2000**, *10*, 295.
(58) Bitter, J. H.; Seshan, K.; Lercher, J. A. *J. Catal.* **1998**, *176*, 93.
(59) Wei, J.; Iglesia, E. *J. Phys. Chem. B* **2004**, *108*, 4094.
(60) Schuurman, Y.; Márquez-Álvarez, C.; Kroll, V. C. H.; Mirodatos, C. *Catal. Today* **1998**, *46*, 185.
(61) Bradford, M. C. J.; Vannice, M. A. *Catal. Today* **1999**, *50*, 87.
(62) Ferreira-Aparicio, P.; Fernández-García, M.; Guerrero-Ruiz, A.; Rodríguez, I. *J. Catal.* **2000**, *190*, 296.
(63) O'Connor, A. M.; Meunier, F. C.; Ross, J. R. H. *Stud. Surf. Sci. Catal.* **1998**, *119*, 819.
(64) Wang, S. B.; Lu, G. Q. M. *Appl. Catal. B: Environ.* **1998**, *16*, 269.
(65) Lu, G. Q.; Wang, S. B. *CHEMTECH* **1999**, *29*, 37.
(66) Zhang, Z. L.; Tsipouriari, V. A.; Efstathiou, A. M.; Verykios, X. E. *J. Catal.* **1996**, *158*, 51.
(67) Tsipouriari, V. A.; Verykios, X. E. *J. Catal.* **1998**, *179*, 292.
(68) Seok, S. H.; Han, S. H.; Lee, J. S. *Appl. Catal. A: Gen.* **2001**, *215*, 31.
(69) Quin, D.; Lapszewicz, J. *Catal. Today* **1994**, *21*, 551
(70) Rostrup-Nielsen, J. R.; Rostrup-Nielsen, T. *Catech* **2002**, *6*, 150.
(71) Astarita, M.; Corcione, F. E.; Vaglieco, B. M. *Exp. Therm. Fluid Sci.* **2002**, *21*, 142.
(72) Naidja, A.; Krishna, C. R.; Butcher, T.; Mahajan, D. *Prog. Energy Combust. Sci.* **2003**, *29*, 155.
(73) Rostrup-Nielsen, J. R. *J. Catal.* **1973**, *31*, 173.
(74) Alstrup, I.; Rostrup-Nielsen, J. R.; Ron, S. *Appl. Catal.* **1981**, *1*, 303.
(75) Rostrup-Nielsen, J. R.; Pedersen, K. *J. Catal.* **1979**, *59*, 395.
(76) Ito, E.; van Veen, R. *Catal. Today* **2006**, *116*, 446.
(77) Wang, L.; Murata, K.; Inaba, M. *Appl. Catal. A: Gen.* **2004**, *257*, 43.
(78) Strohm, J. J.; Zheng, J.; Song, C. *J. Catal.* **2006**, *238*, 309.
(79) Rostrup-Nielsen, J. R.; Tottrup, P. B. Presented at the Symposium on Science of Catalysis and its Applications in Industry, Sindri, India, 1979; Paper 39.
(80) Albright, L. F.; Crynes, B. L.; Corcoran, W. H. In *Pyrolysis. Theory and Industrial Practice*; Academic Press: New York, 1983.
(81) Hartmann, L.; Lucka, K.; Köhne, H. *J. Power Sources* **2003**, *118*, 286.
(82) García, L.; French, R.; Czernik, S.; Chornet, E. *Appl. Catal. A: Gen.* **2000**, *201*, 225.
(83) Natesakhawat, S.; Watson, R. B.; Wang, X.; Ozkan, U. S. *J. Catal.* **2005**, *234*, 496.
(84) Wang, X.; Gorte, R. J. *Appl. Catal. A: Gen.* **2002**, *224*, 209.
(85) Archarya, C. K.; Lane, A. M.; Krause, T. R. *Catal. Lett.* **2006**, *106*, 41.
(86) Krumpelt, M.; Ahmed, S.; Kumar, R.; Rajiv, D. U.S. Patent 5,929,-286, 1999.
(87) Kramarz, K. W.; Bloom, I. D.; Kumar, R.; Ahmed, S.; Wilkenhoener, R.; Krumpelt, M. U.S. Patent 6,303,098, 2001.

(88) Ramírez-Cabrera, E.; Atkinson, A.; Chadwick, D. *Appl. Catal. B: Environ.* **2004**, *47*, 127.
(89) Fornasiero, J. P.; Balducci, G.; Monte, R. D.; Kaspar, J.; Sergo, V.; Gubitosa, G.; Ferrero, A.; Graziani, M. *J. Catal.* **1996**, *164*, 173.
(90) Bartholomew, C. H.; Weatherbee, G. D.; Jarvi, G. A. *Chem. Eng. Commun.* **1980**, *5*, 125.
(91) Borowiecki, T.; Giecko, G.; Panczyk, M. *Appl. Catal. A: Gen.* **2002**, *230*, 85.
(92) Wang, L.; Murata, K.; Matsumura, Y.; Inaba, M. *Energy Fuels* **2006**, *20*, 1377.
(93) Murata, K.; Wang, L.; Saito, M.; Inaba, M.; Takahora, I.; Mimura, N. *Energy Fuels* **2004**, *18*, 122.
(94) Nikolla, E.; Holewinski, A.; Schwank, J.; Linic, S. *J. Am. Chem. Soc.* **2006**, *128*, 11354.
(95) Kepinski, L.; Stasinska, B.; Borowiecki, T. *Carbon* **2000**, *38*, 1845.
(96) Demicheli, M. C.; Duprez, D.; Barbier, J.; Ferretti, O. A.; Ponzi, E. N. *J. Catal.* **1994**, *145*, 437.
(97) Okada, O.; Ipponmatsu, M.; Masuda, M.; Takami, S. *J. Jpn. Fuel Sci. Technol.* **1989**, *68*, 39.
(98) Suzuki, T.; Iwanami, H.; Yomohiro, T. *Int. J. Hydrogen Energy* **2000**, *25*, 119.
(99) Davies, H. S.; Humphries, K. J.; Hebden, D.; Percy, D. A. *Inst. Gas. Eng.* **1967**, *7*, 708.
(100) Rostrup-Nielsen, J. R. *Stud. Surf. Sci. Catal.* **1988**, *36*, 73.
(101) Christensen, T. S. *Appl. Catal. A: Gen.* **1996**, *138*, 285.
(102) Lee, S.; Lanterman, H. B.; Wenzel, J. E.; Edwards, N.; Adams, A.; Wootton, J.; García, A. *Prepr.−Am. Chem. Soc., Div. Pet. Chem.* **2006**, *51*, 487.
(103) Holliday, R. L.; Jong, B. Y. M.; Kolis, J. W. *J. Supercrit. Fluids* **1998**, *12*, 255.
(104) Kljin, J. E.; Engberts, J. B. F. N. *Nature* **2005**, *435*, 746.
(105) Matsumura, Y.; Tode, N. *Phys. Chem. Chem. Phys.* **2001**, *3*, 1284.
(106) Usami, Y.; Kagawa, K.; Matsumura, M.; Sakurai, H.; Haruta, M. *Appl. Catal. A: Gen.* **1998**, *171*, 123.
(107) Matsumura, Y.; Okumura, M.; Usami, Y.; Kagawa, K.; Yamashita, H.; Anpo, M.; Haruta, M. *Catal. Lett.* **1997**, *44*, 189.
(108) Shiozaki, S.; Nagashima, I.; Matsumura, Y.; Haruta, M. *Catal. Lett.* **1998**, *56*, 227.
(109) Shiozaki, S.; Hayakawa, T.; Liu, Y.; Ishii, T.; Kumagai, M.; Harmakawa, S.; Suzuki, K.; Itoh, T.; Shishido, T.; Takehira, K. *Catal. Lett.* **1999**, *58*, 131.
(110) Kapoor, M. P.; Ichihashi, Y.; Kuraoka, K.; Shen, W. J.; Matsumura, Y. *Catal. Lett.* **2003**, *88*, 83.
(111) Kapoor, M. P.; Ichihashi, Y.; Kuraoka, K.; Matsumura, Y. *J. Mol. Catal. A: Chem.* **2003**, *198*, 303.
(112) Shen, W. J.; Matsumura, Y. *Phys. Chem. Chem. Phys.* **2000**, *2*, 1519.
(113) Liu, Y.; Suzuki, K.; Hamakawa, S.; Hayakawa, T.; Murata, K.; Ishii, T.; Kumagai, M. *Catal. Lett.* **2000**, *66*, 205.
(114) Liu, Y.; Hayakawa, T.; Ishii, T.; Kumagai, M.; Yasuda, H.; Suzuki, K.; Hamakawa, S.; Murata, K. *Appl. Catal. A: Gen.* **2001**, *210*, 301.
(115) Sasaki, M.; Hamada, H.; Ito, T. *Appl. Catal. A: Gen.* **2001**, *207*, 191.
(116) Schauermann, S.; Hoffman, J.; Johanek, V.; Hartmann, J.; Libuda, J. *Phys. Chem. Chem. Phys.* **2002**, *4*, 3909.
(117) Ubago-Pérez, R.; Carrasco-Marín, F.; Moreno-Castilla, C. *Appl. Catal. A: Gen.* **2004**, *275*, 119.
(118) Tsoncheva, T.; Rosenholm, J.; Teixeira, C. V.; Dimitrov, M.; Linden, M.; Minchev, C. *Microporous Mesoporous Mater.* **2006**, *89*, 209.
(119) Gotti, A.; Prins, R. *J. Catal.* **1998**, *125*, 302.
(120) Mul, G.; Hirschen, A. S. *Catal. Today* **2001**, *65*, 69.
(121) Sun, K.; Lu, W.; Wang, M.; Xu, X. *Appl. Catal. A: Gen.* **2004**, *268*, 107.
(122) Kapoor, M. P.; Ichihashi, Y.; Nakamori, T.; Matsumura, Y. *J. Mol. Catal. A: Chem.* **2004**, *213*, 251.
(123) Emonts, B.; Hansen, J. B.; Jørgensen, S. L.; Höhlein, B.; Peters, R. *J. Power Sources* **1998**, *71*, 288.
(124) Agaras, H.; Cerella, G. *Appl. Catal.* **1988**, *45*, 53.
(125) Takahashi, K.; Takezawa, N.; Kobayashi, H. *Appl. Catal.* **1982**, *2*, 383.
(126) Takahashi, K.; Kobayashi, H.; Takezawa, N. *Chem. Lett.* **1985**, 759.
(127) Amphlett, J. C.; Evans, M. J.; Mann, R. F.; Weir, R. D. *Can. J. Chem. Eng.* **1985**, *63*, 605.
(128) Jiang, C. J.; Trimm, D. L.; Wainwright, M. S.; Cant, N. W. *Appl. Catal. A: Gen.* **1993**, *93*, 245.
(129) Shimokawabe, M.; Arakawa, H.; Takezawa, N. *Appl. Catal. A: Gen.* **1990**, *59*, 45.
(130) Busca, G.; Costantino, U.; Marmottini, F.; Montanari, T.; Patrono, P.; Pinzari, F.; Ramis, G. *Appl. Catal. A: Gen.* **2006**, *310*, 70.
(131) Twigg, M. V.; Spencer, M. S. *Top. Catal.* **2003**, *22*, 191.
(132) Bartley, G. J. J.; Burch, R. *Appl. Catal. A: Gen.* **1988**, *43*, 141.
(133) Köppel, R. A.; Baiker, A.; Schild, Ch.; Wokaun, A. *Stud. Surf. Sci. Catal.* **1991**, *63*, 59.
(134) Yao, C. Z.; Wang, L. C.; Liu, Y. M.; Wu, G. S.; Cao, Y.; Dai, W. L.; He, H. Y.; Fan, K. N. *Appl. Catal. A: Gen.* **2006**, *297*, 151.
(135) Nitta, Y.; Fujimatsu, T.; Okamoto, T.; Imanaka, T. *Catal. Lett.* **1993**, *17*, 157.
(136) Nitta, Y.; Suwata, O.; Ikeda, Y.; Fujimatsu, T.; Okamoto, Y.; Imanaka, T. *Catal. Lett.* **1994**, *26*, 345.
(137) Matter, P. H.; Braden, D. J.; Ozkan, U. S. *J. Catal.* **2004**, *223*, 340.
(138) Matter, P. H.; Ozkan, U. S. *J. Catal.* **2005**, *234*, 463.
(139) Köppel, R. A.; Stöcker, C.; Baiker, A. *J. Catal.* **1998**, *179*, 515.
(140) Ritzkopf, I.; Vukojevic, S.; Weidenthaler, C.; Grunwaldt, J. D.; Schüth, F. *Appl. Catal. A: Gen.* **2006**, *302*, 215.
(141) Gasser, D.; Baiker, A. *Appl. Catal.* **1988**, *48*, 279.
(142) Mercera, P. D. L.; van Ommen, J. G.; Doesburg, E. B. M.; Burggraaf, A. J.; Ross, J. R. H. *Appl. Catal. A: Gen.* **1991**, *71*, 363.
(143) Breen, J. P.; Ross, J. R. H. *Catal. Today* **1999**, *51*, 521.
(144) York, A. P. E.; Xiao, T. C.; Green, M. L. H. *Top. Catal.* **2003**, *22*, 345.
(145) Rostrup-Nielsen, J. R. *Catal. Today* **2000**, *63*, 159.
(146) Wilhelm, D. J.; Simbeck, D. R.; Karp, A. D.; Dickenson, R. L. *Fuel Process. Technol.* **2001**, *71*, 139.
(147) Guo, H. J.; Lou, H.; Zhu, Y. H.; Zheng, X. M. *Mater. Lett.* **2003**, *57*, 4450.
(148) Provendier, H.; Petit, C.; Estournes, C.; Libs, S.; Kiennemann, A. *Appl. Catal. A: Gen.* **1999**, *180*, 163.
(149) Basile, F.; Basini, L.; D'Amore, M.; Fornasari, G.; Guarinoni, A.; Matteuzzi, D.; Del Piero, G.; Trifirò, F.; Vaccari, A. *J. Catal.* **1998**, *173*, 247.
(150) Shishido, T.; Sukenobu, M.; Morioka, H.; Kondo, M.; Wang, Y.; Takaki, K.; Takehira, K. *Appl. Catal. A: Gen.* **2002**, *223*, 35.
(151) Tsyganok, A. I.; Tsunoda, T.; Hamakawa, S.; Suzuki, K.; Takehira, K.; Hayakawa, T. *J. Catal.* **2003**, *213*, 191.
(152) Dissanayake, D.; Rosynek, M. P.; Kharas, K. C. C.; Lunsford, J. H. *J. Catal.* **1991**, *132*, 117.
(153) Hickman, D. A.; Schmidt, L. D. *J. Catal.* **1992**, *136*, 300.
(154) Hickman, D. A.; Schmidt, L. D. *Science* **1993**, *259*, 343.
(155) Goetsch, D. A.; Schmidt, L. D. *Science* **1996**, *271*, 1560.
(156) Li, C. Y.; Yu, C. C.; Shen, S. K. *Catal. Lett.* **2000**, *67*, 139.
(157) Wang, D.; Dewaele, O.; De Groote, A. M.; Froment, G. F. *J. Catal.* **1996**, *159*, 418.
(158) Tsipouriari, V. A.; Zhang, Z.; Verykios, X. E. *J. Catal.* **1998**, *179*, 283.
(159) Hu, Y. H.; Ruckenstein, E. *Catal. Rev.−Sci. Eng.* **2002**, *44*, 423.
(160) Bitter, J. H.; Hally, W.; Seshan, K.; van Ommen, J. G.; Lercher, J. A. *Catal. Today* **1996**, *29*, 349.
(161) Ruckenstein, E.; Hu, Y. H. *J. Catal.* **1996**, *162*, 230.
(162) Tauster, S. J. *Acc. Chem. Res.* **1987**, *20*, 389.
(163) Nakagawa, K.; Anzai, K.; Matsui, N.; Ikenaga, N.; Suzuki, T.; Teng, Y. H. T.; Kobayashi Haruta, M. *Catal. Lett.* **1998**, *51*, 163.
(164) Choudhary, V. R.; Prabhakar, B.; Rajput, A. M. *J. Catal.* **1995**, *157*, 752.
(165) Nichio, N.; Casella, M. L.; Santori, G. F.; Ponzi, E. N.; Ferretti, O. A. *Catal. Today* **2000**, *62*, 231.
(166) Chang, J. S.; Park, S. E.; Yoo, J. W.; Park, J. N. *J. Catal.* **2000**, *195*, 1.
(167) Miao, Q.; Xiong, G.; Sheng, S.; Cui, W.; Xu, L.; Guo, X. *Appl. Catal. A: Gen.* **1997**, *154*, 17.
(168) Liu, S. L.; Xiong, G. X.; Sheng, S. S.; Yang, W. S. *Appl. Catal. A: Gen.* **2000**, *198*, 261.
(169) Ran, R.; Xiong, G. X.; Yang, W. S. *J. Mater. Chem.* **2002**, *12*, 1854.
(170) Ahluwalia, R. K.; Zhang, Q.; Chmielewski, D. J.; Lauzze, K. C.; Inbody, M. A. *Catal. Today* **2005**, *99*, 271.
(171) Subramanian, R.; Panuccio, G. J.; Kummenacher, J. J.; Lee, I. C.; Schmidt, L. D. *Chem. Eng. Sci.* **2004**, *59*, 5501.
(172) Subramanian, R.; Panuccio, G. J.; Kummenacher, J. J.; Lee, I. C.; Schmidt, L. D. *Chem. Eng. Sci.* **2004**, *59*, 5501.
(173) Flytzani-Stephanopoulos, M.; Voecks, G. E. *Int. J. Hydrogen Energy* **1983**, *8*, 539.
(174) O'Connor, R. P.; Klein, E. J.; Schmidt, L. D. *Catal. Lett.* **2000**, *70*, 99.
(175) Ran, R.; Xiong, G.; Sheng, S.; Yang, W.; Stroh, N.; Brunner, H. *Catal. Lett.* **2003**, *88*, 55.
(176) Yanhui, W.; Diyong, W. *Int. J. Hydrogen Energy* **2001**, *26*, 795.
(177) Krummenacher, J. J.; Schmidt, L. D. *J. Catal.* **2004**, *222*, 429.
(178) Williams, K.; Schmidt, L. D. *Appl. Catal. A: Gen.* **2006**, *299*, 30.
(179) Alejo, L.; Lago, R.; Peña, M. A.; Fierro, J. L. G. *Appl. Catal. A: Gen.* **1997**, *162*, 281.
(180) Wang, Z. F.; Wang, W. P.; Lu, G. X. *Int. J. Hydrogen Energy* **2003**, *28*, 151.
(181) Fierro, J. L. G. *Stud. Surf. Sci. Catal.* **2000**, *130A*, 78.
(182) Espinosa, L.; Lago, R. M.; Peña, M. A.; Fierro, J. L. G. *Top. Catal.* **2003**, *22*, 245.
(183) Russell, J. N.; Gates, S. M.; Yates, J. T. *Surf. Sci.* **1985**, *163*, 516.
(184) Bowker, M.; Madix, R. J. *Surf. Sci.* **1980**, *95*, 190.

(185) Peppley, B. A.; Amphlett, J. C.; Kearns, L. M.; Mann, R. F. *Appl. Catal. A: Gen*. **1999**, *179*, 41.
(186) Peppley, B. A.; Amphlett, J. C.; Kearns, L. M.; Mann, R. F. *Appl. Catal. A: Gen*. **1999**, *179*, 31.
(187) Jiang, C. J.; Trimm, D. L.; Wainwright, M. S.; Cant, N. W. *Appl. Catal. A: Gen*. **1993**, *97*, 145.
(188) Millar, G. J.; Rochester, C. H.; Waugh, K. C. *J. Chem. Soc., Faraday Trans. 1* **1991**, *87*, 2795.
(189) Mavrikakis, M.; Barteau, M. A. *J. Mol. Catal. A: Chem*. **1998**, *131*, 135.
(190) Turco, M.; Bagnasco, G.; Costantino, U.; Marmottini, F.; Montanari, T.; Ramis, G.; Busca, G. *J. Catal*. **2004**, *228*, 56.
(191) Shishido, T.; Yamamoto, Y.; Morioka, H.; Takaki, K.; Takehira, K. *Appl. Catal. A: Gen*. **2004**, *263*, 249.
(192) Navarro, R. M.; Peña, M. A.; Fierro, J. L. G. *J. Catal*. **2002**, *212*, 112.
(193) Cubeiro, M. L.; Fierro, J. L. G. *J. Catal*. **1998**, *179*, 150.
(194) Cubeiro, M. L.; Fierro, J. L. G. *Appl. Catal. A: Gen*. **1998**, *168*, 307.
(195) Iwasa, N.; Masuda, S.; Takezawa, N. *Appl. Catal. A: Gen*. **1995**, *125*, 145.
(196) Agrell, J.; Germani, G.; Jaras, S. G.; Boutonnet, M. *Appl. Catal. A: Gen.* **2003**, *242*, 233.
(197) Chin, Y. H.; Dagle, R.; Hu, J. L.; Dohnalkova, A. C.; Wang, Y. *Catal. Today* **2002**, *77*, 79.
(198) Shekhawat, D.; Gardner, T. H.; Berry, D. A.; Salazar, M.; Haynes, D. J.; Spivey, J. J. *Appl. Catal. A: Gen.* **2006**, *311*, 8.
(199) Tomishige, K.; Kanazawa, S.; Sato, M.; Ikushima, K.; Kunimori, K. *Catal. Lett.* **2002**, *84*, 69.
(200) Dias, J. A.; Assaf, J. M. *J. Power Sources* **2004**, *130*, 106.
(201) Ahmed, S.; Krumplet, K. *Int. J. Hydrogen Energy* **2006**, *26*, 291.
(202) Chan, S. H.; Wang, H. M. *J. Power Sources* **2001**, *101*, 188.
(203) Krumpelt, K.; Krause, T. R.; Carter, J. D.; Kopasz, J. P.; Ahmed, S. *Catal. Today* **2002**, *77*, 3.
(204) Villegas, L.; Guilhaume, N.; Provendier, H.; Daniel, C.; Masset, F.; Mirodatos, C. *Appl. Catal. A: Gen.* **2005**, *281*, 75.
(205) Ferrandon, M.; Krause, T. *Appl. Catal. A: Gen.* **2006**, *311*, 135.
(206) Lenz, B.; Aicher, T. *J. Power Sources* **2005**, *149*, 44.
(207) Wang, A. Q. S.; Fu, Q.; Wu, D. *Appl. Catal. A: Gen.* **2005**, *293*, 71.
(208) Cheekatamarla, P. K.; Lane, A. M. *J. Power Sources* **2005**, *152*, 256.
(209) Navarro, R. M.; Alvarez-Galvan, M. C.; Rosa, F.; Fierro, J. L. G. *Appl. Catal. A: Gen.* **2006**, *297*, 60.
(210) Erry, P.; Dinka, P.; Varma, A. *Chem. Eng. Sci*. **2006**, *61*, 5328.
(211) Liu, D.; Krumpelt, M. *Int. J. Appl. Ceram. Technol.* **2005**, *2*, 301.
(212) Navarro, R. M.; Alvarez-Galvan, M. C.; Villoria de la Mano, J. A.; González-Jiménez, I. D.; Rosa, F.; Fierro, J. L. G. Presented at the 16th World Hydrogen Energy Conference, Lyon, France, 2006.
(213) York, A. P. E. *Chem. Commun.* **1997**, *1*, 39.
(214) Cheekatamarla, P. K.; Thomson, W. J. *J. Power Sources* **2006**, *156*, 520.
(215) Velu, S.; Suzuki, K.; Osaki, T. *Chem. Commun.* **1999**, 2341
(216) Reitz, T. L.; Lee, P. L.; Czaplewski, K. F.; Lang, J. C.; Popp, K. E.; Kung, H. H. *J. Catal*. **2001**, *199*, 193.
(217) Velu, S.; Suzuki, K.; Kapoor, M. P.; Ohashi, F.; Osaki, T. *Appl. Catal. A: Gen*. **2001**, *213*, 47.
(218) Murcia-Mascarós, S.; Navarro, R. M.; Gómez Sainero, L.; Costantino, U.; Nochetti, M.; Fierro, J. L. G. *J. Catal*. **2001**, *198*, 338.
(219) Agrell, J.; Birgersson, H.; Boutonnet, M.; Melián-Cabrera, I.; Navarro, R. M.; Fierro, J. L. G. *J. Catal.* **2003**, *219*, 389.
(220) Purnama, H.; Girgsdies, F.; Ressler, T.; Schattka, J. H.; Caruso, R.; Schomacker, R.; Schlogl, R. *Catal. Lett.* **2004**, *94*, 61.
(221) Velu, S.; Suzuki, K. *Top. Catal.* **2003**, *22*, 235.
(222) Lin, S.; Harada, M.; Suzuki, Y.; Hatano, H. *Fuel* **2002**, *81*, 2079.
(223) Higman, C.; van der Burgt, M. In *Gasification*; Elsevier Science: New York, 2003.
(224) Lin, S.; Harada, M.; Suzuki, Y.; Hatano, H. *Fuel* **2002**, *81*, 2079.
(225) Molina, A.; Mondragón, F. *Fuel* **1998**, *77*, 1831.
(226) Hausseman, W. B. *Int. J. Hydrogen Energy* **1994**, *19*, 413.
(227) Vamvuka, D. *Energy Explor. Exploit.* **1999**, *17*, 515.
(228) Biassi, V. *Gas Turbine World* **2003**, *33*, 12.
(229) Pierce, J. *Engineer* **2003**, *292*, 10.
(230) Ruby, J.; Johnson, A. A.; Ziock, H. *SME Annu. Meet. Prepr*. **2004**, 961.
(231) Cox, A. W. *Energy World* **2004**, *321*, 10.
(232) Ohtsuka, Y.; Asami, K. *Catal. Today* **1997**, *39*,111
(233) Kuznetsov, B.; Shchipko, M. L. *Chem. Sustainable Dev.* **1996**, *4*, 419.
(234) Orio, A.; Corella, J.; Narvaez, I. *Ind. Eng. Chem. Res.* **1997**, *36*, 3800.
(235) Mondal, K.; Piotrowski, K.; Dasgupta, D.; Hippo, E.; Wiltowski, T., *Ind. Eng. Chem. Res.* **2005**, *44*, 5508.
(236) Carrazza, J.; Tysoe, W. T.; Heinemann, H.; Somorjai, G. A. *J. Catal*. **1985**, *96*, 234.
(237) Ohtsuka, Y.; Tomita, A. *Fuel* **1986**, *65*, 1653.
(238) Balasubramanian, B.; Ortiz, A. L.; Kaytakuglu, S.; Harrison, D. P. *Chem. Eng. Sci*. **1999**, *54*, 3543.
(239) Lin, S.; Harada, M.; Suzuki, Y.; Hatano, H. *Fuel* **2004**, *83*, 869.
(240) Curran, G. P.; Clancey, J. T.; Scarpiello, D. A.; Fink, C. E.; Gorin, E. *Chem. Eng. Prog*. **1966**, *62*, 80.
(241) McCoy, D. C.; Curran, G. P.; Sudbury, J. D. *Automot. Ind.* **1976**, *33*.
(242) Lin, S.; Suzuki, Y.; Hatano, H.; Harada, M. *Energy Fuels* **2001**, *15*, 339.
(243) Wang, J.; Takarada, T. *Energy Fuels* **2001**, *15*, 356.
(244) Arakawa, H.; Areasta, M.; Armor, J. N.; Barteau, M. A.; Beckman, E. J.; Bell, A. T.; Bertcaw, J. E.; Creutz, C.; Dinjus, E.; Dixon, D. A.; Domen, K.; DuBois, D. L.; Eckert, J.; Fujita, E.; Gibson, D. H.; Goddart, W. A.; Goodman, D. W.; Keller, J.; Kubas, G. J.; Kung, H. H.; Lyons, J. E.; Manzer, L. E.; Marks, T. J.; Morokuma, K.; Nicholas, K. M.; Periana, R.; Que, L.; Rostrup-Nielsen, J. R.; Sachtler, W. M. H.; Schmidt, L. D.; Sen, A.; Somorjai, J. A.; Stair, P. C.; Stults, B. R.; Tumas, W. *Chem. Rev.* **2001**, *101*, 953.
(245) Ogden, J.; Kreitz, T.; Kartha, S; Iwan, L. *Princeton University Center for Energy and Environmental Studies Draft Report*; Princeton University: Princeton, NJ, Nov 1996.
(246) Shinke, N.; Higashiguchi, S.; Hirai, K. *2000 Fuel Cell Seminar Abstracts*, Portland, OR, 2000; p 292.
(247) Shah, M.; Dmevich, R. F.; Balachandran, U. In *Proceedings of the 2000 Hydrogen Program Review*; NREL/CP-570-28890; National Renewable Energy Laboratory: Golden, CO, 2000.
(248) Anderson, R. P. *Hydrogen Research, Development and Demonstration Activities at the Idaho National Engineering and Environmental Laboratory (INEEL)*; presented at the 12th National Hydrogen Association Meeting, March 6−8, 2001; National Hydrogen Association: Washington, DC, 2001.
(249) Sircar, S.; Anand, M.; Carvill, B.; Hufton, J.; Mayorga, S.; Miller, B. *U.S. DOE Hydrogen R&D Program Review Meeting*; U.S. GPO: Washington, DC, 1996.
(250) Hufton, J.; Waldron, W.; Weigel, S.; Rao, M.; Nataraj, S.; Sircar, S. In *Proceedings of the 2000 Hydrogen Program Review*; NREL/CP-570-28890; National Renewable Energy Laboratory: Golden, CO, 2000.
(251) Sekiguchi, H.; Mori, Y. *Thin Solid Films* **2003**, *435*, 44.
(252) Iskenderova, K.; Porshnev, P.; Gutsol, A.; Saveliev, A.; Fridman, A.; Kennedy, L.; Rufael, T. In *Proceedings of the 15th International Symposium on Plasma Chemistry*; 2001; Vol. 7, p 2849.
(253) Paulmier, T.; Fulcheri, L. *Chem. Eng. J.* **2005**, *106*, 59.
(254) Hu, J.; Wang, Y.; van der Wiel, D. P.; Chin, Y.; Palo, D. R.; Rozmiarek, R.; Dagle, R. A.; Holladay, J. D.; Baker, E. G. *Chem. Eng. J.* **2003**, *93*, 55.
(255) Hu, J.; Wang, Y.; Cao, C.; Elliott, D. C.; Stevens, D. J.; White, J. F. *Ind. Eng. Chem. Res.* **2005**, *44*, 1722.
(256) Tonkovich, A. Y.; Perry, S. T.; Wang, Y.; Qiu, D.; LaPlante, T.; Rogers, W. A. *Chem. Eng. Sci.* **2004**, *59*, 4819.
(257) Tonkovich, A. Y.; Yang, B.; Perry, S. T.; Fitzgerald, P.; Wang, Y. *Catal. Today* **2007**, *120*, 21.
(258) Poirier, M. G.; Spundzhiev, C. *Int. J. Hydrogen Energy* **1997**, *22*, 429.
(259) Steinberg, M. *Int. J. Hydrogen Energy* **1998**, *23*, 419.
(260) Muradov, N. Z. *Energy Fuels* **1998**, *12*, 41.
(261) Choudhary, T. V.; Aksoylu, E.; Goodman, D. W. *Catal. Rev.−Sci. Eng.* **2003**, *45*, 151.
(262) Nakagawa, K.; Ikenaga, N.; Teng, Y.; Kobayashi, T.; Suzuki, T. *J. Catal*. **1999**, *186*, 405.
(263) Kalk, T.; Mahlendorf, F.; Roes, J. *2000 Fuel Cell Seminar Abstracts*; Portland, OR, 2000; p 317.
(264) Cox, K.; Williamson, K. In *Hydrogen: Its Technology and Implications*; CRC Press: Boca Raton, FL, 1977; Vol. 1.
(265) (a) Noyes, G. P. U.S. Patent 4,836,898, 1989. (b) Kalk, T.; Mahlendorf, F.; Roes, J. *2000 Fuel Cell Seminar Abstracts*; Portland, OR, 2000; p 317.
(266) Kim, M. S.; Rodríguez, N. M.; Baker, R. T. K. *J. Catal*. **1992**, *134*, 253.
(267) Rodríguez, N. M.; Chambers, A.; Baker, R. T. K. *Langmuir* **1995**, *11*, 3862.
(268) Boelland, E.; de Box, P. K.; Knock, A. I. J. M.; Geus, J. W. *J. Catal*. **1985**, *96*, 481.
(269) De Jong, K. P.; Geus, J. W. *Catal. Rev.−Sci. Eng.* **2000**, *42*, 481.
(270) Otsuka, K.; Ogihara, H.; Takenaka, S. *Carbon* **2003**, *41*, 223.
(271) Takenaka, S.; Shigeta, Y.; Tanabe, E.; Otsuka, K. *J. Catal*. **2003**, *220*, 468.
(272) Zhang, T. J.; Amiridis, M. D. *Appl. Catal. A: Gen*. **1998**, *167*, 161.
(273) Guil-López, R.; LaParola, V.; Peña, M. A.; Fierro, J. L. G. *Catal. Today* **2006**, *116*, 289.

(274) Wang, H. Y.; Rukenstein, E. *Carbon* **2002**, *40*, 1911.
(275) Takahashi, K.; Kobayashi, H.; Takezawa, N. *Chem. Lett*. **1985**, 759.
(276) Amphlett, J. C.; Evans, M. J.; Mann, R. F.; Weir, R. D. *Can. J. Chem. Eng.* **1985**, *63*, 605.
(277) Jiang, C. J.; Trimm, D. L.; Wainwright, M. S.; Cant, N. W. *Appl. Catal. A: Gen*. **1993**, *93*, 245.
(278) Au, C. T.; Ng, C. F.; Liao, M. S. *J. Catal*. **1999**, *185*, 12.
(279) Tornianen, P. M.; Chu, X.; Schmidt, L. D. *J. Catal*. **1994**, *146*, 1.
(280) Au, C. T.; Wang, H. Y. *J. Catal*. **1997**, *167*, 337.
(281) Shimokawabe, M.; Arakawa, H.; Takezawa, N. *Appl. Catal. A: Gen*. **1990**, *59*, 45.
(282) Bartley, G. J. J.; Burch, R. *Appl. Catal. A: Gen.* **1988**, *43*, 141.
(283) Koeppel, R. A.; Baiker, A.; Schild, Ch.; Wokaun, A. *Stud. Surf. Sci. Catal*. **1991**, *63*, 59.
(284) Tan, P. L.; Au, C. T.; Lai, S. Y. *Appl. Catal. A: Gen*. **2007**, *324*, 36.
(285) Xu, Y.; Liu, S.; Wang, L.; Xie, M.; Guo, X. *Catal. Lett.* **1995**, *30*, 135.
(286) Solymosi, F.; Erdohelyi, A.; Szöke, A. *Catal. Lett.* **1995**, *32*, 43.
(287) Solymosi, F.; Cserényi, J.; Szöke, A.; Bánsági, T.; Oszkó, A. *J. Catal.* **1997**, *165*, 50.
(288) Wang, D.; Lunsford, J. H.; Rosynek, M. P. *J. Catal.* **1997**, *169*, 347.
(289) Shu, Y.; Ma, D.; Liu, X.; Han, X.; Xu, Y.; Bao, X. *J. Phys. Chem. B* **2000**, *104*, 8245.
(290) Liu, S.; Dong, Q.; Ohnishi, R.; Ichikawa, M. *Chem. Commun.* **1997**, 1455.
(291) Wang, L.; Ohnishi, R.; Ichikawa, M. *J. Catal.* **2000**, *190*, 276.
(292) Zeng, J.; Xiong, Z.; Zhang, H.; Lin, G.; Tsai, K. *Catal. Lett.* **1998**, *53*, 119.
(293) Weckhuysen, B. M.; Wang, D.; Rosynek, M. P.; Lunsford, J. H. *J. Catal.* **1998**, *175*, 347.
(294) Zhang, C.; Li, S.; Yuan, Y.; Zhang, W.; Wu, T.; Lin, L. *Catal. Lett.* **1998**, *56*, 207.
(295) Shu, Y.; Xu, Y.; Wong, S.; Wang, L.; Guo, X. *J. Catal.* **1997**, *170*, 11.
(296) Weckhuysen, B. M.; Rosynek, M. P.; Lunsford, J. H. *Catal. Lett.* **1998**, *52*, 31.
(297) Bouchy, C.; Derouane-Abd Hamid, S. B.; Derouane, E. G. *Chem. Commun.* **2000**, 125.
(298) Liu, H.; Bao, X.; Xu, Y. *J. Catal.* **2006**, *239*, 441.
(299) Liu, B. S.; Leung, J. W. H.; Li, L.; Au, C. T.; Cheung, A. S. C. *Chem. Phys. Lett.* **2006**, *430*, 210.
(300) Ma, D.; Wang, D. Z.; Su, L. L.; Shu, Y.; Xu, Y.; Bao, *J. Catal.* **2002**, *208*, 260.
(301) Liu, H.; Li, T.; Tian, B.; Xu, Y. *Appl. Catal. A: Gen.* **2001**, *213*, 103.
(302) Wang, D.; Lunsford, J. H.; Rosynek, M. P. *Top. Catal.* **1996**, *3*, 289.
(303) Ohnishi, R.; Liu, S.; Dong, Q.; Wang, L.; Ichikawa, M. *J. Catal.* **1999**, *182*, 92.
(304) Demirbas, A. *Energy Sources* **2002**, *24*, 59.
(305) Ni, M.; Leung, D. Y. C.; Leung, M. K. H.; Sumathy, K. *Fuel Process. Technol.* **2006**, *87*, 461.
(306) Milne, T. A.; Abatzoglou, N.; Evans, R. J. *National Renewable Energy Laboratory Technical Report*; NREL/TP-570-25357; National Renewable Energy Laboratory: Golden, CO, 1998.
(307) Corella, J.; Aznar, M. P.; Gil, J.; Caballero, M. A. *Energy Fuels* **1993**, *13*, 122.
(308) Sutton, D.; Kelleher, B.; Ross, J. *Fuel Process. Technol.* **2001**, *73*, 155.
(309) Arvelakis, S.; Koukios, E. G. *Biomass Bioenergy* **2002**, *22*, 331.
(310) Narvaez, I.; Corella, J.; Orio, A. *Ind. Eng. Chem. Res.* **1997**, *36*, 317.
(311) Arvelakis, S.; Gehrmann, H.; Beckmann, M.; Koukios, E. G. *Biomass Bioenergy* **2002**, *22*, 55.
(312) Turn, S. Q.; Kinoshita, C. M.; Ishimura, D. *Biomass Bioenergy* **1997**, *12*, 241.
(313) Milne, T. A.; Evans, R. J; Abatzoglou, N. *Biomass Gasifier Tars: Their Nature, Formation and Conversion*; Report NRELTP-570-25357; National Renewable Energy Laboratory: Golden, CO, 1998.
(314) Sato, S.; Lin, S. Y.; Suzuki, Y.; Hatano, H. *Fuel* **2003**, *82*, 561.
(315) Antal, M. J. In *Toward a Solar Civilization*; Williams, R. H., Ed.; MIT Press: Cambridge, MA, 1978; p 80.
(316) Antal, M. J. In *Energy from Biomass and Wastes*; Klass, D. L., Ed.; IGT: Chicago, IL, 1978; p 495.
(317) Antal, M. J. In *Solar Energy*; Boer, K. W., Duffie, J. A., Eds.; Plenum Press: New York, 1982; p 61.
(318) Antal, M. J. *Ind. Eng. Chem. Res.* **1983**, *22*, 366.
(319) Modell, M. In *Fundamentals of Thermochemical Biomass Conversion*; Overend, R. P., Milne, T. A., Mudge, L. K., Eds.; Elsevier: London, U.K., 1985; p 95.
(320) Grønli, M.; Varhegyi, G.; Antal, M. J. *Ind. Eng. Chem. Res.* **1999**, *38*, 2238.
(321) Mok, W. S. L.; Antal, M. J. *Ind. Eng. Chem. Res.* **1992**, *31*, 1157.
(322) Antal, M. J.; Leesonboom, T.; Mok, W. S.; Richards, G. N. *Carbohydr. Res.* **1991**, *217*, 71.
(323) Bobleter, O. *Prog. Polym. Sci.* **1994**, *19*, 797.
(324) Holgate, H. R.; Meyer, J. C.; Tester, J. W. *AIChE J*. **1995**, *41*, 637.
(325) Kabyemela, B. M.; Adschiri, T.; Malaluan, R.; Arai, K. *Ind. Eng. Chem. Res.* **1997**, *36*, 2025.
(326) Kabyemela, B. M.; Adschiri, T.; Malaluan, R.; Arai, K. *Ind. Eng. Chem. Res.* **1997**, *36*, 1552.
(327) Kabyemela, B. M.; Takigawa, M.; Adschiri, T.; Malaluan, R. M.; Arai, K. *Ind. Eng. Chem. Res.* **1998**, *37*, 357.
(328) Minowa, T.; Fang, Z.; Ogi, T.; Varhegyi, G. *J. Chem. Eng. Jpn.* **1998**, *31*, 131.
(329) Kabyemela, B. M.; Adschiri, T.; Malaluan, R. M.; Arai, K. *Ind. Eng. Chem. Res.* **1999**, *38*, 2888.
(330) Jakab, E.; Liu, K.; Meuzelar, H. L. C. *Ind. Eng. Chem. Res.* **1997**, *36*, 2087.
(331) Manarungson, S.; Mok, W. S. L.; Antal, M. J. In *Advances in Thermochemical Biomass Conversion*; Bridgwater, A. V., Ed.; Blackie Academic and Professional: London, U.K., 1993; p 1367.
(332) Xu, X.; Matsumura, Y.; Stenberg, J.; Antal, M. J. *Ind. Eng. Chem. Res.* **1996**, *35*, 2522.
(333) Matsumura, Y.; Minowa, T.; Potic, B.; Kersten, S. R. A.; Prins, W.; van Swaaij, W. P. M.; van de Beld, B.; Elliott, D. C.; Neuenschwander, G. C.; Kruse, A.; Antal, M. J. *Biomass Bioenergy* **2005**, *29*, 269.
(334) Elliott, D. C.; Sealock, L. J.; Baker, E. G. *Ind. Eng. Chem. Res*. **1993**, *32*, 1542.
(335) Shin, H. Y.; Matsumoto, K.; Higashi, H.; Iwai, Y.; Arai, Y. *J. Supercrit. Fluids* **2001**, *21*, 105.
(336) Minowa, T.; Zhen, F.; Ogi, T. *J. Supercrit. Fluids* **1998**, *13*, 253.
(337) Kruse, A.; Meier, D.; Rimbrecht, P.; Schacht, M. *Ind. Eng. Chem. Res.* **2000**, *39*, 4842.
(338) Elliott, D. C.; Sealock, L. J. *Ind. Eng. Chem. Prod. Res. Dev*. **1983**, *22*, 426.
(339) Watanabe, M.; Inomata, H.; Arai, K. *Biomass Bioenergy* **2002**, *22*, 405.
(340) Watanabe, M.; Inomata, H.; Osada, M.; Sato, T.; Adschiri, T.; Arai, K. *Fuel* **2003**, *82*, 545.
(341) Saxena, S. K. *Int. J. Hydrogen Energy* **2003**, *28*, 49.
(342) Ishida, M.; Otsuka, K.; Takenaka, S.; Yamanaka, I. *J. Chem. Technol. Biotechnol.* **2005**, *80*, 281.
(343) Frusteri, F.; Freni, S.; Spadaro, L.; Chiodo, V.; Bonura, G.; Donato, S.; Cavallaro, S. *Catal. Commun*. **2004**, *5*, 611.
(344) Llorca, J.; de la Piscina, P. R.; Sales, J.; Homs, N. *Chem. Commun*. **2001**, 641.
(345) Fatsikostas, A. N.; Kondarides, D. I.; Verykios, X. E. *Chem. Commun*. **2001**, 851.
(346) Marino, F. J.; Jobbagy, M.; Baronetti, G.; Laborde, M. *Stud. Surf. Sci. Catal.* **2000**, *130*, 2147.
(347) Llorca, J.; Homs, N.; Sales, J.; de la Piscina, P. R. *J. Catal*. **2002**, *209*, 306.
(348) Breen, J. P.; Burch, R.; Coleman, H. M. *Appl. Catal. B: Environ.* **2002**, *39*, 65.
(349) Liguras, D. K.; Kondarides, D. I.; Verykios, X. E. *Appl. Catal. B: Environ.* **2003**, *43*, 345.
(350) Fierro, V.; Akdim, O.; Mirodatos, C. *Green Chem.* **2003**, *5*, 20.
(351) Navarro, R. M.; Alvarez-Galván, M. C.; Sánchez-Sánchez, M. C.; Rosa, F.; Fierro, J. L. G. *Appl. Catal. B: Environ.* **2005**, *55*, 229.
(352) Fatsikostas, A. N.; Kondarides, D. I.; Verykios, X. E. *Catal. Today* **2002**, *75*, 145.
(353) Sánchez-Sánchez, M. C.; Navarro, R. M.; Fierro, J. L. G. *Catal. Today* **2007**, in press.
(354) Frusteri, F.; Freni, A.; Chiodo, V.; Spadaro, L. *Appl. Catal. A: Gen.* **2004**, *270*, 1.
(355) Navarro, R. M.; Sánchez-Sanchez, M. C.; Fierro, J. L. G *Int. J. Hydrogen Energy* **2007**, in press.
(356) Llorca, J.; Homs, N.; Sales, J.; Fierro, J. L. G.; de la Piscina, P. R. *J. Catal*. **2004**, *222*, 470.
(357) Cavallaro, S.; Freni, S. *Int. J. Hydrogen Energy* **1996**, *21*, 465.
(358) Freni, S. *J. Power Sources* **2001**, *94*, 14.
(359) Cavallaro, S. *Energy Fuels* **2000**, *14*, 1195.
(360) Freni, S.; Cavallaro, S.; Mondello, N.; Spadaro;, L.; Frusteri, F. *J. Power Sources* **2002**, *108*, 53.
(361) Sheng, P. Y.; Yee, A.; Bowmaker, G. A.; Idriss, H. *J. Catal.* **2002**, *208*, 393.
(362) Auprête, G.; Descorme, C.; Duprez, D. *Catal. Commun.* **2002**, *3*, 263.
(363) Cavallaro, S.; Chiodo, V.; Freni, S.; Mondello, N.; Frusteri, F. *Appl. Catal. A: Gen.* **2003**, *249*, 119.
(364) Mattos, L. V.; Noronha, F. B. *J. Catal*. **2003**, *233*, 453.
(365) Salge, J. R.; Deluga, G. A.; Schimidt, L. D. *J. Catal*. **2005**, *235*, 69.
(366) Yee, Y.; Morrison, S. J.; Idriss, H. *Catal. Today* **2000**, *63*, 327.
(367) Mattos, L. V.; Noronha, F. B. *J. Power Sources* **2000**, *152*, 50.

(368) Wheeler, C.; Jhalani, A.; Klein, E. J.; Tummala, S.; Schimdt, L. D. *J. Catal.* **2004**, *223*, 191.
(369) Huber, G. W.; Chheda, J. N.; Barrett, C. J.; Dumesic, J. A. *Science* **2005**, *300*, 2075.
(370) Huber, G. W.; Dumesic, J. A. *Catal. Today* **2006**, *111*, 119.
(371) Huber, G. W.; Cortright, R. D.; Dumesic, J. A. *Angew. Chem. Int. Ed.* **2004**, *43*, 1549.
(372) Davda, R. R.; Shabaker, J. W.; Huber, G. W.; Cortright, R. D.; Dumesic, J. A. *Appl. Catal. B: Environ.* **2003**, *43*, 1.
(373) Shabaker, J. W.; Huber, G. W.; Davda, R., R.; Cortright, R. D.; Dumesic, J. A. *Catal. Lett.* **2003**, *88*, 1.
(374) Huber, G. W.; Shabaker, J. W.; Evans, S. T.; Dumesic, J. A. *Appl. Catal. B: Environ.* **2006**, *62*, 226.
(375) Shabaker, J. W.; Simonetti, D. A.; Cortright, R. D.; Dumesic, J. A. *J. Catal.* **2005**, *231*, 67.
(376) Fu, Q.; Flytzani-Stephanopoulos, M. *Science* **2003**, *301*, 935.
(377) Hardacre, C.; Ormerod, R. M.; Lambert, R. M. *J. Phys. Chem.* **1994**, *98*, 10901.
(378) Genciu, A. F. *Curr. Opin. Solid State Mater. Sci.* **2002**, *6*, 389.
(379) Yeung, C. M. Y.; Yu, K. M. K.; Fu, Q. J.; Thompsett, D.; Petch, M. I.; Tsang, S. C. *J. Am. Chem. Soc.* **2005**, *127*, 18010.
(380) Twigg, M.V., Ed. *Catalyst Handbook*, 2nd ed.; Wolfe Press: London, U.K., 1989; Chapters 5−7.
(381) Rhodes, C.; Hutchings, G. J.; Ward, A. M. *Catal. Today* **1995**, *23*, 43.
(382) Ovesen, C. V.; Clausen, B. S.; Hammershoi, B. S.; Steffensen, G.; Askgaard, T.; Chorkendorff, I.; Nørskov, J. K.; Rasmussen, P. B.; Stoltze, P.; Taylor, P. *J. Catal.* **1996**, *158*, 170.
(383) Hu, X. D.; Wagner, J. P. U.S. Patent 5,990,040, 1999.
(384) Klier, K.; Herman, R. G.; Vedage, G. A. U.S. Patent 5,021,231, 1991.
(385) Campbell, C. T. In *The Chemical Physics of Solid Surfaces and Heterogeneous Catalysis*; King, D. A., Woodruff, D. P., Eds.; Elsevier: Amsterdam, The Netherlands, 1993; Vol. 6, Chapter 9, p 287.
(386) Meyers, D. J.; Krebs, J. F.; Krause, T. R.; Carter, J. D. *Prepr. Pap.−Am. Chem. Soc., Div. Fuel Chem.* **2002**, *222*, 110.
(387) Patt, J.; Moon, D. J.; Phillips, C.; Thompson, L. *Catal. Lett.* **2000**, *65*, 193.
(388) Lehrmann, P.; Nielsen, P. E. H.; Aasberg-Petersen, K.; Schiodt, N. C. Can. Patent CA 2,345,515, 2001.
(389) Sauvignon, G.; Caillod, J. Eur. Patent 0189701, 1990.
(390) Newsome, D. S. *Catal. Rev.−Sci. Eng.* **1980**, *21*, 275.
(391) Andreev, A. A.; Kafedjiyski, V. J.; Edreva-Kardjieva, R. M. *Appl. Catal. A: Gen.* **1999**, *179*, 223.
(392) Trovarelli, A. *Catal. Rev.−Sci. Eng.* **1996**, *34*, 439.
(393) Gandhi, H. S.; Graham, G. W.; McCabe, R. *J. Catal.* **2003**, *216*, 433.
(394) Larese, C.; López-Granados, M.; Mariscal, R.; Fierro, J. L. G.; Lambrou, P. S.; Efstathiou, A. M. *Appl. Catal. B: Environ.* **2005**, *59*, 13.
(395) López-Granados Cabello Galisteo, F.; Lambrou, P. S.; Mariscal, R.; Sanz, J.; Sobrados, I.; Fierro, J. L. G.; Efstathiou, A. M. *J. Catal.* **2006**, *239*, 410.
(396) Li, Y.; Fu, Q.; Flyztani-Stephanopoulos, M. *Appl. Catal. B: Environ.* **2000**, *27*, 179.
(397) Bunluesin, T.; Gorte, R. J.; Graham, G. W. *Appl. Catal. B: Environ.* **1998**, *15*, 107.
(398) Hilaire, S.; Wang, X.; Luo, T.; Gorte, R. J.; Wagner, J. *Appl. Catal. A: Gen.* **2001**, *215*, 271.
(399) Iwasawa, Y. In *Elementary Reaction Steps in Heterogeneous Catalysis*; Joyner, R. W., Van Santen, R. A., Eds.; Kluwer Academic: Dordrecht, The Netherlands, 1993; p 287.
(400) Golunski, S.; Rajaram, R.; Hodge, N.; Hutchings, G. J.; Kiely, C. J. *Catal. Today* **2002**, *72*, 107.
(401) Zalc, J. M.; Sokolovskii, V.; Loffler, D. G. *J. Catal.* **2002**, *206*, 169.
(402) Liu, X.; Ruettinger, W.; Xu, X.; Farrauto, R. *Appl. Catal. B: Environ.* **2005**, *56*, 69.
(403) Ruettinger, W.; Ilinich, O.; Farrauto, R. J. *J. Power Sources* **2003**, *118*, 61.
(404) Haruta, M.; Date, M. *Appl. Catal. A: Gen.* **2001**, *222*, 427.
(405) Iida, H.; Tahara, K.; Higashi, H.; Igarashi, A. *Adv. Technol. Mater. Mater. Process. J.* **2002**, *4*, 62.
(406) Bond, G. C. *Catal. Today* **2002**, *72*, 5.
(407) Golunski, S.; Rajaram, R.; Hodge, N.; Hutchings, G. J.; Kiely, C. J. *Catal. Today* **2002**, *72*, 107.
(408) Fu, Q.; Weber, A.; Flyztani-Stephanopoulos, M. *Catal. Lett.* **2001**, *77*, 87.
(409) Andreeva, D.; Idakiev, V.; Tabakova, T.; Ilieva, L.; Falaras, P.; Bourlinos, A.; Travlos, A. *Catal. Today* **2002**, *72*, 51.
(410) Boccuzzi, F.; Chiorino, A.; Manzoli, M.; Andreeva, D.; Tabakova, T.; Ilieva, L.; Iadakiev, V. *Catal. Today* **2002**, *75*, 169.
(411) Andreeva, A.; Tabakova, T.; Idakiev, V.; Christov, P.; Giovanoli, R. *Appl. Catal. A: Gen.* **1998**, *169*, 9.
(412) Rohland, B.; Plzak, V. *J. Power Sources* **1999**, *84*, 183.
(413) Liu, W.; Flytzani-Stephanopoulos, M. *J. Catal.* **1995**, *153*, 317.
(414) Li, Y.; Fu, Q.; Flytzani-Stephanopoulos, M. *Appl. Catal. B: Environ.* **2000**, *27*, 179.
(415) Gorte, R. J.; Zhao, S. *Catal. Today* **2005**, *104*, 18.
(416) Hilaire, S.; Sharma, S.; Gorte, R. J.; Vohs, J. M.; Jen, H.-W. *Catal. Lett.* **2000**, *70*, 131.
(417) Yeung, C. M. Y.; Meunier, F.; Burch, R.; Thompsett, D.; Tsang, S. C. *J. Phys. Chem. B* **2006**, *110*, 8540.
(418) Shido, T.; Iwasawa, Y. *J. Catal.* **1993**, *141*, 71.
(419) Jacobs, G.; Williams, L.; Graham, U.; Thomas, G. A.; Sparks, D. E.; Davis, B. H. *Appl. Catal. A: Gen.* **2003**, *252*, 107.
(420) Jacobs, G.; Williams, L.; Graham, U.; Sparks, D.; Davis, B. H. *J. Phys. Chem. B* **2003**, *107*, 10398.
(421) Jacobs, G.; Graham, U. M.; Chenu, E.; Patterson, P. M.; Dozier, A.; Davis, B. H. *J. Catal.* **2005**, *229*, 499.
(422) Iida, H.; Igarashi, A. *Appl. Catal. A: Gen.* **2006**, *303*, 48.
(423) Chenu, E.; Jacobs, G.; Crawford, A. C.; Keogh, R. A.; Patterson, P. M.; Sparks, D. E.; Davis, B. H. *Appl. Catal. B: Environ.* **2005**, *59*, 45.
(424) Jacobs, G.; Chenu, E.; Patterson, P. M.; Williams, L.; Sparks, D.; Thomas, G.; Davis, B. H. *Appl. Catal. A: Gen.* **2004**, *258*, 203.
(425) Jacobs, G.; Patterson, P. M.; Williams, L.; Chenu, E.; Sparks, D.; Thomas, G.; Davis, B. H. *Appl. Catal. A: Gen.* **2004**, *262*, 177.
(426) Weibel, M.; Garin, F.; Bernhardt, P.; Maire, G.; Prigent, M. In *Catalysis and Automotive Pollution Control II*; Elsevier: Amsterdam, The Netherlands, 1991; Vol. 71, p 195.
(427) Huang, J.; El-Azzami, L.; Ho, W. S. W. *J. Membr. Sci.* **2005**, *261*, 67.
(428) Xue, E.; O'Keeffe, M.; Ross, J. R. H. *Catal. Today* **1996**, *30*, 107.
(429) Criscuoli, A.; Basile, A.; Drioli, E. *Catal. Today* **2000**, *56*, 53.
(430) Armor, J. N. *J. Membr. Sci.* **1998**, *147*, 217.
(431) Giessler, S.; Jordan, L.; Diniz da Costa, J. C.; Lu, G. Q. *Sep. Purif. Technol.* **2003**, *32*, 255.
(432) Tosti, S.; Basile, A.; Ciappetta, G.; Rizello, C.; Violante, V. *Chem. Eng. J.* **2003**, *93*, 23.
(433) Lee, D. W.; Lee, Y. G.; Nam, S. E.; Sea, B.; Lee, K. H. *Sep. Purif. Technol.* **2003**, *32*, 4.
(434) Gray, P. G.; Petch, M. I. *Plat. Met. Rev.* **2000**, *44*, 108.
(435) Dudfield, C. D.; Chen, R.; Adcock, P. L. *J. Power Sources* **2000**, *86*, 214.
(436) Korotkikh, O.; Farrauto, R. *Catal. Today* **2000**, *62*, 249.
(437) Liu, X.; Korotkikh, O.; Farrauto, R. *Appl. Catal. A: Gen.* **2002**, *226*, 293.
(438) Watanabe, M.; Uchida, H.; Ohkubo, K.; Igarashi, H. *Appl. Catal. B: Environ.* **2003**, *46*, 595.
(439) Haruta, M.; Ueda, A.; Tsubota, S.; Torres-Sanchez, R. M. *Catal. Today* **1996**, *29*, 443.
(440) Okumura, M.; Coronado, J. M.; Soria, J.; Haruta, M.; Conesa, J. C. *J. Catal.* **2001**, *203*, 168.
(441) Macieiewski, M.; Fabrizioli, P.; Grundwaldt, J. D.; Becker, O. S.; Baiker, A. *Phys. Chem. Chem. Phys.* **2001**, *3*, 3846.
(442) Liu, H.; Kozlov, A.; Kozlova, A.; Shido, T.; Iwasawa, Y. *Phys. Chem. Chem. Phys.* **1999**, *1*, 2851.
(443) Grisel, R. J. H.; Nieuwenhuys, B. E. *Catal. Today* **2001**, *64*, 69.
(444) Son, I. H.; Lane, A. M. *Catal. Lett.* **2001**, *76*, 151.
(445) Suh, D. J.; Kwak, C.; Kim, J.-H.; Kwon, S. M.; Park, T.-J. *J. Power Sources* **2005**, *142*, 70.
(446) Ko, E.-Y.; Park, E. D.; Seo, K. W.; Lee, H. C.; Lee, D.; Kim, S. *Korean J. Chem. Eng.* **2006**, *23*, 182.
(447) Kwak, C.; Park, T.-J.; Suh, D. J. *Appl. Catal. A: Gen.* **2005**, *278*, 181.
(448) Cho, S.-H.; Park, J.-S.; Choi, S.-H.; Kim, S.-H. *J. Power Sources* **2006**, *156*, 260.
(449) Vgouropoulos, G.; Ioannides, T.; Papadopoulou, C.; Batista, J.; Hocevar, S.; Matralis, H. K. *Catal. Today* **2002**, *75*, 157.
(450) Kim, D. H.; Cha, J. E.; *Catal. Lett.* **2003**, *86*, 107
(451) Grisel, R.; Westrate, K. J., Cluhoi, A.; Nieuwenhuys, B. E. *Gold Bull.* **2002**, *35*, 39.
(452) Kahlich, M. J.; Gasteiger, H. A.; Behm, R. J. *J. Catal.* **1997**, *171*, 93.
(453) Shubert, M. M.; Kahlich, M. J.; Gasteiger, H. A.; Behm, R. J. *J. Power Sources* **1999**, *84*, 175.
(454) Wang, M. *GREET 1.5-Transportation Fuel-Cycle Model, Vol. 1: Methodology, Development, Use and Results*; Argonne National Laboratory Report PB2000-101157INW; Argonne National Laboratory: Argonne, IL, 1999.
(455) Granovskii, M.; Dincer, I.; Rosen, M. A. *J. Power Sources* **2007**, *167*, 461.

CR0501994